LABORATORY MODELING OF

ENERGY DISSIPATION IN SIX-FOOT DROP

BROKEN-BACK CULVERTS

By

JAMES ALFRED BROWN

Bachelor of Science in Civil Engineering

Oklahoma State University

Stillwater, Oklahoma

2006

Submitted to the Faculty of the
Graduate College of the
Oklahoma State University
in partial fulfillment of
the requirements for
the Degree of
MASTER OF SCIENCE
December, 2012

LABORATORY MODELING OF

ENERGY DISSIPATION IN SIX-FOOT DROP

BROKEN-BACK CULVERTS

Thesis Approved:

Dr. Avdhesh K. Tyagi

Thesis Adviser

Dr. Garey A. Fox

Dr. Dee Ann Sanders

ACKNOWLEDGEMENTS

I would like to express my sincere gratitude and appreciation to my advisor, Dr. Avdhesh K. Tyagi, for his assistance and guidance during the process of this research. Sincere thanks are due to my committee members, Dr. Dee Ann Sanders and Dr. Garey A. Fox for their help in my Masters program. I would especially like to thank my wife, Jeannette, for her moral support. In addition, a special thanks to the engineers and staff of the U.S. Department of Agricultural Research Service for contributions of ideas, time and effort. The support of my fellow students at Oklahoma State Abdelfatah Ali and Nicholas Johnson was invaluable in facilitating this research. My family has been the foundation of all my achievements. This project was supported by the Research Investigation Transportation Agency, Federal Highway Administration and Oklahoma Department of Transportation.

Name: JAMES ALFRED BROWN

Date of Degree: DECEMBER, 2012

Title of Study: LABORATORY MODELING OF ENERGY DISSIPATION IN SIX-FOOT DROP BROKEN-BACK CULVERTS

Major Field: CIVIL ENGINEERING WATER RESOURCES

Abstract:

Scope and Method of Study: Current mitigations for scour include expensive external energy dissipators such as large riprap basins or concrete stilling basins at culvert outlets. The research presented in this thesis examines the effectiveness of inexpensive internal energy dissipators to maximize the energy loss within the culvert by forming a hydraulic jump inside the culvert barrel. A broken-back culvert in the laboratory represents a 1 (vertical) to 2 (horizontal) slope after the upstream inlet and then continues 138 feet at a 1 percent slope to the downstream outlet. The prototype for these experiments was either a two barrel 10-foot by 10-foot, or a two barrel 10-foot by 20-foot reinforced concrete culvert. The drop between inlet and outlet was selected as 6 feet. Three flow conditions were simulated, consisting of 0.8, 1.0 and 1.2 times the culvert depth.

Findings and Conclusions: The Froude number of the hydraulic jump created in the flat part of the culvert ranges between 1.8 and 2.3. This Froude number classifies the jump as a weak jump. The jump in experiments began nearly at the toe by placing weirs in the flat part. The optimal location was determined at a distance of 69 feet (21 meters) from the outlet face of the culvert under pressure flow conditions. The outlet momentum was reduced 22-40% from the approach momentum. The reduction in velocity was dependent on approach velocity and varied from 1.9 to 3.1 ft./s (0.6 to 0.9 m/s). For new culvert construction, the best option to maximize energy dissipation under open channel flow condition is to use one 3.0 ft. (0.9 meter) high sill located 69 feet (21 meters) from the outlet. The maximum length of the culvert can then be reduced between 42 to 56 feet (12.8 to 17 meters). Such a scenario is important where right-of-way problems exist for culvert construction. Both designs are effective in reducing outlet velocity, momentum, and energy, all of which will decrease the need for downstream scour mitigation.

TABLE OF CONTENTS

Chapter Page

LIST OF TABLES

Table Page

LIST OF FIGURES

Figure Page

NOMENCLATURE

Symbol/Variable	Description
H	Head upstream of culvert, inch; Pressure head above culvert, inch
$V_{u/s}$	Velocity at upstream of culvert, fps
y_s	Water depth at inclined channel, inch
y_t	Water depth at toe of culvert, inch
y_1	Water depth before hydraulic jump in supercritical flow, inch
V_1	Velocity before hydraulic jump in supercritical flow, fps
V_2	Velocity after hydraulic jump in subcritical flow, fps
L	Length of hydraulic jump, inch
X	Location of toe of the hydraulic jump to the beginning of the sill, inch
y_2	Water depth after hydraulic jump in subcritical flow, inch
h	Weir height, inch
$y_{d/s}$	Water depth at downstream of culvert, inch (sometimes known as
$V_{d/s}$	Velocity downstream of culvert, fps
M_1	Momentum force before the hydraulic jump at y_1, pound

Symbol/Variable	Description
M_2	Momentum force after the hydraulic jump at y_2, pound
y_c	Critical water depth, inches
W	Weight of fluid within the control volume, pound
F_f	Friction force, pound
P_1	Pressure force before the hydraulic jump at y_1, pound
P_2	Pressure force after the hydraulic jump at y_2, pound
ϕ	Bed slope angle from the horizontal, percent
A	Cross-sectional area, square feet
L	Length, inches or feet
Vol	Volume, cubic inches or cubic feet
T	Time, seconds or minutes
V	Velocity, fps
Q	Flow rate through channel, cfs
p	Prototype (subscript)
m	Model (subscript)
r	Ratio (subscript)
g	Acceleration due to gravity, feet per square second
ρ	Fluid density, slugs per cubic feet

Symbol/Variable	Description
ρ	Fluid density, slugs per cubic feet
μ	Fluid viscosity, pound second per square feet
$\bar{z}$	Distance from the water surface to the centroid of A, feet
$(\bar{z}A)$	Centroid area, cubic feet
$(\bar{z}A)'$	Dimensionless centroid area = $(\bar{z}A)/BD^2$
β_1, β_2	Velocity distribution coefficients, dimensionless
β_a	Air entrainment ratio, dimensionless = $0.0066(F_{r1}-1)^{1.4}$
D	Height of culvert, feet
y'_1	Ratio of water depth before hydraulic jump to conduit height
y'_2	Ratio of water depth after hydraulic jump to conduit height
$H.J.$	Hydraulic jump
F_{r1}	Approach Froude number
ΔE	Energy loss due to hydraulic jump, inches
THL	Total head loss for entire culvert, inches
E_2/E_1	Efficiency of hydraulic jump
$U.P.$	Under Pressure
N	No hydraulic jump occurred
Y	Hydraulic jump occurred

CHAPTER I

INTRODUCTION

1.1 RESEARCH OVERVIEW

Culverts are designed to safely pass water underneath roadways in hilly topography or on the side of a relatively steep hill. Some topography situations require culvert designs with one or more breaks in the profile slope; these culverts are known as broken-back culverts (FHWA, 2011). Broken-back culverts have steep sloped sections to overcome elevation differences, which increases water velocity and produces high-energy flows at the culvert outlet. These high-energy flows can scour and erode the natural channel bed and cause undercutting of the culvert foundation (Hotchkiss and Larson, 2005), leading to collapse of the structure (Figure 1.1). Culverts at risk of imminent foundation failure are called scour-critical culverts (Tyagi and Schwarz, 2002).

A recent research study conducted by the Oklahoma Transportation Center at Oklahoma State University indicated that there are 121 scour-critical culverts on the Interstate System (ISTAT), the National Highway System (NHS), and the State Transportation Program (STP) in Oklahoma (Tyagi and Schwarz, 2002). The approximate replacement cost of these culverts is about $121M. Current mitigations for scour include expensive external energy dissipators such as large riprap basins or

Figure 1.1 Example of a scour-critical culvert.

concrete stilling basins at culvert outlets. The research presented in this thesis examines the effectiveness of inexpensive internal energy dissipators to maximize the energy loss within the culvert. This energy loss minimizes the scour around the culvert thus decreasing the degradation downstream in the channel. This would in turn reduce the construction and rehabilitation costs of culverts in Oklahoma.

One of the most efficient means of internal energy dissipation is to force a hydraulic jump. A hydraulic jump is a natural phenomenon of a sudden rise in water level due to the change from supercritical flow to subcritical flow, which results in a sudden decrease in velocity of the flow (Chow, 1959) (Figure 1.2). This sudden change in the velocity causes considerable turbulence and loss of energy. Consequently, the hydraulic jump has been recognized as an effective method for energy dissipation for many years.

1.2 PROJECT GOAL AND OBJECTIVES

The purpose of this project is to develop a methodology to analyze broken-back culverts in Oklahoma such that the energy is mostly dissipated within the culverts to minimize the degradation downstream. A survey of culverts in Oklahoma indicates that the drop in flowline between upstream and downstream ends range between 6 and 24 feet. In previous research a drop of 24 feet was investigated (Tyagi et al., 2006/2009). In this research, a drop of 6 feet was used in the laboratory model because it is the lower limit. The culvert dimensions and hydraulic parameters for the scale model were provided during a communication with the Bridge Division, Oklahoma Department of Transportation (personal communication with B. Rusch, 2008). These hydraulic parameters are based on current field practice of culverts in Oklahoma such as seasonal

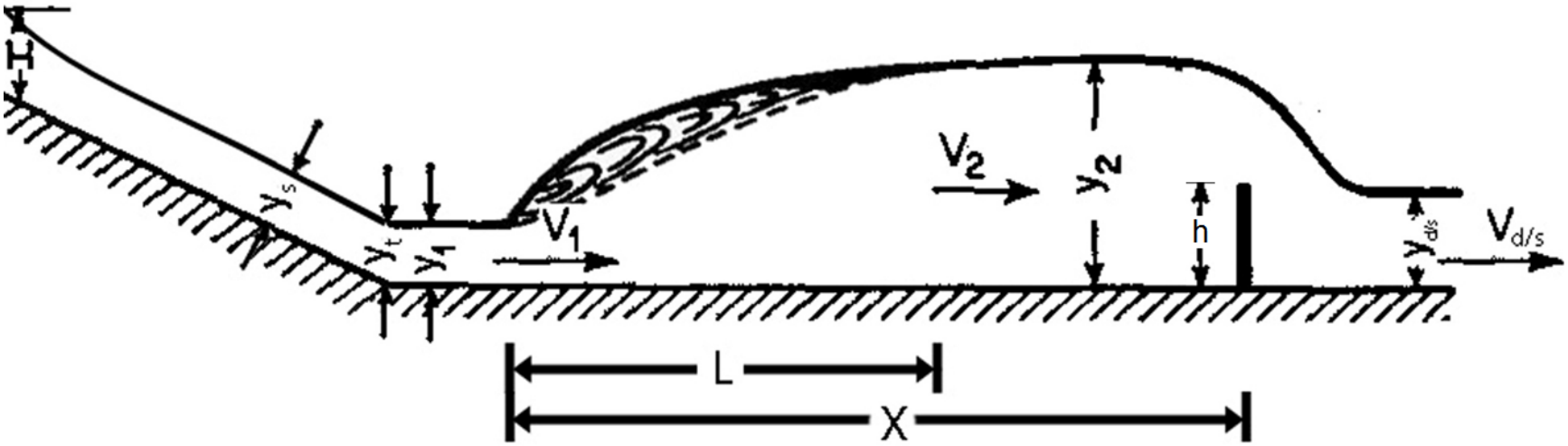

Figure 1.2 Hydraulic jump variables in a broken-back culvert.

flow patterns, acceptance downstream velocities based on soil textures, etc. It is the author's belief that the findings presented could be applied universally to similarly dimensioned culverts in similar Froude number ranges.

The research investigation includes the following tasks: 1) to obtain and review existing research currently available for characterizing the hydraulic jump in culverts; 2) to build a scale model to represent a prototype of a broken-back culvert 150 feet long, with two barrels of 10 by 10 feet, and a vertical drop of 6 feet; 3) to simulate different flow conditions for 0.8, 1.0 and 1.2 times the culvert depth (d) in the scale model constructed in Task 2; 4) to evaluate the energy dissipation between upstream and downstream ends of the broken-back culvert with and without friction blocks of different shapes; 5) to observe the efficiency of the hydraulic jump with and without friction blocks between upstream and downstream ends of the culvert and the location of the hydraulic jump from the toe of the drop in the culvert.

1.3 THESIS CHAPTER OVERVIEW

This thesis is divided into six chapters. Chapter two provides a review of existing knowledge of energy dissipaters, forced hydraulic jumps, including several types of energy dissipaters and their theoretical basis and applicability. Also included is a review of Acoustic Doppler Velocimeter (ADV) sampling and data fitting techniques in order to reduce data spikes and other signal noise from the raw data set. The last part of this chapter concerns dimensional analysis of model characteristics related to real world prototype culvert attributes. Chapter three describes the experimental methods for the tests. Presented is the design and construction of the broken-back culvert model including

supply tank, downstream channel, weirs, and friction blocks. Also there is a discussion of the construct of ADV mount to reduce vibrations to ensure accurate velocity readings. In chapter four, testing procedures are presented to show how each experiment was conducted. In chapter five, the results of data analysis and post-processing of the test are introduced. Chapter six provides conclusions about the effectiveness of different dissipation designs. Future research is also identified in this chapter.

CHAPTER II

LITERATURE REVIEW

2.1 INTRODUCTION

In this chapter, a literature search was performed for forced hydraulic jumps, hydraulic jump, acoustic doppler velocimeter (ADV) and dimension analysis related to the theoretical foundation of this project. These are discussed in the following sections.

2.2 BROKEN-BACK CULVERTS

An alternative to installing a steeply sloped culvert is to break the slope into a steeper portion near the inlet followed by a horizontal runout section. This configuration is referred to as a broken-back culvert and may be considered another internal (integrated) energy dissipator strategy if it is designed so that a hydraulic jump occurs in the runout section to dissipate energy. Figure 2.1 illustrates two cases: a double broken-back culvert, and a single broken- back culvert. In both cases, the exit or runout section is assumed to be horizontal. Under certain conditions of culvert properties and tailwater levels, a hydraulic jump will form in the runout section and reduce the outlet velocity from that associated with a supercritical depth to that associated with a subcritical depth. Modifications to the runout section may be used to induce a hydraulic jump within the culvert

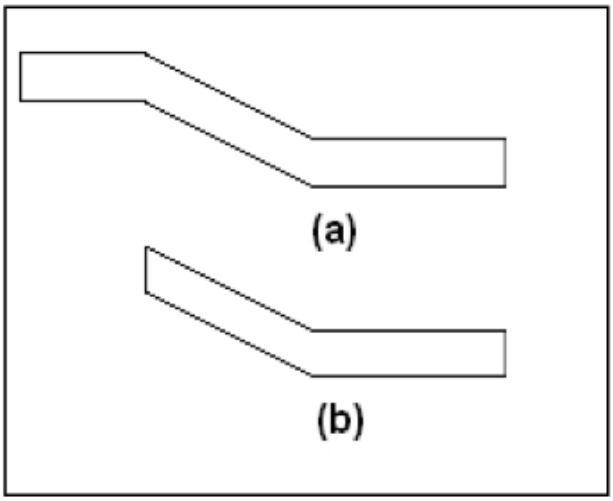

Figure 2.1 Elevation views of a) Double and b) Single Broken-back Culvert. (FHWA, 2011)

2.2.1 INLET CONTROLLED CULVERTS

Inlet control usually occurs if the culvert is operating on a steep slope such as a broken back culvert. For inlet control, the entrance characteristics of the culvert are such that the entrance head losses are predominant in determining in the headwater of the culvert. The barrel will carry water through the culvert more efficiently than the water can enter the culvert.

In inlet controlled culverts, as the name suggests, only the headwater and the inlet configuration affect the culvert performance. The headwater depth is measured from the invert of the inlet control section to the top surface of the upstream water column (Figure 1.2). The inlet area is the cross-sectional area of the face of the culvert. In Figure 2.2 there are several illustrates of the inlet-controlled culverts. The type of flow depends on the submergence of the inlet and outlet ends of the culvert. Depending on the tailwater, a hydraulic jump may occur downstream of the inlet.

Figure 2.2 A depicts a condition where neither the inlet nor the outlet end of the culvert is submerged. The flow passes through critical depth just downstream of the culvert entrance and the flow in the barrel is supercritical. The barrel flows party full over its length and the flow approaches normal depth at the outlet end.

Figure 2.2 B shows that submergence of the outlet end of the culvert does not assure outlet control. In the case, the flow just downstream of the inlet is supercritical and a hydraulic jump forms in the culvert barrel.

Figure 2.2 C is a typical design situation. The inlet end is submerged and the outlet end flows freely. Once again the flow is supercritical and barrel flows partly full over its

2.2 A Inlet/Outlet Unsubmerged

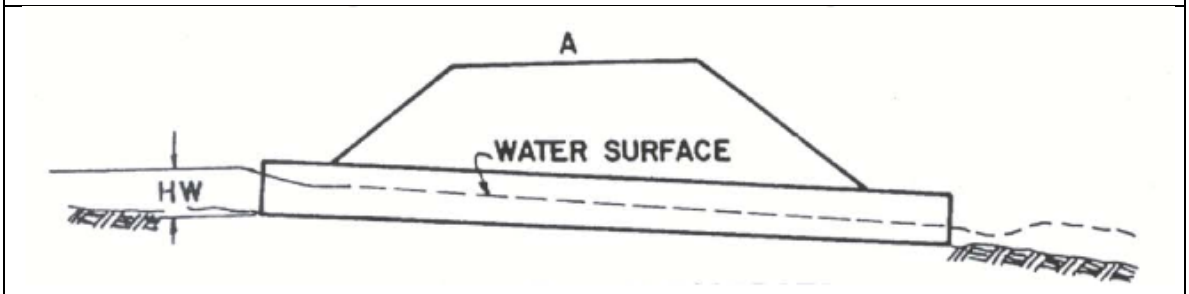

2.2 B Outlet Submerged, Inlet Unsubmerged

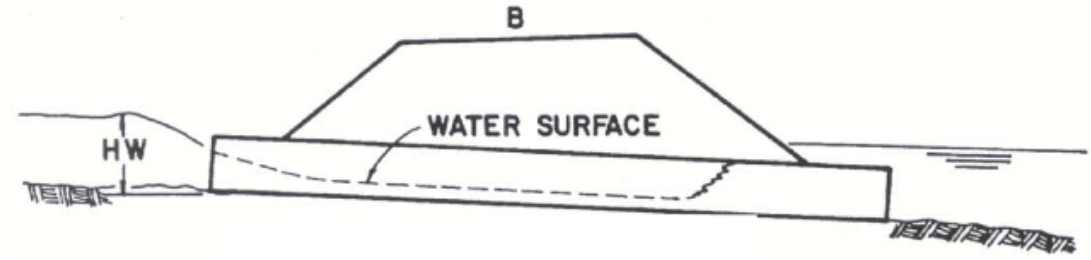

2.2 C Inlet Submerged

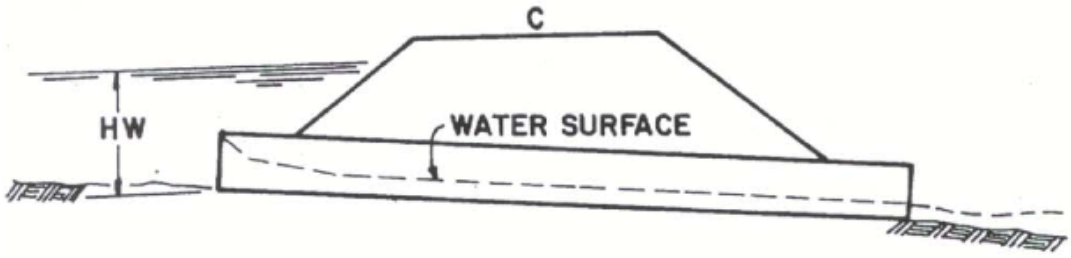

2.2 D Inlet/Outlet Submerged

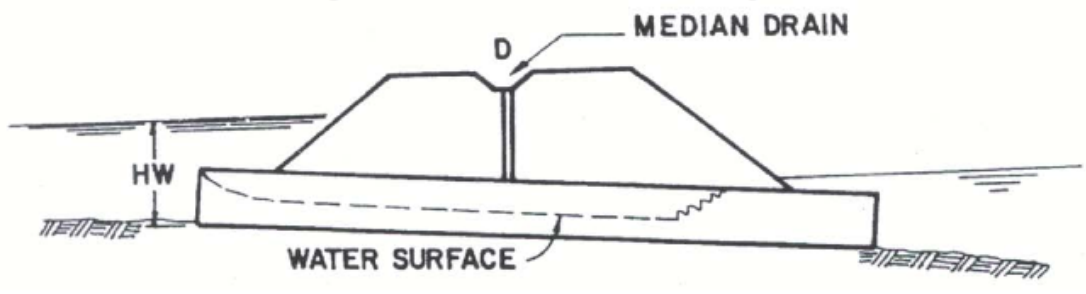

Figure 2.2 Inlet controlled culverts (FHWA, 1998)

length. Critical depth is located just downstream of the culvert entrance, and the flow is approaching normal depth at the downstream end of the culvert.

Figure 2.2 D is an unusual condition illustrating the fact that even submergence of both the inlet and the outlet ends of the culvert does not assure full flow. In this case, a hydraulic jump will form in the barrel.

2.2.2 FIELD USE OF MULTIBARREL CULVERTS

According to Gary and Blake (2008), multibarrel culverts including broken-back culverts are commonly used through the United States. They surveyed state transportation engineers in February 2007, to gain some understanding of the extent to which multibarrel culverts are used throughout the United States. Half of those states (25) responded and a summary is presented in Table 2.1.

Table 2.1 Survey of culverts by states. (Gary et al. 2008)

State	Multiple culvert use	Circular or box	Lowered invert on one barrel
Alaska, Arkansas, Colorado, Connecticut, Maine, Maryland, Michigan, Minnesota, Nebraska, Nevada, North Dakota, South Carolina	Yes	Both	Yes
Montana, Utah	Yes	Box	Yes
Georgia, Hawaii, New Mexico, Wyoming	Yes	Both	No
Iowa	Yes	Box	No
California, Idaho, Kentucky	Yes	Circular	No, or uncommon
Indiana, Ohio, Washington	No	—	—

2.3 FORCED HYDRAULIC JUMPS

The hydraulic jump is an example of rapidly varied flow in which supercritical flow abruptly converts to subcritical, typically due to high tailwater (Chow 1959; Rajaratnam 1967). In this process, the water surface passes upwards through critical depth as kinetic energy is converted to potential energy (Franzini and Finnemore 1997; Thompson and

Kilgore 2006). The transition is always accompanied by an energy loss. Energy is lost as kinetic energy is converted into turbulence and then into sound and heat (Haindl 1957; Sturm 2001).

Extensive research effort has been devoted to the use of appurtenances (Rand 1965; Karki and Kumar 1996) especially with rectangular weirs and sills to force hydraulic jumps in horizontal rectangular channels. Sills and weirs are used to force a hydraulic jump and to stabilize the jump location on a horizontal channel. A weir is when the defined as ratio of the depth of flow over the crest (y_c) to block height (h) when it is equal to less than ten (Figure 1.2). Conversely, a sill is defined as this ratio equal to or greater than ten. The current research was performed using weirs. Hydraulic jumps forced by sills and weirs are known to dissipate more energy than classical or free hydraulic jumps (Forster and Skrinde 1950). A classical hydraulic jump is a jump caused by subcritical downstream flow depth in a constant width horizontal rectangular channel, with no appurtenances (Chow 1959).

Chow states that a hydraulic jump will form in a channel if either of the following two conditions occurs: (1) the momentum in the tailwater downstream from the culvert exceeds that in the barrel, or (2) the supercritical Froude number in the barrel is reduced to approximately 1.7 in a decelerating flow environment (Chow, 1959).

A weir or a sill located near the toe of the jump has proven to be an effective energy dissipator. Both experimental and theoretical considerations have shown that the thickness of the weir has no discernable effect on the flow pattern, or on the energy dissipation mechanism (Hager, 1992). Thus a weir thickness of sufficient strength to

resist the flow water was considered for these experiments.

Most jumps vary in appearance between two extremes cases as shown Figure 2.3 (Hager et al. 1990). The first is a fully-developed surface roller, which is characterized by a relatively smooth and continuous water surface, as flow continues along the channel bottom and diverges downstream called a submerged sill (Figure 2.3a). At this point, bubbles rise intensively to a stagnation point, where flow either proceeds downstream or circulates back towards the toe of the jump to yield a roller. The second extreme is a standing wave, in which flow is immediately deflected to the surface at the toe called a non-submerged sill (Figure 2.3b). The toe moves downstream while the end of the jump moves upstream, creating a shorter jump, characterized by heavy surface waves and eruptions. The second extreme has a very limited capacity for energy dissipation since non-submerged sills fail to produce a fully-developed jump, allowing supercritical flow to persist well beyond the sill (Hager et al. 1990).

From the previously mentioned extreme cases, an expanded range of jump behavior observations have led to various systems of classification that differentiate between those cases and provide a universal language among hydraulicians to communicate such behavior more easily (Figure 2.4).

First, the A-jump is defined as a jump where the end roller is just above the front face of the sill. The A-jump corresponds to the flow configuration with maximum tailwater (Figure 2.4a). By decreasing the tailwater depth, the toe of the jump moves toward the sill. In a B-jump the sill considerably modifies the flow and the streamline pattern becomes curved (Figure 2.4b). Also the height of the bottom roller

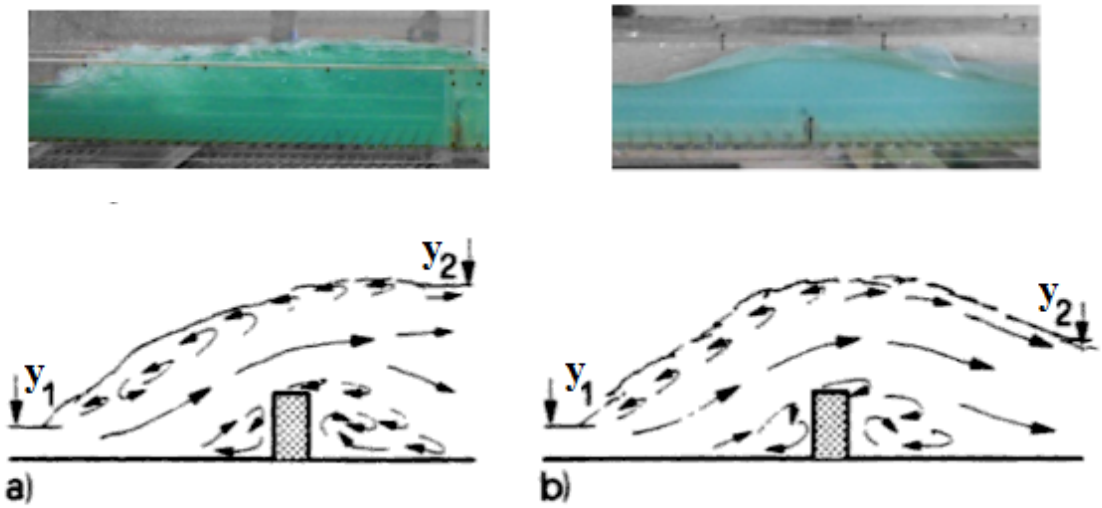

Figure 2.3 Hydraulic jump at a sill: a) Submerged sill flow, b) Non-submerged sill flow.(Hager and Li, 1992)

increases and a surface boil or roller emerges behind the sill; neither changes the water surface profile significantly. As the tailwater depth decreases, the distance between the toe of the jump and the upstream face of the sill diminishes. Additionally, the water surface profile becomes more convex due to plunging currents foaming behind the sill. The minimum B-jump further degrades to the lowest tailwater before the main flow begins striking the channel bottom. A C-jump is characterized by heavy plunging flows, which strike the channel bottom. A wave type jump forms a standing wave that passes over the sill. The flow is entirely supercritical and scouring becomes likely (Hager et al. 1990).

There are two main parameters of interest in predicting hydraulic jump behavior: (1) the subcritical sequent depth (y_2), and (2) the length of the jump (L) (Thompson and Kilgore 2006). Not only do these parameters describe the size of the jump, but if the subcritical sequent depth is compared to the tailwater profile, the location may be found as well (Chow 1959). Furthermore, once both sequent depths are known, energy loss may be determined by Bernoulli's equation (Thompson and Kilgore 2006).

In open channel jumps Montes (1998) has related the tailwater depth to location of the jump in the channel. If the tailwater increases, the hydrostatic pressure downstream will increase, causing a net force in the upstream direction, which will push the jump upstream. Conversely, if the tailwater decreases, the jump will move downstream. Likewise, if the upstream velocity increases, the momentum flux upstream will increase, causing a net force in the downstream direction, which will increase the size of the jump and push it downstream. Conversely, if the upstream velocity decreases, the jump will decrease in size and move upstream. Therefore, in the absence of channel friction, the

size and location of the hydraulic jump is highly sensitive to fluctuations in depth and

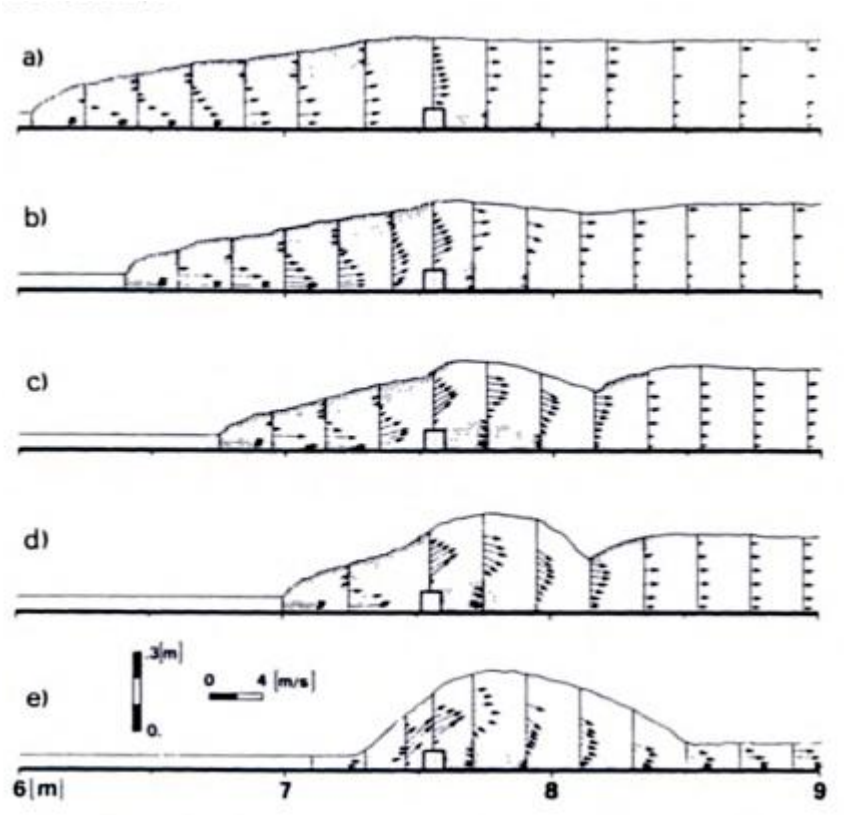

Figure 2.4 Hydraulic jump at sill: a) A-jump b) B-jump c) Minimum B-jump d) C-jump e) Wave type flow. (Hager and Li, 1992).

velocity (Montes 1998).

The hydraulic jump has many useful applications in hydraulic design. Among these are: (1) to dissipate energy in water flowing over dams, weirs, and other hydraulic structures and thus prevent scouring downstream from these structures; (2) to raise the water level on the downstream side of a measuring flume to maintain a high water level in the channel for irrigation or other water-distribution purposes; (3) to increase weight on an apron and thus reduce uplift pressure under a masonry structure by raising the water depth on the apron; (4) to increase the discharge of a sluice gate by holding back tailwater, since the effective head will be reduced if tailwater is allowed to drown the jump; (5) to mix chemicals used for water purification; (6) to aerate water for city water supplies; and (7) to remove air pockets from water-supply lines and thus prevent air locking (Chow 1959).

2.4 LITERATURE ON HYDRAULIC JUMP

Hydraulic jumps have been the focus of interest among engineers for almost 200 years. Although first described by De Vinci in the 16th Century, the phenomenon's engineering concerns started with Giorgio Bidone, an Italian, in 1818 (Chow 1959), and then with the French hydraulician Jean-Baptiste Bélanger, who developed his famous equation in 1838 relating the supercritical and subcritical depths to the upstream Froude number (Hager 1999). Comprehensive histories of the study of hydraulic jumps may be found in several hydraulics texts, including Chow (1959), Rajaratnam (1967), Hager (1992), and Montes (1998). An extended discussion is summarized in the following paragraphs.

Preliminary studies of Blee (1929) and Shukry (1957) pointed out the relative importance of the sill position relative to the toe of jump. Rand (1957; 1965; 1967) conducted a number of systematic observations on sill flow, including a classification of flow types. The ratio of sequent depths as a function of sill height and type of jump, the length characteristics, and the energy loss were analyzed.

Harleman investigated the effect of baffle piers on the properties of the hydraulic jump using one row of stepped blocks and two rows of cavitation-free blocks. In addition to the Froude number, Harleman (1954) recognized the importance of the location of the baffle piers, relative to the toe of the jump, as a design parameter. He also determined the length and depth reduction caused by the baffle piers by comparing properties of the forced jump with the classical hydraulic jump. Harleman (1954) also applied a momentum theory that observed depth reductions were consistent with measured drag forces on the baffle piers.

Bradley and Petreka (1957) produced well-known design curves for a variety of stilling basins based on extensive studies of free and forced hydraulic jumps. They recommended the use of baffle blocks and a continuous end sill. Pillai and Unny (1964) studied forced hydraulic jumps using baffle blocks with a continuous end sill. Both studies performed open channel jump experiments which lend themselves to design curves provided by the Bélanger equation – that is, expressing the ratio between sequent depths as a function of the upstream Froude number.

Rajaratnam (1964) extensively studied forced jumps with a wide range of appurtenances including a sill, baffle blocks, two sills, two baffle block rows, baffle basin

(sill and baffle blocks), and sunk basin (abrupt rise in channel bed). Rajaratnam connected, using the momentum equation, the drag force coefficient with the distance between the appurtenance and the toe of the jump in one general relationship for each type of appurtenances. Design curves were developed for the calculation of downstream water depth for variable distances between the toe of the jump and the appurtenances.

Bhutto et al. (1989) provided analytical solutions for computing sequent depth and relative energy loss for a free hydraulic jump in horizontal and sloping rectangular channels from their experimental studies. They used the ratio of jump length to jump depth and the Froude number to compute the length of the free jump on a horizontal bed. Jump factor and shape factor were evaluated experimentally for the free jump on a sloping bed. To check the efficiency of the jump, they made comparisons with previous solutions by other researchers and found that the equations they derived could be used instead of equations by Ludin, Bakhmateff, Silvester and Chertoussove.

Gharanglk and Chaudhry (1991) present three models for the numerical simulation of hydraulic jumps in a rectangular channel while factoring in the considerable effect of nonhydrostatic pressure distribution. The one-dimensional Boussinesq equations are solved in time subject to appropriate boundary conditions which numerically simulate the hydraulic jump. The results were compared to experimental data which indicate that four-order models with or without Boussinesq terms give similar results for all Froude numbers tested. The Froude numbers ranged from 2.3 to 7.0. The MacCormack scheme and a dissipative two-four scheme were used to solve the governing equations subject to specified end conditions until a steady state was achieved.

Ohtsu et al. (1996) evaluated incipient hydraulic jump conditions on flows over vertical sills. They identified two methods of obtaining an incipient jump: (1) increasing the sill height, or (2) increasing the tailwater depth until a surface roller forms upstream of the sill. For wide channels, predicted and experimental data were in agreement, but in the case of narrow channels, incipient jump was affected by channel width.

Ohtsu, et al (2001) investigated undular hydraulic jump conditions in a smooth rectangular horizontal channel. They found that the formation of an undular jump depends only on the inflow Froude number and the boundary-layer development at the toe of the jump. At these Froude number ranges, they found that the effects of the aspect ratio and the Reynolds number on the flow characteristics were negligible. Under experimental investigation, it was found that the upper limits of the Froude numbers range between 1.3 and 2.3 at the inflow. Furthermore, a Froude number of 1.7 was found to be the critical velocity point in which inflow was fully developed. They obtained the ratio thickness of the boundary layer to the depth of the toe of the jump to be 0.45 to 1.0, which agreed with predicted values from experimental results.

Hotchkiss and Donahoo (2001) developed a computer program to analyze Broken-back culverts. Broken-back Culvert Analysis Program (BCAP) is a simple but powerful tool for analyzing broken-back culverts and hydraulic jumps. This program utilizes classical hydraulic jump energy and momentum equations. It is able to plot rating curves for the headwater, outlet depth and outlet velocity.

Finnemore, et al. (2002) states that the characteristics of the hydraulic jump depend on the Froude number (Fr). The Froude number is the ratio between inertial and

gravitational forces. They added that in order for the hydraulic jump to occur, the flow must be supercritical, i.e. a jump can occur only when the Froude number is greater than 1.0. The hydraulic jump is classified according to its Froude number. When Fr is between 1.7 and 2.5, the flow is classified as a weak jump and will have a smooth rise in the water surface with less energy dissipation. An Fr between 2.5 and 4.5 results in an oscillating jump with 15-45% energy dissipation. A steady jump will occur when Fr ranges from 4.5 to 9.0 and results in energy dissipation from 45% to 70%. When Fr is above 9.0, a strong jump will occur with energy losses ranging from 70% to 85%.

Hotchkiss et al (2003) describe the available predictive tools for hydraulic jumps, the performance of the Broken-back Culvert Analysis Program (BCAP) in analyzing the hydraulics of a broken-back culvert, and the current applications and distribution of BCAP. They conducted tests on the broken-back culvert made of Plexiglas® to assess the performance of BCAP in predicting headwater rating curves, the locations of hydraulic jumps, and the lengths of hydraulic jumps. They conclude that accounting for the losses within the jump because of the friction in corrugated metal pipes and more accurate predicting of the locations of hydraulic jumps may be improved by predictions of flow hydraulics within the culvert barrel.

The Utah Department of Transportation (UDOT) addresses aspects of broken-back culverts and hydraulic jumps in the state's Manual of Instruction – Roadway Drainage (US Customary units), Culverts (2004). This manual illustrates steps for the design of broken-back culverts which include: 1) Establish a flow-line profile, 2) sizing the culvert, 3) beginning to calculate a supercritical profile, 4) completing profile calculations, and 5) considering hydraulic jump cautions. Section F of Appendix 9 of the manual, covers

aspects of hydraulic jumps in culverts, including cause and effect, momentum friction, comparison of momentum and specific energy curves, and the potential occurrence of hydraulic jumps. The manual also takes into account the sequent depth of jump for rectangular conduits, circular conduits, and conduits of other shapes.

Larson, E. (2004), in her Master's thesis entitled "Energy Dissipation in Culverts by Forcing a Hydraulic Jump at the Outlet", suggests that outlet energy could be reduced by forcing a hydraulic jump. She considered two designs to create a hydraulic jump within the culvert barrel: (1) a rectangular weir placed on a flat apron and (2) a vertical drop along with a rectangular weir. These two designs were used to study the energy reduction in the flow at the outlet. From these experiments she found that both designs were effective in reduction of outlet velocity, momentum, and energy. The author found that these reductions would decrease the need for downstream scour mitigation.

Hotchkiss et al. (2005) proposed that by controlling the water velocity at the outlet of a culvert, scour could be reduced. He compared the effectiveness of a simple weir near the culvert outlet to a weir with a drop upstream of the culvert barrel. Both designs are intended to reduce the specific energy of the water at the outlet by inducing a hydraulic jump within the culvert barrel, without the aid of tailwater. A design procedure was proposed based on the geometry and effectiveness of each jump type in energy reduction. In this research, they found the Froude number ranged from 2.6 to 6.0. It was determined that both weir designs were effective in reducing the velocity of water along with the energy and momentum, which would decrease the need for downstream scour mitigation.

The Hydraulic Design of Energy Dissipators for Culverts and Channels (July,

2006), from the Federal Highway Administration, provides design information for analyzing and mitigating problems associated with the energy dissipation at culvert outlets and in open channels. It recommends the use of the broken-back culvert design as an internal energy dissipator. The proposed design for a broken-back culvert is limited to the following conditions: 1) the slope of the steep section must be less than or equal to 1.4:1 (V: H) and 2) the hydraulic jump must be completed within the culvert barrel.

According to this report, for situations where the runout section is too short and/or there is insufficient tailwater for a jump to be completed within the barrel, modifications may be made to the outlet that will induce a jump. The design procedure for stilling basins, streambed level dissipaters, riprap basins and aprons, drop structures and stilling wells is also discussed.

Pagliara et. al. (2008) analyzed the hydraulic jump that occurs in homogeneous and nonhomogeneous rough bed channels. They investigated the sequent flow depth and the length of the jump, which are the influence parameters of the hydraulic jump. In this research, they drew on the general jump equation to analyze the jump phenomenon. In analyzing the rough bed data, they were able to formulate a representative equation to explain the phenomenon. The equations found in their study may be used to design stilling basins downstream of hydraulic structures.

Hotchkiss et al. (2008) analyzed the accuracy of the following seven programs on culvert hydraulics: HY-8, FishXing, Broken-back Culvert Analysis Program (BCAP), Hydraflow Express, CulvertMaster, Culvert, and Hydrologic Engineering Center River Analysis system (HEC-RAS). The software was tested on the accuracy of three

calculations: headwater depths, flow control, and outlet velocities. The software comparison was made between software output values and hand calculations, not from laboratory experimental data. The hand calculations used were derived from laboratory experiments done by the National Bureau of Standards (NBS). Hotchkiss et al. concluded HEC-RAS is the most comprehensive program for both accuracy and features for culverts affected by upstream structures.

Tyagi et al. (2009) investigated hydraulic jump under pressure and open channel flow conditions in a broken-back culvert with a 24 foot drop. It was found that for pressure flow a two sill solution induced the most desirable jump, and for open channel a single sill close to the middle of the culvert was most desirable. The investigation was funded by the Oklahoma Transportation Center, Research and Innovative Technology Administration, Federal Highway Administration, and Oklahoma Department of Transportation.

Varol et al. (2009) carried out many experiments to determine the effect of a water jet device at varying upstream Froude numbers and flow rates on hydraulic jump characteristics. They analyzed hydraulic jump experiments by high speed (SVHS camera) image processing techniques. Flow structure, roller lengths, water surface profiles, and energy losses were studied experimentally for both free jump and jump modified by water jet. It was observed that the roller of the hydraulic jump moved upstream as the water jet flow increased. Moreover, it was noted that the downstream water depth (y2) and roller length increased with increased water jets discharge. Furthermore, they found that forced hydraulic jumps initiated by water jet had higher energy losses than free jumps.

Mignot and Cienfuegos (2010) focused on an experimental investigation of energy dissipation and turbulence production in weak hydraulic jumps. Froude numbers ranged from 1.34 to 1.99. They observed two peak turbulence production regions for the partially developed inflow jump, one in the upper shear layer and the other in the near-wall region. The energy dissipation distribution in the jumps was measured and revealed a similar longitudinal decay of energy dissipation, which was integrated over the flow sections and maximum turbulence production values from the intermediate jump region towards its downstream section. It was found that the energy dissipation and the turbulence production were strongly affected by the inflow development. Turbulent production showed a common behavior for all measured jumps. It appeared that the elevation of maximum Turbulent Kinetic Energy (TKE) and turbulence production in the shear layer were similar.

Alikhani et al. (2010) conducted many experiments to evaluate effects of a continuous vertical end sill in a stilling basin. They measured the effects of sill position on the depth and length of a hydraulic jump without considering the tailwater depth. In the experiments, they used five different sill heights placed at three separate longitudinal distances in their 1:30 scaled model. The characteristics of the hydraulic jump were measured and compared with the classical hydraulic jump under varied discharges. They proposed a new relationship between sill height and position, and sequent depth to basin length ratio. The study concluded that a 30% reduction in basin length could be accomplished by efficiently controlling the hydraulic jump length through sill height.

Tyagi et al. (2010a) performed many experiments for open channel culvert conditions. Optimum energy dissipation was achieved by placing one sill at 40 feet from

the outlet. Friction blocks and other modifications to the sill arrangement were not as effective.

Tyagi et al. (2010b) carried out many experiments to optimize flow condition and energy dissipation in a broken-back culvert under pressure flow. It was found that two sills, the first 5 ft high and 25 feet from the outlet and the second 3.34 ft high and 45 feet from the outlet, gave the best results. The culvert could not be shortened since it was full under the tested conditions.

Comparison of current research to Literature

There are some differences between the current research and the literature data. First, the approach supercritical flow is developed with a steeply sloped channel, not a sluice gate. Second, the depth of flow downstream from the weir was uncontrolled which is not practice in some studies. In the field controls are rarely installed to affect the water level downstream of the culvert outlet. (Zhu, 2008) Third, the current research unitized both weirs and friction blocks in the flume simultaneously, often a weir(s) are use singly in literature.

2.5 LITERATURE ON ACOUSTIC DOPPLER VELOCIMETER (ADV)

Acoustic Doppler Velocimeter (ADV) is a sonar device which tracks suspended solids (particles) in a fluid medium to determine an instantaneous velocity of the particles in a sampling volume. In general, ADV devices have one transmitter head and two to four receiver heads. Since their introduction in 1993, acoustic Doppler velocimeters have quickly become valuable tools for laboratory and field investigations of flow in oceans,

rivers, canals, reservoirs, hydraulic structures and laboratory scale models (Sontek, 2001).

Wahl (2000) discusses methods for filtering raw ADV data using a software application called WinADV. Wahl suggests that ADV data present unique requirements compared to traditional current-metering equipment, due to the types of data obtained, the analyses that are possible, and the need to filter the data to ensure that any technical limitations of ADVs do not adversely affect the quality of the results. According to Wahl, the WinADV program is a valuable tool for filtering, analyzing, and processing data collected from ADVs. Further, this program can be used to analyze ADV files recorded using the real time data acquisition programs provided by ADV manufacturers.

Goring and Nikora (2002) formulated a new post processing method for despiking raw ADV data. The method combines three concepts, including:

1. That differentiation of the data enhances the high frequency portion of a signal, which is desirable in sonar measurements.
2. That the expected maximum of a random series is given by the "Universal threshold function".
3. That good data clusters are a dense cloud in phase space maps.

These concepts are used to construct an ellipsoid in three-dimensional phase space, while points lying outside the ellipsoid are designated as spikes (bad data). The algorithm presented by Goring and Nikora has superior performance over past methods (RC Filter Method, Tukey 53H Method, Acceleration Thresholding Method and Wavelet Thresholding Method) and with the added advantage of requiring no algorithm

parameters. Several methods for replacing sequences of spurious data are presented. Goring and Nikora prefer a method of polynomial fitted to good data on either side of the spike event, then interpolated across the event.

Mori et al. (2007) investigates measuring velocities in aerated flows using ADV techniques. ADV measurements are useful and powerful for measurements of mean and turbulent components of fluids in both hydraulic experimental facilities and fields. However, it is difficult to use the ADV in bubbly flows because air bubbles generate spike noise in the ADV velocity data. This study describes the validity of the ADV measurements in bubbly flows. The true three-dimensional phase space method is significantly useful to eliminating the spike noise of ADV recorded data in bubbly flow as compared to the classical low correlation method (Goring and Nikora, 2002). The results of the data analysis suggest that:

1. There is no clear relationship between velocity and ADV's correlation/signal-to-noise ratio in bubbly flow;
2. Spike noise filtering methods based on low correlation and signal-to-noise ratio are not adequate for bubbly flow; and
3. The true 3D phase space method significantly removes spike noise of ADV velocity in comparison with the original 3D phase space method.

In addition the study found that ADV velocity measurements can be valid for 1% to 3% air void flows. The limitations of the ADV velocity measurements for high void fractions were not studied.

Chanson et al. (2008) investigated the use of ADVs to determine the velocity in turbulent open channel flow conditions in both laboratory and field experiments. They demonstrated that the ADV is a competent set of devices for steady and unsteady turbulent open channel flows. However, in order to accurately measure velocity, the ADV raw data must be processed and the unit must be calibrated to the suspended sediment concentrations. Accurately processing your ADV data requires practical knowledge and experience with the device's capabilities and limitations. Chanson concluded that turbulence properties should not be derived from unprocessed ADV signals and some despiking methods were not directly applicable to many field and laboratory applications.

Birjandia and Bibeau, (2011) discovered that Acoustic Doppler Velocimetry (ADV) could measure flow velocities in three directions in experimental facilities and field applications. Based on the Doppler shift effect, ADV can accurately resolve the quasi-instantaneous flow field at frequencies of up to approximately 200 Hz. However, this technique is sensitive to operating conditions that can lead to contaminated signals containing large amplitude spikes, a disadvantage of ADV. Aliasing of the Doppler signal creates these spikes. Such a situation occurs when large particles intersect the sampling volume or acoustic waves. For example during the characterization of river velocities, sediments floating near the riverbed cause aliasing from particles, and more importantly, surface entrained air bubbles contaminate the ADV signal. Spikes due to air bubbles not only increase the standard deviation of the velocity, but also corrupt the autocorrelation and power spectra. As some of these spikes appear like velocity fluctuations, developing accurate despiking procedures is an important requirement during post-processing of

ADV velocity measurements in bubbly flow applications. A new hybrid method is introduced which has advantages over conventional despiking methods such as the acceleration threshold method and the phase-space threshold method when using ADV in bubbly flow. ADV river velocity measurements near kinetic turbines demonstrate the proposed method. This method is applicable to other bubbly flow applications to characterize the liquid phase using ADV.

2.6 DIMENSIONAL ANALYSIS

In engineering and physics, the Buckingham π theorem is a key theorem in dimensional analysis. It is a formalization of Rayleigh's method of dimensional analysis. The theorem loosely states that if we have a physically meaningful equation involving a certain number (n), of physical variables (p) and these variables are expressible in terms of k independent fundamental then the original expression is equivalent to an equation involving a set of $p = n - k$ dimensionless parameters constructed from the original variables. This provides a method for computing sets of dimensionless parameters from the given variables, even if the form of the equation is still unknown. However, the choice of dimensionless parameters is not unique: Buckingham's theorem only provides a way of generating sets of dimensionless parameters, and will not choose the most physically meaningful.

2.6.1 DIMENSIONAL ANALYSIS OF WEIR FORCED HYDRAULIC JUMP

The weir forced hydraulic jump depends on many variables to characterize. Consider a culvert in which a rectangular continuous weir located a distance of X from the entrance is used to develop a forced hydraulic jump (Figure 1.2). The following functional relationship among significant parameters is used to characterize the forced

hydraulic jump due to the presence of a continuous weir in a rectangular channel. Thus, if f represents a unknown function;

$$f\left(h, y_1, y_2, y_{d/s}, V_1, L, X, \phi, g, \rho, \mu\right) = 0 \quad (1)$$

where; h is the height of the weir, y_1 and V_1 are depth and average velocity of the supercritical stream at distance X upstream of the weir, $y_{d/s}$ is the sequent depth of jump (or in fact flow depth immediately after for a forced jump), y_2 is maximum flow depth upstream of the weir. X is the length of the stilling basin or distance from the beginning of the flat part of the channel to upstream face of the weir, L is the length of the hydraulic jump, ϕ is channel slope, g is gravity, ρ and μ are water density and viscosity respectively. Assuming a horizontal stilling basin ($\phi = 0$) and fully turbulent flow independent of Reynolds number, the dimensionless parameters are summarized as:

$$f\left(\frac{h}{y_1}, \frac{y_{d/s}}{y_1}, \frac{y_2}{y_1}, \frac{L}{X}, \frac{X}{y_1}, Fr_1\right) = 0 \quad (2)$$

2.6.2 HYDRAULIC SIMILITUDE THEORY

Similarity between a hydraulic model and a prototype may be achieved in three basic forms: a) geometric similarity, b) kinematic similarity, and c) dynamic similarity (Chow, 1959). All similitude nomenclature is defined in the nomenclature tables starting on page xi.

BROKEN-BACK CULVERT SIMILARITIES

a. Geometric similarity implies similarity of physical form. The model is a geometric reduction of the prototype and is accomplished by maintaining a fixed ratio for

all homologous lengths between the physical quantities involved in geometric similarity: length (L), area (A), and volume (Vol). To keep the homologous lengths in the prototype (p) and the model (m) at a constant ratio (r), they may be expressed as:

$$\frac{L_p}{L_m} = L_r \tag{3}$$

An area (A), is the product of two homologous lengths; hence, the ratio of the homologous area is also a constant given as:

$$\frac{A_p}{A_m} = \frac{L_p^2}{L_m^2} = L_r^2 \tag{4}$$

A volume (Vol.) is the product of three homologous lengths; the ratio of the homologous volume can be represented as:

$$\frac{Vol_p}{Vol_m} = \frac{L_p^3}{L_m^3} = L_r^3 \tag{5}$$

b. Kinematic similarity implies similarity of motion. Kinematic similarity between the model and the prototype is attained if the homologous moving particles have the same velocity ratio along geometrically similar paths. This similarity involves the scale of time and length. The ratio of times required for homologous particles to travel homologous distances in a model and prototype is given by:

$$\frac{T_p}{T_m} = T_r \tag{6}$$

The velocity (V) is defined as distance per unit time; thus, the ratio of velocities may be expressed as:

$$\frac{V_p}{V_m} = \frac{\left(L_p / T_p\right)}{\left(L_m / T_m\right)} = \frac{L_r}{T_r} \tag{7}$$

The flow (Q) is expressed as volume per unit time and may be given by:

$$\frac{Q_p}{Q_m} = \frac{\left(L_p^3 / T_p\right)}{\left(L_m^3 / T_m\right)} = \frac{L_r^3}{T_r} \tag{8}$$

c. Dynamic similarity implies similarity in forces involved in motion. In broken-back culverts, inertial force and gravitational (g) force are considered dominant forces in fluid motion. All experiments conformed to the Froude law constraints listed in Table 2.2. The Froude number is defined as:

$$F_r = \frac{\left[V_p / \left(g_p L_p\right)^{1/2}\right]}{\left[V_m / \left(g_m L_m\right)^{1/2}\right]} = 1 \tag{9}$$

Table 2.2 Froude Limitations and current model parameters. (Larson 2004)

Modeling Limitation	Reason	Current Model	Reference
Model/Prototype<1/60	Minimize scale effects	1/20	Rajaratnam et al. 1968
y > 15 mm	Eliminate surface tension	54.1 mm	Husain et al. 1994
V > 230 mm/s	For gravitational waves to occur	701-1981.2 mm/s	Husain et al. 1994
h > 3 mm	Reduce effects of viscous forces	25.4-63.5 mm	Gunal et al. 1996

Continuing on, as g_p and g_m are the same in a model and the prototype, these cancel in Equation 9, yielding:

$$\frac{V_r}{\left(L_r\right)^{1/2}} = 1 \tag{10}$$

$$V_r = \frac{V_p}{V_m} = \left(L_r\right)^{1/2} \tag{11}$$

$$V_p = V_m \left(L_r\right)^{1/2} \tag{12}$$

Using the three similarities, a variable of interest can be extrapolated from the model to the prototype broken-back culvert.

CHAPTER III

EXPERIMENTAL EQUIPMENT DESIGN

3.1 INTRODUCTION

During the initial period of discussion regarding the construction of a scale model representing a 150-feet long broken-back culvert with two barrels of 10 x 10 feet each and a vertical drop of 6 feet, the research group visited the USDA Agricultural Research Service Hydraulic Engineering Research Laboratory in Stillwater, Oklahoma. This was the facility at which testing was done. The group visited with facility personnel and inspected the equipment that would be used to conduct tests including the flow capacity of the system.

3.2 BROKEN-BACK MODEL

The 1 to 20 scale was adopted due to space limitations at the testing facility, and in consideration of the potential need to expand the model depending on where the hydraulic jump occurred. If the hydraulic jump did not form within the model, the smaller scale would leave room to double the length of the culvert. In addition, a lower flow rate would be required during testing if a smaller scale were used.

3.3 SUPPLY WATER TANK AND DOWNSTREAM CHANNEL

The materials considered were wood and Plexiglas®. Plexiglas® was found preferable because it offered visibility as well as durability, and a surface which would more closely simulate the surface being modeled (Figures 3.4 through 3.10). The Manning's roughness value for Plexiglas® is 0.010 which is close to the roughness of finished concrete at 0.012. Half-inch Plexiglas® proved to be sturdy and was thick enough to allow connection hardware to be installed in the edges of the plates. This material also fit well into the proposed scale of 1 to 20, which equated one-half inch in the model to one foot in the prototype. The model was constructed at the test facility. During the course of the test runs, it became apparent that a flow straightener would have to be installed inside the reservoir in order to calm the inlet flow. A sealed plywood divider was constructed with a series of openings covered with coarse mesh (Figure 3.12). Also, a divider wall was placed between the two inlet sections in the reservoir to better ensure equal flow into channels in the culvert barrel.

In addition to the Plexiglas® model of the culvert, a reservoir was constructed upstream of the model to collect and calm the fluid entering the model. The reservoir was constructed with plywood because it was not necessary to observe the behavior of the fluid at that stage (Figure 3.6 and 3.7). Within the reservoir, wing walls at an angle of 60 degrees were constructed to channel flow into the model opening. The base of the wing walls was constructed with plywood and the exposed wing wall models were formed with Plexiglas®. The same design was used for the outlet structure of the culvert.

Friction blocks were mounted in different arrangements on a sheet of Plexiglas® the same width as the barrels, and placed in the barrel. Three friction block shapes were selected: a regular flat faced, a semi-circular faced, and a c-shaped face blocks (Figure 3.9). Sills were located only on the horizontal portion of the model.

Two sections were constructed and added to the model for several experiments. These sections served two purposes. During initial experimentation, it was observed that the original design was under pressure and that a theoretical hydraulic jump would occur above the confines of the existing culvert ceiling. The additional sections were inverted and mounted to the top of the original model making a culvert with 2 barrels 6 inches wide by 12 inches high and the original length of 90 inches (Figure 3.10). Figure 3.11 shows the downstream channel after wingwall made from plywood.

3.4 ACOUSTIC DOPPLER VELOCIMETER (ADV) MOUNT

In order to ensure the ADV unit would not move during a velocity readings resulting in a false motion being recorded as flow a custom mount was constructed (Figure 3.13). As well the ADV unit mounted rode on a set of horizontal rails to enable a velocity reading to be taken easily at most locations. Access holes were cut into the top of the barrel sections to allow for placement of a velocity meter.

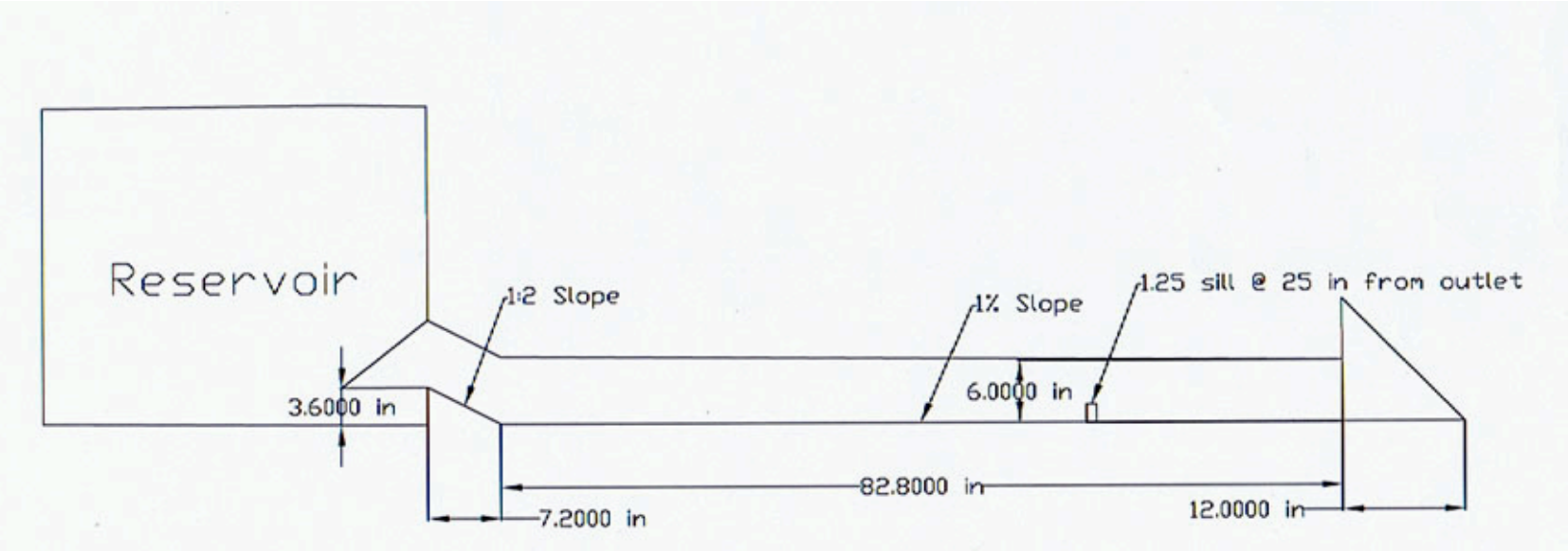

Figure 3.1 Profile view of model at 1:20 scale.

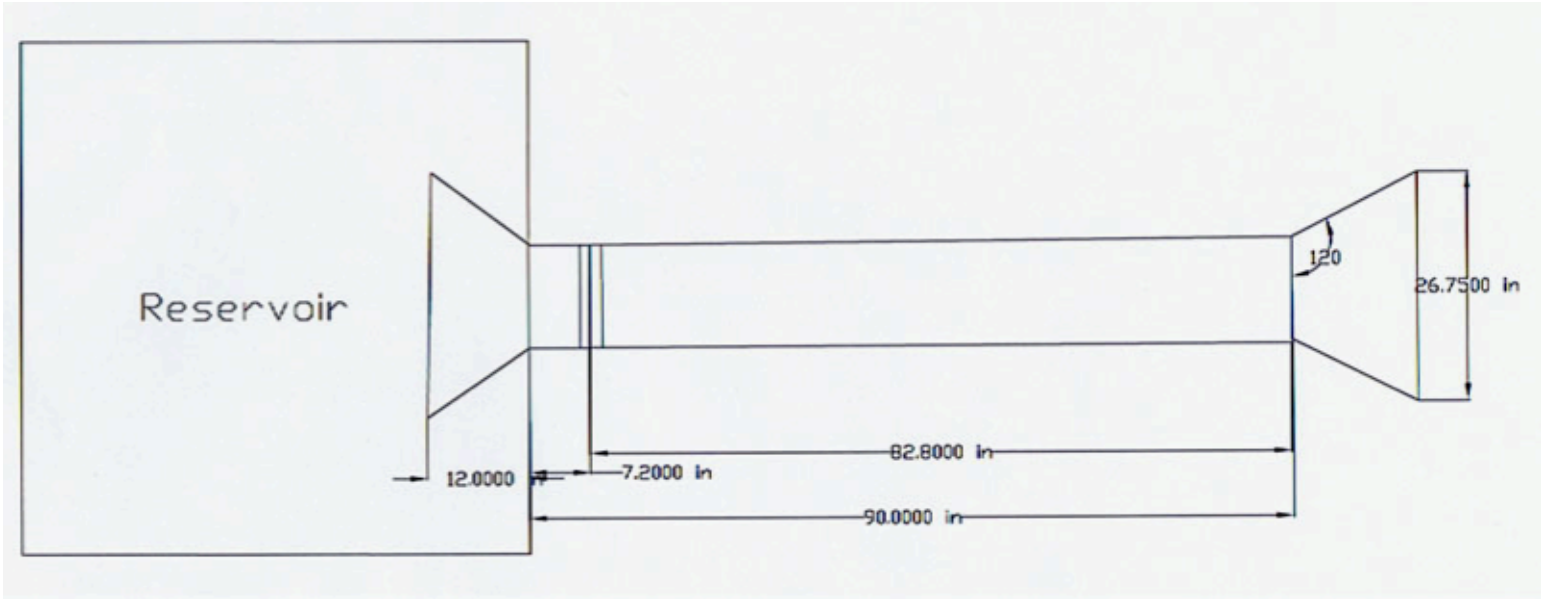

Figure 3.2 Plan view of model at 1:20 scale.

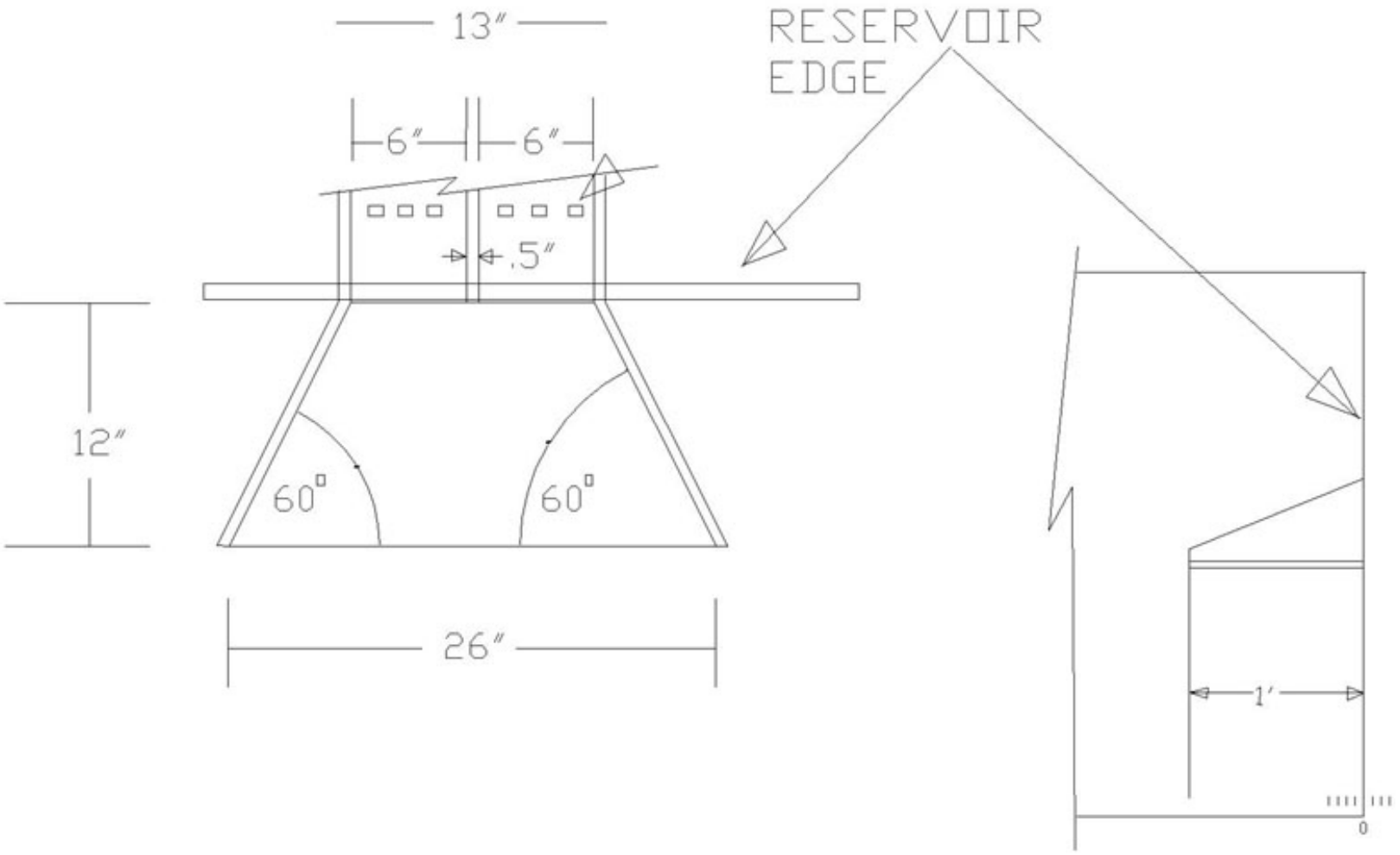

Figure 3.3 Inlet and outlet details.

Figure 3.4 Typical sill dimensions.

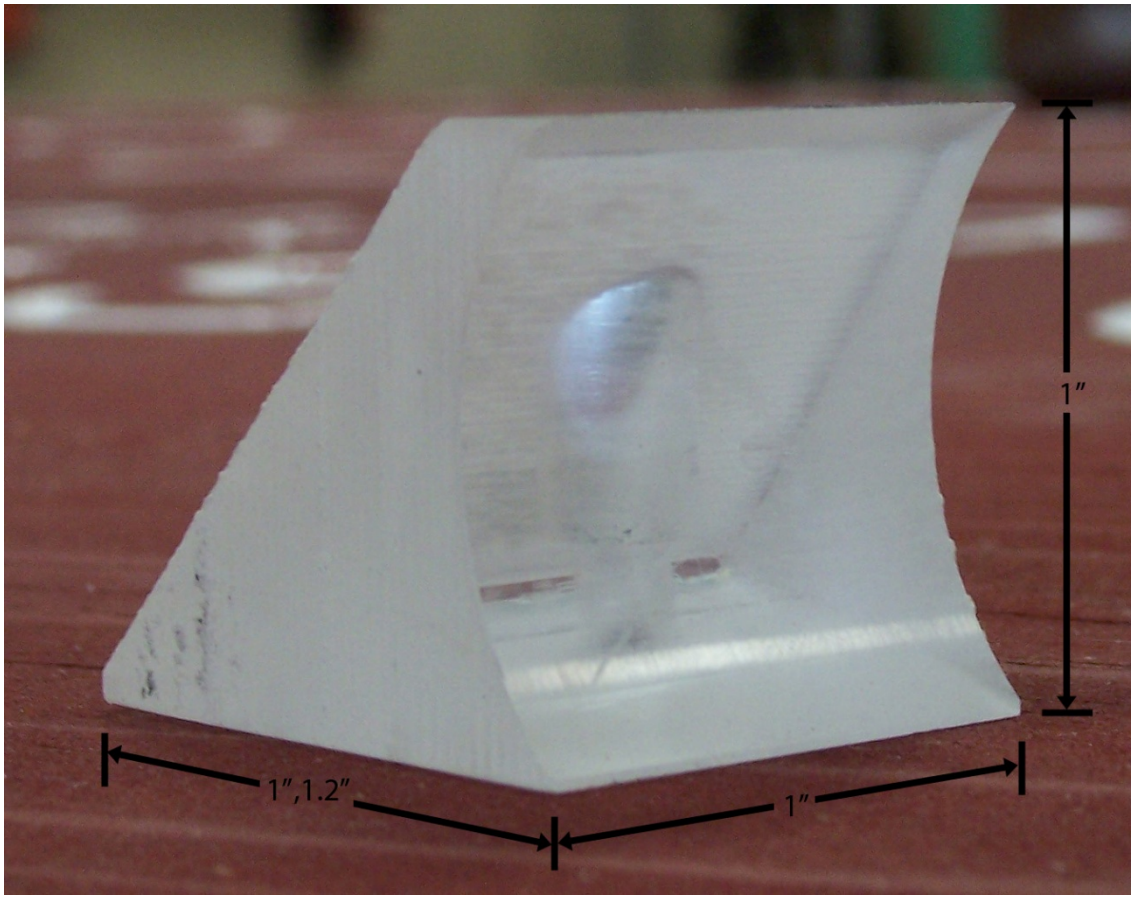

Figure 3.5 Example of friction block.

Figure 3.6 Front view of laboratory model.

Figure 3.7 Side view of laboratory model.

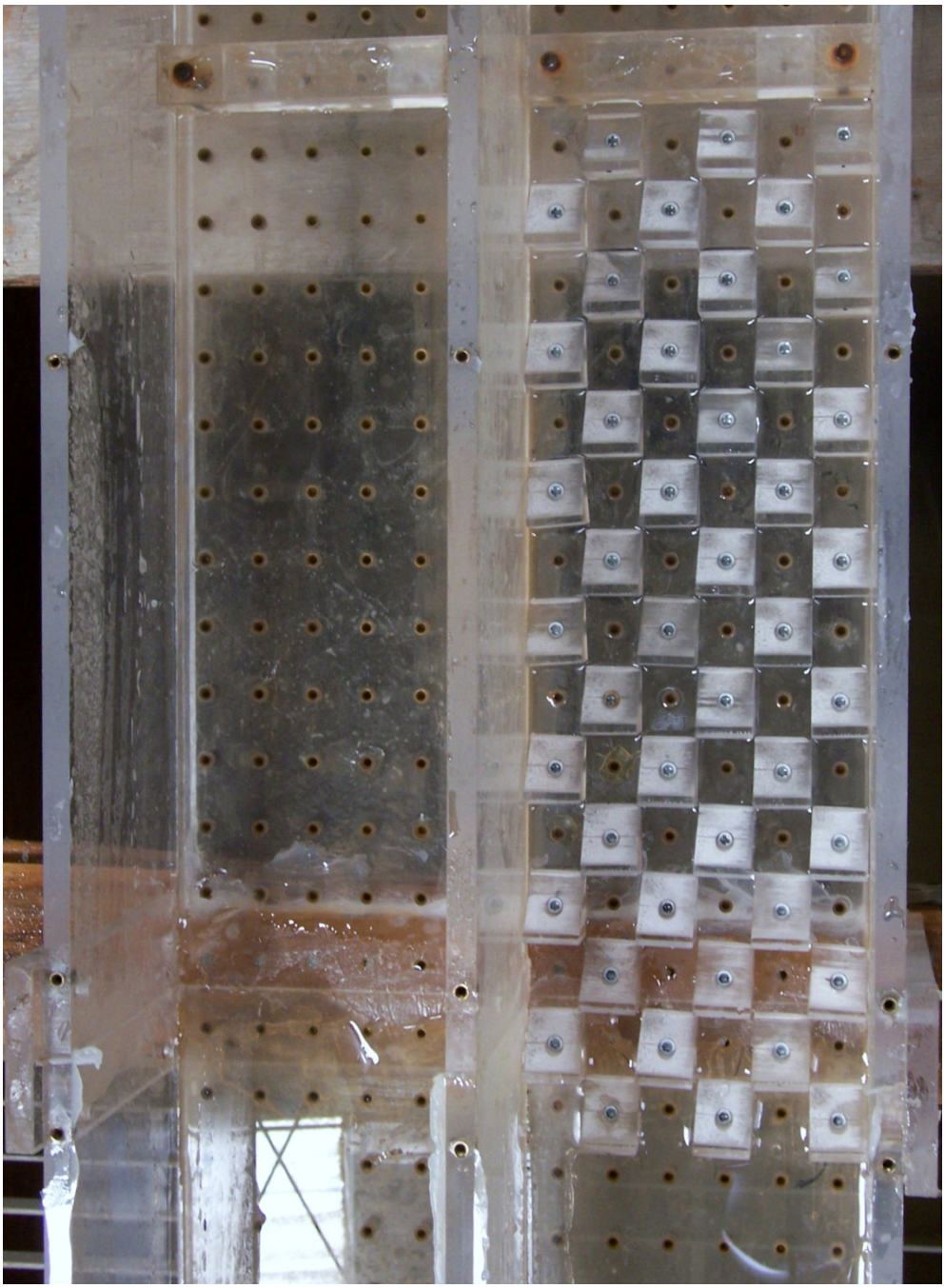

Figure 3.8. Example of flat faced friction blocks arranged on model bottom.

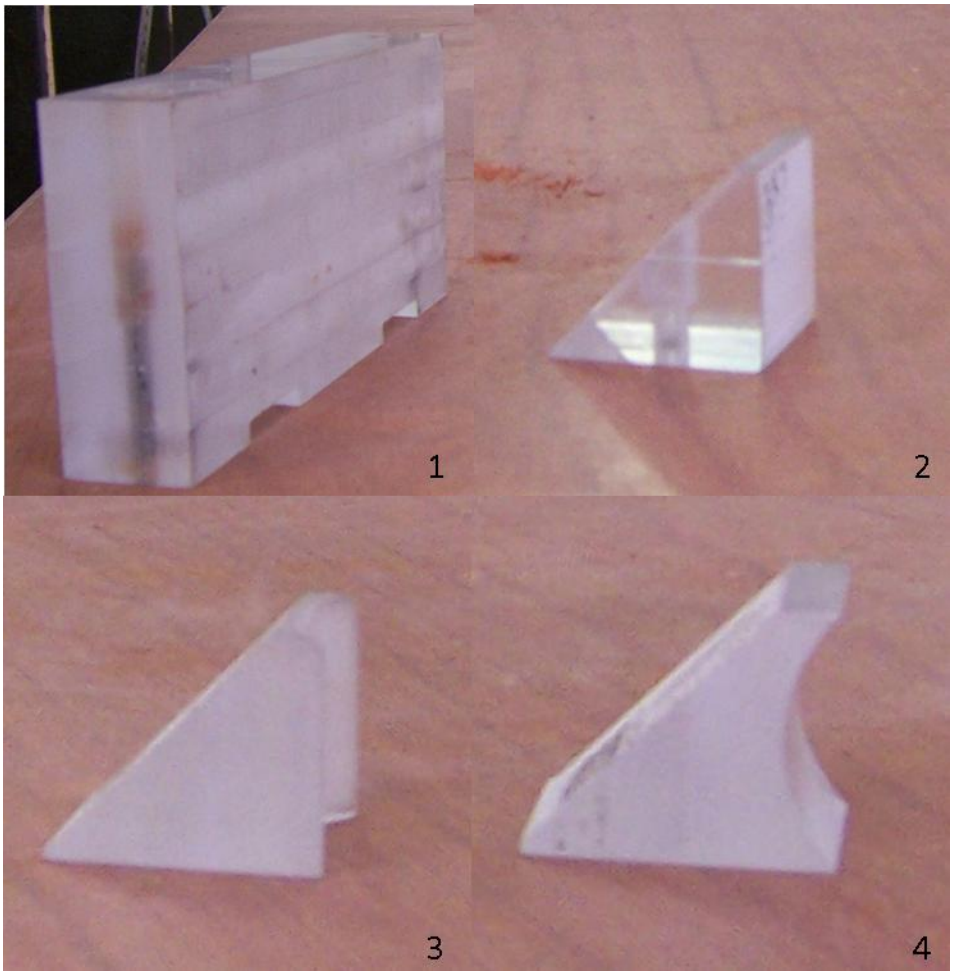

Figure 3.9 Example of friction block shapes and sill. (1. 3” Sill, 2. Regular flat-faced friction block, 3. Semi-circular friction block, 4. C-shaped friction block)

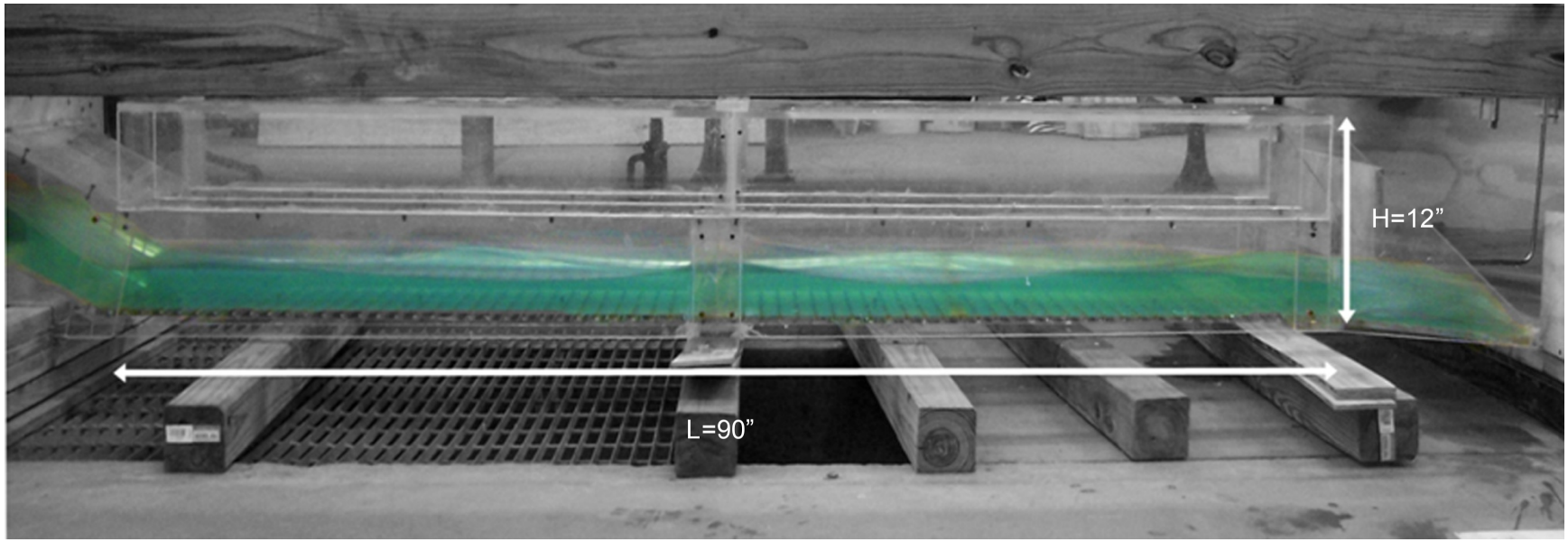

Figure 3.10 Example of extended channel height to apply open channel condition.

Figure 3.11 Downstream plywood channel after wingwall.

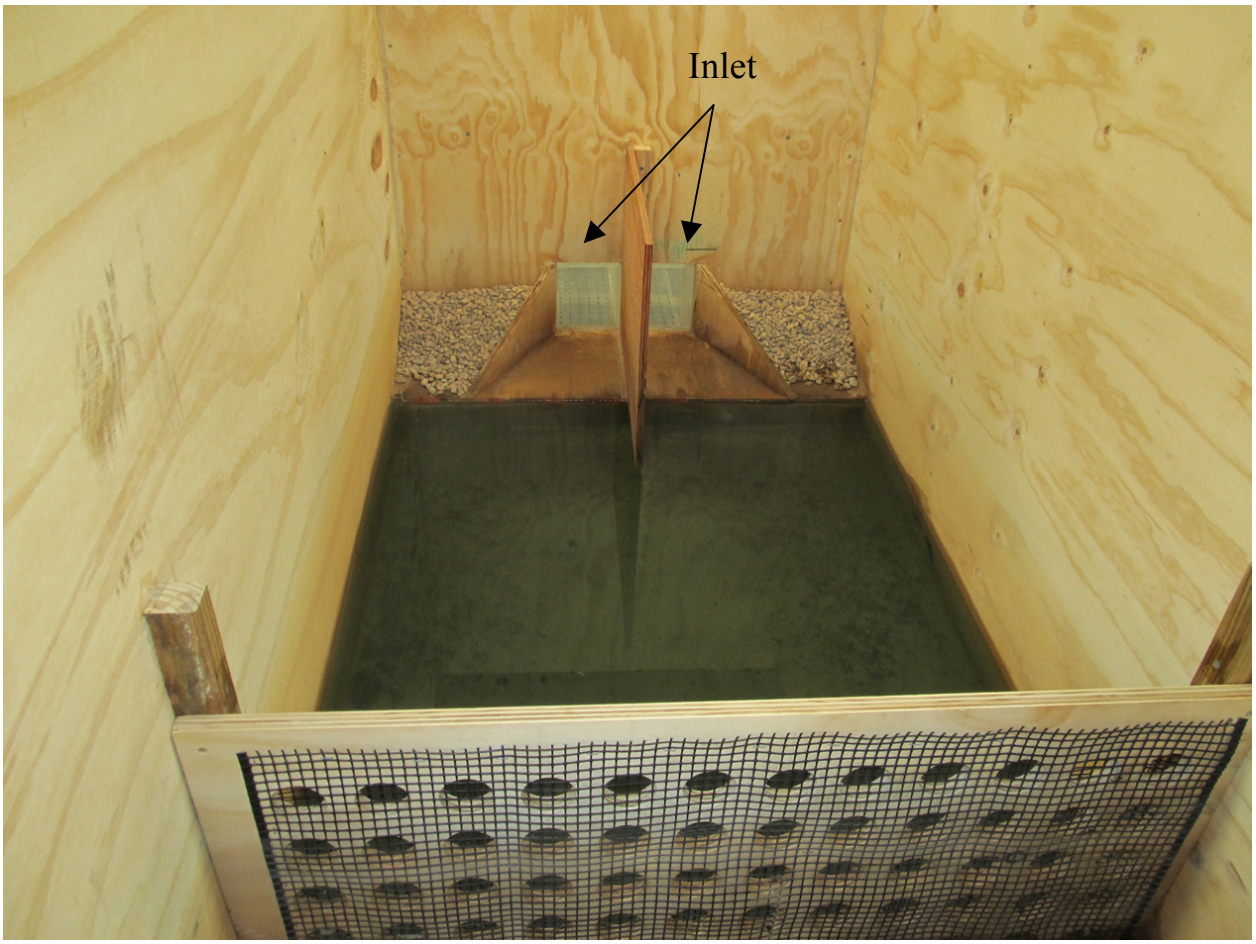

Figure 3.12 Reservoir and channel inlet for culvert model.

Figure 3.13 Acoustic Doppler Velocimeter (ADV) Mount over flume.

CHAPTER IV

TESTING METHODS

4.1 INTRODUCTION

Many experiments were conducted to create energy dissipation within a broken-back culvert. Thirty-two experiments were done for this model with variations in length, height, width, and energy dissipaters used. Each experiment tested three scenarios. They were run with upstream heads of 0.8d, 1.0d, and 1.2d with each depth denoted by A, B, or C, respectively. For example, 8A represents the 8th experiment run at 0.8d, 8B represents the 8th experiment run at 1.0d, and 8C represents the 8th experiment run at 1.2d.

4.2 TEST PROCEDURE

A SonTek 2D-side looking MicroADV sonar velocimeter was used to measure the velocity at the intake of the structure, after the hydraulic jump, and at the downstream end of the culvert. 2D-side looking denotes it has two receiver arms to give readings in the x and y planes. Also, a pitot tube was used to measure velocity at the toe before the hydraulic jump. The flow rates for all experiments were the same. For 0.8d, the flow rate was 1.0 cfs; for 1.0d, the flow rate was 1.3 cfs; and for 1.2d, the flow rate was 1.7 cfs. Also the velocity at the intake of the structure was the same for all experiments. For 0.8d, the velocity was 2.5 fps; for 1.0d, the velocity was 2.7 fps; and for 1.2d the velocity was

2.8 fps.

Experiments 1 through 17 were run on a model with 2 barrels measuring 6 inches by 6 inches in area (existing culverts) and a length of 6.9 feet which represented under pressure flow condition. For Experiments 18 through 32, the height of the culvert was raised to 12 inches (modified culvert) with the original length of 6.9 feet and width of 6 inches which represented the open channel condition. Different configurations of friction blocks, and sills were used in the experiments. All results are shown in Table A1 to A17 for pressure flow experiments and Table A17 to A32 for open channel flow experiments, and selected experiment photos can be seen in Appendix A.

In these experiments, the length of the hydraulic jump (L), the depth before the jump (y_1), the depth after the jump (y_2), the distance from the beginning of the hydraulic jump to the beginning of the sill (X), the depth of the water in the inclined channel (y_s), and the depth of the water downstream of the culvert ($y_{d/s}$) were measured. All dimensions were measured by using a rule and point gage. The flowrate was measured by a orifice plate between which measures the pressure difference in a fixed pipe opening size. A full description of the process of calculating the flowate and detail on the device is in Appendix B. As mentioned above, the velocity before the jump (V_1) was measured by a pitot tube and the velocity at the inlet of structure as seen in Figure 3.12 ($V_{u/s}$), the velocity after the jump (V_2), and the velocity downstream of culvert ($V_{d/s}$) were all measured by ADV.

The procedure of the experiment is as follows:

1. Install energy dissipation (such as sills and/or friction blocks) in the model

2. Set point gage to the correct height in the reserve (for example, Experiment 1A means the head equal to 0.8d)
3. Turn on pump in station
4. Adjust valve and coordinate the opening to obtain the amount of head for the experiment
5. Record the reading for flow rate (using a orifice plate connected to a manometer)
6. Run the model for 10 minute before taking measurements (to allow for the flow to establish)
7. Measure Ys, Y1, Y2, L, X, and YD/S, as seen in Figure 13
8. Measure velocities along the channel Vu/s, V1, V2, and VD/S
9. Post process the raw ADV data to determine final velocity values

Post-processing the raw ADV data was essential to maintain data validity. A software program from the Bureau of Reclamation called WinADV was obtained to process the ADV data. The MicroADV was calibrated according to water temperature, salt content, and total suspended solids. The unit was calibrated to the manufacturer's specification for total suspended solids based on desired trace solution water content. At the end of each day of experiments, the reservoir was drained to prevent mold growth, which could affect the suspended solid concentration of the water. If this change in sediment concentration were to occur, it could minimally affect velocity readings.

4.3 BASELINE TESTS

Experiments 1 and 32 were run without any energy dissipation devices or sill in order to evaluate the hydraulic characteristics of the model, including the Froude number and supercritical flow conditions. Experiment 32 utilized an extended flume, which effectively doubled the vertical height. This experiment is also an example of the current field practice to allow the kinetic energy of fluid to be transferred downstream without energy reduction. This experiment did not produce a hydraulic jump. The results can be found in Table 4.1 and 4.2, below. All experiment variables are defined in the nomenclature tables starting on page xi.

Table 4.1 Experiment 1 using Open channel Flow Condition with no sill in the culvert.

H.J.	Run	H	W_{temp}	Q	$V_{u/s}$	Y_s	Y_{toe}	Y_1	Y_2	$Y_{d/s}$	Fr1	V_1	V_2	$V_{d/s}$	L	X	ΔE	THL	E_2/E_1
N	1A	0.8d	-	1.0092	2.500	2.50	2.50	-	-	2.13	2.2343	5.78698	-	6.00533	-	-	-	0.714598	-
N	1B	1.0d	-	1.3145	2.700	2.83	3.37	-	-	2.63	1.9791	5.95147	-	6.419968	-	-	-	0.648387	-
N	1C	1.2d	-	1.7117	2.800	4.13	4.00	-	-	3.13	1.8330	6.00533	-	6.61755	-	-	-	0.970876	-

Table 4.2 Experiment 32 using Open channel Flow Condition with no sill in the extended height culvert.

H.J.	Run	H	W_{temp}	Q	$V_{u/s}$	Y_s	Y_{toe}	Y_1	Y_2	$Y_{d/s}$	Fr1	V_1	V_2	$V_{d/s}$	L	X	ΔE	THL	E_2/E_1
N	32A	0.8d	53.4	0.9852	2.500	2.75	2.38	-	-	2.00	2.3118	5.8423	-	6.0587	-	-	-	0.724625	-
N	32B	1.0d	53.3	1.3444	2.700	2.50	3.25	-	-	2.63	1.9969	5.8971	-	6.34429	-	-	-	0.828382	-
N	32C	1.2d	53.6	1.7348	2.800	3.78	4.00	-	-	3.25	1.8412	6.03208	-	6.444998	-	-	-	1.270870	-

4.4 SILL HEIGHT AND LOCATION SELECTION

Thirty-two experiments were performed in the hydraulic laboratory. These experiments show model runs without friction blocks, the effect of a sill at the end of the

model, and with friction blocks of different shapes as well as the sill. The friction blocks were comprised of three different shapes, including flat-faced friction blocks, semi-circular faced friction blocks, and C-shaped blocks (see Figure 3.8). After the effectiveness was evaluated, the numbers of blocks were varied by 15, 30, and 45.

In these experiments, the optimum sill height was determined first, the optimum sill location was found next, and finally the effectiveness of friction blocks in combination with the optimum sill parameters was determined.

CHAPTER V

RESULTS

5.1 OVERVIEW OF RESULTS

Eight experiments were selected from thirty-two experiments performed in the hydraulic laboratory. These eight experiments were chosen based the following criteria; (a) All flow conditions (A, B and C) produced a hydraulic jump and (b) There were no drowned hydraulic jumps in any of flow conditions. These experiments show model runs without friction blocks, the effect of a sill at the end of the model, and with friction blocks of different shapes as well as the sill. The friction blocks were comprised of three different shapes, including flat-faced friction blocks, semi-circular faced friction blocks, and C-shaped blocks (see Figure 3.9). After the effectiveness was evaluated, the numbers of blocks were varied by 15, 30, and 45.

In these experiments, the optimum sill height was determined first, the optimum sill location was found next, and finally the effectiveness of friction blocks in combination with the optimum sill parameters was determined. Weir heights were selected to test a full range of jumps. Non-Submerged or incomplete jumps, complete jumps, and standing waves were all observed.

5.2 HYDRAULIC JUMP VALIDATION

Momentum at the outlet, Froude number and reduction in velocity were used to

determine jump effectiveness. Recall that Chow (1959) stated that a hydraulic jump will form in a channel if either of the following two conditions occurs: (1) the momentum in the tailwater downstream from the culvert exceeds that in the barrel, or (2) the supercritical Froude number in the barrel is reduced to approximately 1.7 in a decelerating flow environment (Chow, 1959).

The specific momentum function was used to find the approach and outlet momenta:

$$M_1 = \beta_1 \rho_1 Q V_1 \quad (13)$$

$$M_2 = \beta_2 \rho_2 Q V_2 \quad (14)$$

by assuming uniform velocity distributions at section (1) and (2) (i.e. $\beta_1 = \beta_2 = 1$), continuity, $V_1 = Q/A_1$ and $V_2 = Q/A_2$ and substituting the area function for a rectangular section. The momentum equation reduces to

$$M = \frac{q^2}{g*y} + \frac{y^2}{2} \quad (15)$$

where M is the specific momentum and y is the flow depth. The approach momentum exceeded the outlet or tailwater momentum in every experiment, which formed a hydraulic jump (Figure 5.1).

Next in a hydraulic jump the downstream velocity is always reduced compare to approach. The velocity change is compared to the approach velocity is shown in Figure 5.2.

$$V_1 - V_2 = \Delta V \quad (16)$$

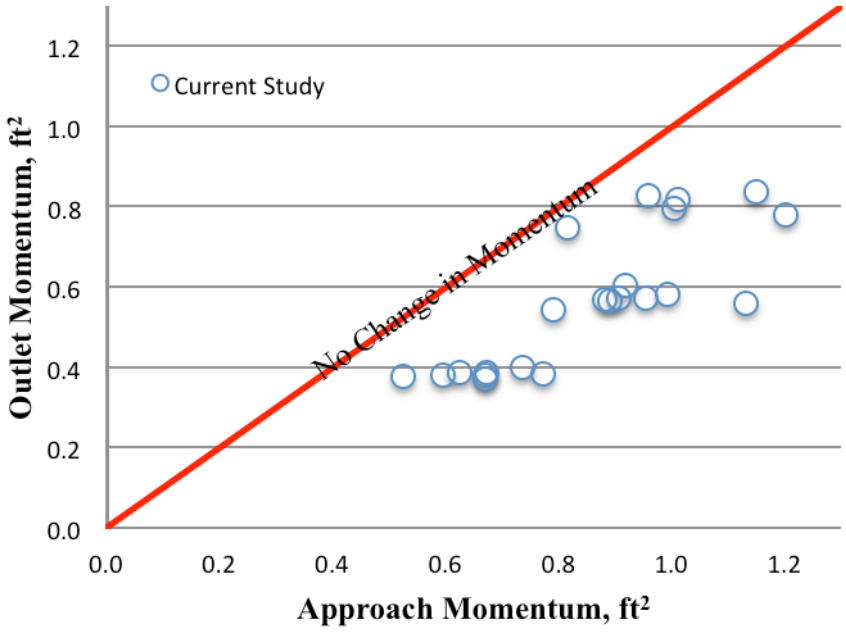

Figure 5.1 Outlet momentum versus Inlet momentum.

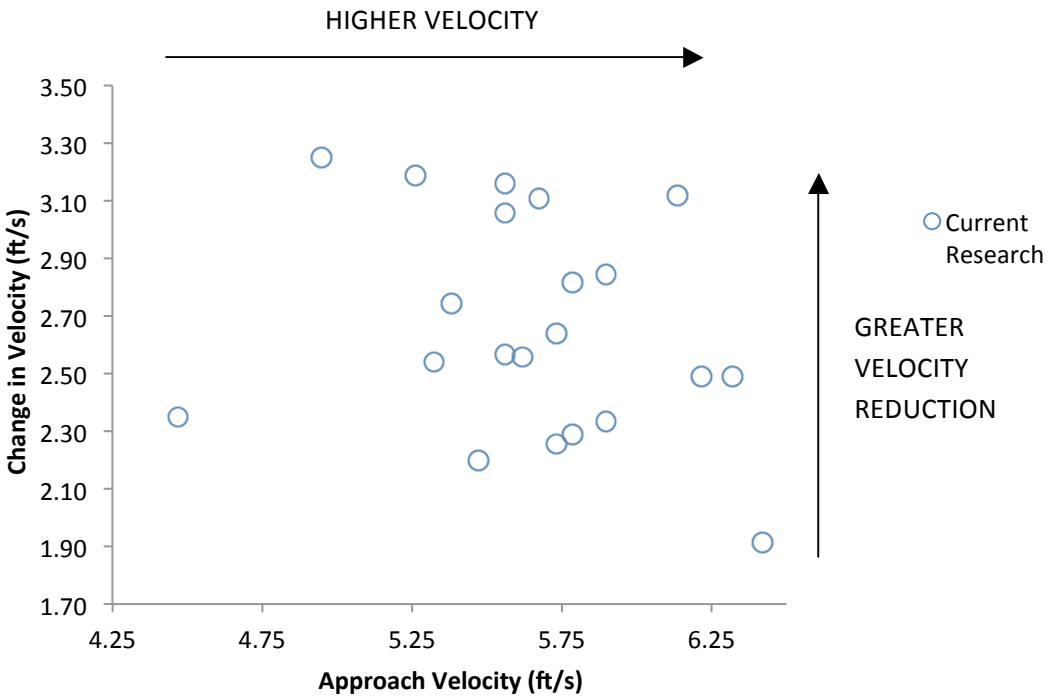

Figure 5.2 Change in velocity vs. approach velocity.

where V_1 is the approach or supercritical flow velocity and the V_2 is the tailwater or subcritical flow velocity. As shown in Figure 5.2, the majority of the experiments collect toward the maxima of greatest inlet velocity and lowest outlet velocity. The spread in data is a result of variants of hydraulic jump strength produced as a property of weir height and location.

The current weir data were compared with the trend lines from Forester and Skrinde (1950) in Figure 5.3. Forester and Skrinde (1950) recommend that jump length (X) be five times the jump depth. For a given approach Froude number and h/y_1 value, the Forester and Skrinde data. They recommended that the distance between the slope break and the weir equal the jump length:

$$L = 5 * y_2 \qquad (17)$$

where L is the distance from the jump toe to the weir and y_2 is the sequent depth for a classic hydraulic jump. Forester and Skrinde (1950) found the minimum weir height that creates a jump terminating at the weir:

$$h = y_1(0.0331Fr_1 + 0.4385Fr_2 - 0.6534) \qquad (18)$$

where h is the weir height, y_1 is the approach flow depth, and Fr_1 is the approach Froude number. This is the equation for line "$X/y_2 = 5$" from Figure 5.3. As shown in Figure 5.3 the data collected near the "$X/y_2 = 5$" line suggesting that current research matches Forester and Skrinde (1950) results.

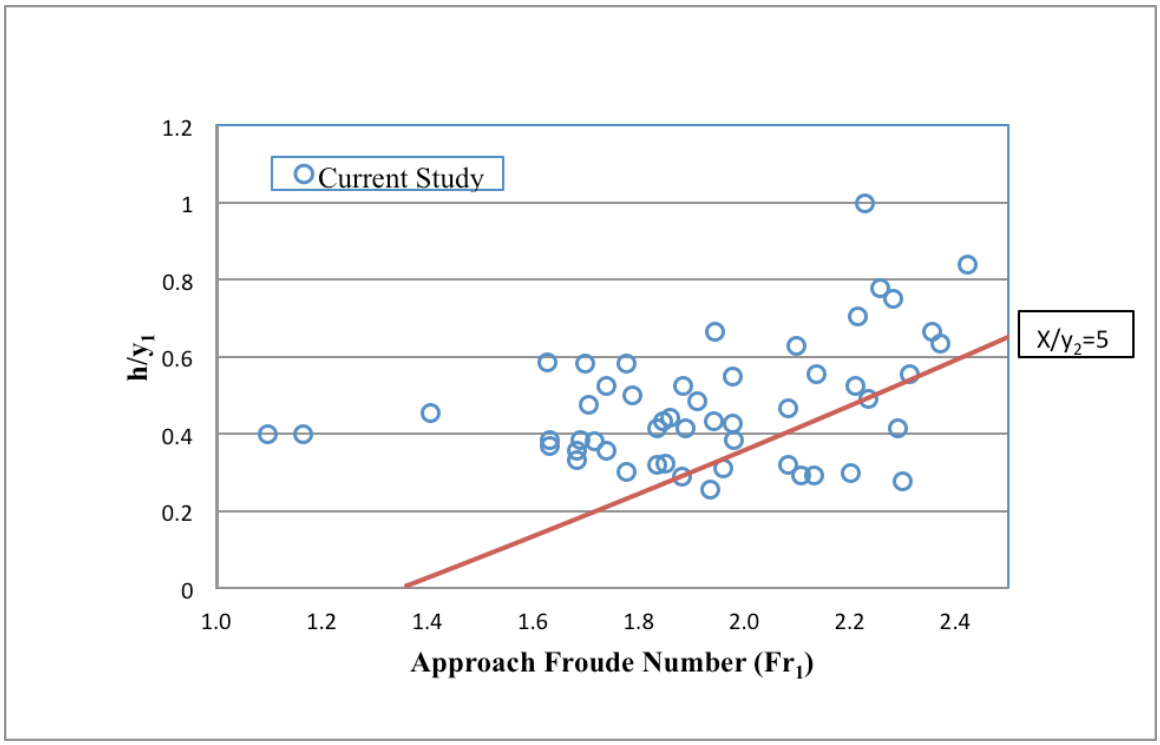

Figure 5.3 Current study data (circles) compared to Forster and Skrinde (1950).

5.3 DATA ANALYSIS

5.3.1 ENERGY DISSIPATION

The loss of energy or energy dissipation in the jump was calculated by taking the difference between the specific energy before the jump and after the jump

$$\Delta E = E_1 - E_2 = \frac{(Y_2 - Y_1)^3}{4Y_1Y_2} \tag{19}$$

The efficiency of the jump was calculated by taking the ratio of the specific energy before and after the jump:

$$\frac{\mathrm{E_2}}{\mathrm{E_1}} = \frac{\left(8\mathrm{Fr_1}^2+1\right)^{3/2} - 4\mathrm{Fr_1}^2+1}{8\mathrm{Fr_1}^2\left(2+\mathrm{Fr_1}^2\right)} \tag{20}$$

If the downstream depth was unknown, the following equation was used to calculate the Froude number (Fr) of the hydraulic jump:

$$F_{r1} = \frac{V_1}{\sqrt{gY_1}} \tag{21}$$

Belanger equation for sequent depth in classical hydraulic jump (free jump);

$$\frac{y_2}{y_1} = \frac{\sqrt{\left(1+8Fr_1^2\right)-1}}{2} \tag{22}$$

The total head loss between upstream of structure and downstream of structure was calculated by applying the Bernoulli equation:

$$THL = \left(H + \frac{V_{u/s}^2}{2g} + Z\right) - \left(Y_{d/s} + \frac{V_{d/s}^2}{2g}\right) \tag{23}$$

where THL is the total head loss between the upstream and downstream ends (inches); H is the water depth upstream of the culvert (inches) and $Z$is drop between upstream and downstream ends of the model equal to 0.3 feet for a 6 foot drop in prototype.

Open channel flow Hydraulic Jumps

Where the downstream depth was known, the following equation was used to calculate the upstream supercritical flow Froude number (Fr) of the hydraulic jump:

$$Fr_1 = \sqrt{\frac{\left(\frac{2Y_2}{Y_1}+1\right)^2 - 1}{8}} \qquad (24)$$

Pressure flow Hydraulic Jumps

Pressure flow hydraulic jumps occur when the fluid in the flume exerts pressure against the top. Subsequently, the sequent depth y_2 in these pressure flow jumps cannot be reached because of the confines of the flume. They may be estimated using momentum theory (Lowe, 2008). A listing of incomplete or pressure flow hydraulic jump is below in Table 5.1.

Table 5.1 Pressure flow experiments.

H.J.	Run	H	W_{temp}	Q	$V_{u/s}$	Y_s	Y_{toe}	Y_1	Y_2	$Y_{d/s}$	Fr1	V_1	V_2	$V_{d/s}$	L	X	□E	THL	E_2/E_1
Y	12C	1.2d	50.3	1.6883	2.800	3.88	4.00	3.88	6 (u.p.)	3.75	1.8777	6.05871	-	6.05871	7.00	-	0.10	1.670876	0.929
Y	13B	1.0d	50.5	1.3145	2.700	2.88	2.38	3.13	6 (u.p.)	3.38	2.0348	5.89710	-	5.32316	8.00	-	0.31	-0.321621	0.904
Y	13C	1.2d	50.6	1.7187	2.800	4.25	4.13	4.13	6 (u.p.)	4.25	1.7878	5.95150	-	5.89710	7.00	-	0.07	1.530909	0.942

The nature of the hydraulic jump cannot be accounted for by use of the energy equation, because there is a substantial dissipation of energy owning to the turbulence associated with the jump. However, because momentum is conserved across hydraulic jumps under assumptions discuss later, momentum theory may be applied to determine the jump size and location (Hotchkiss et al. 2003). Momentum theory states that the sum

of the external forces acting upon a system equals the change in momentum across that system (Thompson and Kilgore 2006). This principle can successfully be applied to complete or incomplete hydraulic jumps such as those shown in Figure B2-2. According to this figure, and using an axis parallel to the channel, a one-dimensional form of the momentum equation may be written:

$$P_1 - P_2 + W \sin\phi - F_f = M_2 - M_1 \qquad (25)$$

where P_1 and P_2 are the pressure forces (lbs, N) at sections (1) and (2), respectively; W is the weight (lbs, N) of the fluid within the control volume; ϕ is the bed slope angle (degrees) from the horizontal; F_f is the force of friction (lbs, N) caused by the channel or conduit; and M_1 and M_2 are the momentum fluxes (lbs, N) at sections (1) and (2), respectively.

A complete derivation of momentum theory of incomplete hydraulic jumps can be reviewed in Appendix B; the following equations are obtained for sequent depth of incomplete jumps (Lowe, 2008):

$$y'_2 = \frac{1}{2} + \left(Fr_1^2 + \frac{1}{2}\right)(y'_1)^2 - Fr_1^2(y'_1)^3 \qquad (26)$$

The dimensionless form of the sequent depth;

$$y'_2 = y_2/D \qquad (27)$$

The following method used to obtain sequent depths y_2 (Lowe 2008), for experiments in Table 5.1;

Step 1: Calculate dimensionless upstream depth

$$y'_1 = \frac{y_1}{D} \tag{28}$$

Step 2: Calculate upstream Froude number

$$F_{r1} = \frac{V_1}{\sqrt{g y_1}} \tag{29}$$

Step 3: Calculate downstream depth (y_2)

$$y'_2 = \frac{1}{2} + \left(Fr_1{}^2 + \frac{1}{2}\right) y'_1{}^2 - Fr_1{}^2 y'_1{}^3 \tag{30}$$

$$y_2 = y'_2 * D$$

Once the sequent depth is known, a new Froude number can be calculated for calculated y_2;

$$Fr'_1 = \sqrt{\frac{\left(\frac{2y_2}{y_1}+1\right)^2 - 1}{8}} \tag{31}$$

The efficiency of the jump can be calculated using this new Froude number (Chow, 1959);

$$\frac{E_2}{E_1} = \frac{\left(8Fr'_1{}^2+1\right)^{3/2} - 4Fr'_1{}^2 + 1}{8Fr_1{}^2\left(2+Fr'_1{}^2\right)} \tag{32}$$

The sequent depths and jump efficiencies were calculated for all incomplete or pressure flow jumps, the results are listed in Table 5.2. The jump efficiencies are higher for the calculated deeper sequent depths. This results because the differences between the approach and outlet specific energies widen.

Table 5.2 Incomplete jump experiments compared observed and calculated sequent depths.

	Experiment 12C For 1.0d	**Experiment 13B For 1.0d**	**Experiment 13C For 1.2d**
Observed y_2	6 in. (U.P.)	6 in. (U.P.)	6 in. (U.P.)
E_2/E_1	0.929	0.904	0.942
Calculated y_2	7.38 in.	7.05 in.	7.25 in.
E'_2/E'_1	0.959	0.920	0.979

5.3.2 SELECT EXPERIMENTS

Experiment 2 was run with one 1.25-inch sill located 25 inches from the end of the culvert. Experiment 2 demonstrates the use of one sill to control the hydraulic jump under open channel and pressure flow conditions. When the fluid in flume exerts pressure against the top of the model it's defined as Pressure Flow. A hydraulic jump was observed in all three flow conditions. The results show that the Froude number values ranged from 1.8 to 2.3. These ranges of Froude number values are indicative of a weak hydraulic jump. The energy dissipation due to hydraulic jump ranges between 0.1 inches to 0.26 inches and the total head loss for the whole culvert ranges between 1.89 inches to 2.38 inches. Additional results can be seen in Table 5.3.

Table 5.3 Experiment 2 using Pressure Flow Condition with a 1.25 inch sill at 25 inches from the end of the culvert.

H.J.	Run	H	W_{temp}	Q	$V_{u/s}$	Y_s	Y_{toe}	Y_1	Y_2	$Y_{d/s}$	Fr1	V_1	V_2	$V_{d/s}$	L	X	ΔE	THL	E_2/E_1
Y	2A	0.8d	-	0.9893	2.500	2.50	2.40	2.55	4.90	2.90	2.2123	5.78688 P-tube	-	4.88139 P-tube	5.00	-	0.26	2.224602	0.874
Y	2B	1.0d	-	1.3853	2.700	2.88	3.38	3.25	5.90	3.25	2.0153	5.95147 P-tube	-	5.58874 P-tube	4.00	-	0.24	1.888382	0.907
Y	2C	1.2d	-	1.6930	2.800	4.25	4.00	3.90	6.00	3.40	1.8729	6.05871 P-tube	-	5.89712 P-tube	4.50	-	0.10	2.380865	0.929

Experiment 11 was run with one 1.25-inch sill located 25 inches from the end of the culvert. In addition, 15 flat faced friction blocks were placed in the horizontal portion of the channel in the pattern as shown in Figure 3.8. Experiment 11 demonstrates the use of one sill to control the hydraulic jump under open channel and pressure flow conditions. Pressure flow is defined by the fluid excreting pressure against the top of the model. A hydraulic jump was observed in all three flow conditions. The results show that the Froude number values ranged from 1.8 to 2.0. These ranges of Froude number values are indicative of a weak hydraulic jump. The energy dissipation due to hydraulic jump ranges between 0.02 inches to 0.13 inches and the total head loss for the whole culvert ranges between 1.3 inches to 2.9 inches. Additional results can be seen in Table 5.4.

Table 5.4 Experiment 11 using Pressure Flow Condition with a 1.25 inch sill 25 inches from the end of the culvert and 15 flat-faced friction blocks in front of the sill.

H.J.	Run	H	W_{temp}	Q	$V_{u/s}$	Y_s	Y_{toe}	Y_1	Y_2	$Y_{d/s}$	Fr1	V_1	V_2	$V_{d/s}$	L	X	ΔE	THL	E_2/E_1
Y	11A	0.8d	49.3	0.9893	2.500	2.75	2.38	3.00	5.00	2.50	2.0199	5.73100	-	4.67932	5.75	-	0.13	2.984590	0.906
Y (?)	11B	1.0d	49.7	1.3205	2.700	2.75	3.50	3.50	5.00	3.00	1.9243	5.89710	-	5.73097	4.50	-	0.05	-1.161615	0.921
Y (?)	11C	1.2d	49.8	1.7302	2.800	4.25	4.00	4.25	5.38	4.00	1.7624	5.95150	-	6.11163	4.00	-	0.02	1.300866	0.946

Experiment 12 was run with one 1.25-inch sill located 25 inches from the end of the culvert. In addition, 30 flat faced friction blocks were placed in the horizontal portion of the channel in the pattern as shown in Figure 3.8. Experiment 12 demonstrates the use of one sill to control the hydraulic jump under open channel and pressure flow

conditions. Pressure flow is defined by the fluid excreting pressure against the top of the model. A hydraulic jump was observed in all three flow conditions. The results show that the Froude number values ranged from 1.8 to 2.5. These ranges of Froude number values are indicative of a weak hydraulic jump. The energy dissipation due to hydraulic jump ranges between 0.03 inches to 0.97 inches and the total head loss for the whole culvert ranges between 1.67 inches to 3.10 inches. Additional results can be seen in Table 5.5.

Table 5.5 Experiment 12 using Pressure Flow Condition with a 1.25 inch sill at 25 inches from the end of the culvert with 30 flat-faced friction blocks in front of the sill.

H.J.	Run	H	W_{temp}	Q	$V_{u/s}$	Y_s	Y_{toe}	Y_1	Y_2	$Y_{d/s}$	Fr1	V_1	V_2	$V_{d/s}$	L	X	ΔE	THL	E_2/E_1
Y	12A	0.8d	50.3	0.9812	2.500	2.50	2.38	2.00	5.50	2.50	2.4739	5.73096	-	4.609989	8.00	-	0.97	3.104597	0.829
Y	12B	1.0d	50.4	1.3621	2.700	3.50	3.75	4.13	5.50	3.25	1.8040	6.00533	-	5.3232	3.50	-	0.03	2.428300	0.940
Y	12C	1.2d	50.3	1.6883	2.800	3.88	4.00	3.88	6 (u.p.)	3.75	1.8777	6.05871	-	6.05871	7.00	-	0.10	1.670876	0.929

Experiment 15 was run with a 1.25-inch sill located 25 inches from the downstream end of the culvert. In addition, 30 curved friction blocks were placed in the horizontal portion of the channel in the pattern shown in Figure 3.8. Experiment 15 was chosen for two reasons: (1) a hydraulic jump formed inside the horizontal section of the model for all three flow conditions, and (2) it is an example of the field being under pressure due to the confines of the model. This experiment produced a hydraulic jump for all three conditions. The total head loss ranges between -0.68 inches to 2.24 inches. The results of this experiment are shown in Table 5.6.

Table 5.6 Experiment 15 using Pressure Flow Condition with a 1.25 inch sill at 25 inches from the end of the culvert with 30 curved-face friction blocks in front of the sill.

H.J.	Run	H	W_{temp}	Q	$V_{u/s}$	Y_s	Y_{toe}	Y_1	Y_2	$Y_{d/s}$	Fr1	V_1	V_2	$V_{d/s}$	L	X	ΔE	THL	E_2/E_1
Y	15A	0.8d	48.2	1.0132	2.500	2.50	2.63	2.38	6 (u.p.)	2.88	2.2678	5.73097	-	4.88139	12.00	-	0.83	2.244597	0.864
Y	15B	1.0d	47.0	1.3084	2.700	3.00	3.38	3.50	6 (u.p.)	3.25	1.8701	5.73097	-	5.50164	7.50	-	0.19	-0.681615	0.930
Y	15C	1.2d	47.1	1.7325	2.800	4.38	4.00	4.50	6 (u.p.)	4.25	1.7282	6.00530	-	5.95147	5.00	-	0.03	1.410870	0.951

Experiment 22 was run with a 1.75-inch sill in the middle of the culvert with an increased culvert height of 12 inches. Experiment 22 illustrates the open channel flow condition, the fluid at atmosphere pressure throughout the model, and the use of a single sill at the end to control the hydraulic jump. A hydraulic jump was observed in all three flow conditions. The results show that the Froude number values ranged from 1.7 to 1.9. This range of Froude number values is indicative of a weak type of hydraulic jump. In a weak jump, a series of small rollers develops on the surface of the jump, but the downstream water surface remains smooth (Chow, 1959). The energy dissipation due to the hydraulic jump ranges between 0.64 inches to 0.92 inches and the total head loss for the whole culvert ranges between 1.668 inches to 2.37 inches. Additional results can be seen in Table 5.7.

Table 5.7 Experiment 22 using Open Channel Condition with a 1.75 inch sill at the middle of the culvert.

H.J.	Run	H	W_{temp}	Q	$V_{u/s}$	Y_s	Y_{toe}	Y_1	Y_2	$Y_{d/s}$	Fr1	V_1	V_2	$V_{d/s}$	L	X	ΔE	THL	E_2/E_1
Y	22A	0.8d	56.3	0.9893	2.500	2.63	2.50	2.50	6.38	2.75	2.1289	4.94692	2.40749	4.88139	8.50	38.50	0.92	2.374602	0.888
Y	22B	1.0d	56.8	1.3385	2.700	3.00	3.38	3.50	7.50	3.63	1.8350	5.4428	3.10805	5.50164	12.00	-	0.61	1.688377	0.935
Y	22C	1.2d	57.4	1.6954	2.800	4.36	4.00	4.00	8.36	4.00	1.7970	5.5599	3.0027	5.95147	14.00	-	0.62	1.660870	0.941

Experiment 26 was run with a 1.75-inch sill 25 inches from the end of the culvert with 30 flat faced friction blocks with an increased culvert height of 12 inches. Experiment 26 was chosen to show a single sill located midway in the horizontal barrel with friction blocks under an open channel flow condition. A hydraulic jump was observed in all three flow conditions. The results show that the Froude number values ranged from 1.7 to 2.1. These ranges of Froude number values are indicative of a weak hydraulic jump. The energy dissipation due to the hydraulic jump ranges between 0.89 inches to 0.96 inches and the total head loss for the whole culvert ranges between 2.11 inches to 2.23 inches. Additional results can be seen in Table 5.8.

Table 5.8 Experiment 26 using Open Channel Condition with a 1.75 inch sill at 25 inches from the end of the culvert with 30 flat-faced friction blocks in front of the sill.

H.J.	Run	H	W_{temp}	Q	$V_{u/s}$	Y_s	Y_{toe}	Y_1	Y_2	$Y_{d/s}$	Fr1	V_1	V_2	$V_{d/s}$	L	X	ΔE	THL	E_2/E_1
Y	26A	0.8d	56.8	0.9893	2.473	2.38	2.38	2.38	6.38	2.63	2.2211	5.32316	2.7799	5.011586	14.00	54.00	1.05	2.229808	0.892
Y	26B	1.0d	56.8	1.3296	2.659	3.00	3.50	4.13	7.50	3.38	1.5990	5.6745	3.30877	5.3833	13.00	51.00	0.31	2.137657	0.954
Y	26C	1.2d	57.1	1.7279	2.880	4.38	3.88	4.88	8.38	3.75	1.5274	5.89712	3.20998	5.89712	14.00	48.50	0.26	2.115357	0.963

Experiment 27 was run with one 1.75-inch sill located 25 inches from the end of the culvert. In addition, 45 flat faced friction blocks were placed in the horizontal portion of the channel in the pattern shown in Figure 3.8. A hydraulic jump was observed in all three flow conditions. The results show that the Froude number values ranged from 1.7 to 2.1. These ranges of Froude number values are indicative of a weak hydraulic jump. The energy dissipation due to hydraulic jump ranges between 0.4 inches to 1.1 inches and the total head loss for the whole culvert ranges between 2.11 inches to 2.20 inches. Additional results can be seen in Table 5.9.

Table 5.9 Experiment 27 using Open Channel Condition with a 1.75 inch sill at 25 inches from the end of the culvert with 45 flat-faced friction blocks in front of the sill.

H.J.	Run	H	W_{temp}	Q	$V_{u/s}$	Y_s	Y_{toe}	Y_1	Y_2	$Y_{d/s}$	Fr1	V_1	V_2	$V_{d/s}$	L	X	ΔE	THL	E_2/E_1
Y	27A	0.8d	57.0	0.9893	2.473	2.63	2.38	2.38	6.50	2.75	2.2572	5.3833	2.8934	5.01159	13.00	54.00	1.13	2.109801	0.888
Y	27B	1.0d	57.1	1.3355	2.671	3.00	3.50	3.50	7.38	3.25	1.8103	5.61747	3.49799	5.44280	13.00	52.50	0.57	2.159348	0.935
Y	27C	1.2d	57.2	1.7094	2.849	3.88	4.00	4.38	8.25	3.75	1.6479	5.78688	3.8486	5.84230	14.00	52.25	0.40	2.202360	0.956

Experiment 29 was run with a 1.75-inch sill located 25 inches from the end of the culvert. In addition, 30 curved faced friction blocks were placed in the horizontal portion of the channel in the pattern shown in Figure 3.8. A hydraulic jump was observed in all three flow conditions. The results show that the Froude number values ranged from 1.7 to 1.9. These ranges of Froude number values are indicative of a weak hydraulic jump. The energy dissipation due to the hydraulic jump ranges between 0.88 inches to 0.95 inches and the total head loss for the whole culvert ranges between -0.32 inches to 2.25 inches. Additional results can be seen in Table 5.10.

Table 5.10 Experiment 29 using Open Channel Condition with a 1.75 inch sill at 25 inches from the end of the culvert with 30 curved-face friction blocks in front of the sill.

H.J.	Run	H	W_{temp}	Q	$V_{u/s}$	Y_s	Y_{toe}	Y_1	Y_2	$Y_{d/s}$	Fr1	V_1	V_2	$V_{d/s}$	L	X	ΔE	THL	E_2/E_1
Y	29A	0.8d	59.1	0.9973	2.500	2.38	2.50	2.50	6.50	2.75	2.1633	5.01159	2.53715	4.94692	10.00	56.00	0.98	2.254593	0.882
Y	29B	1.0d	59.7	1.3084	2.700	2.88	3.25	3.25	7.50	3.38	1.9536	5.55986	2.89344	5.32316	12.00	53.00	0.79	-0.321621	0.917
Y	29C	1.2d	59.8	1.7140	2.800	4.13	4.00	4.13	8.38	4.13	1.7530	5.78688	3.10805	5.95147	12.00	49.00	0.55	1.530870	0.947

Experiment 31 was run with one 1.75-inch sill located 25 inches from the end of the culvert and utilized the increased culvert height of 12 inches. In addition, 30 c-shaped friction blocks were placed in the horizontal portion of the channel in the pattern shown in Figure 3.8. A hydraulic jump was observed in all three flow conditions. The results show that the Froude number values ranged from 1.5 to 2.2. These ranges of Froude

number values are indicative of a weak type of hydraulic jump. The energy dissipation due to the hydraulic jump ranges between 0.88 inches to 0.97 inches and the total head loss for the whole culvert ranges between 1.53 inches to 2.37 inches. Additional results can be seen in Table 5.11.

Table 5.11. Experiment 31 using Open Channel Condition with a 1.75 inch sill at 25 inches from the end of the culvert with 15 C-shaped friction blocks in front of the sill.

H.J.	Run	H	W_{temp}	Q	$V_{u/s}$	Y_s	Y_{toe}	Y_1	Y_2	$Y_{d/s}$	Fr1	V_1	V_2	$V_{d/s}$	L	X	ΔE	THL	E_2/E_1
Y	31A	0.8d	60.8	0.9937	2.500	2.63	2.50	2.50	6.50	2.88	2.1633	5.07543	2.77992	4.94690	10.00	55.50	0.98	2.12463	0.882
Y	31B	1.0d	61.1	1.3175	2.700	3.00	3.38	4.00	7.50	3.25	1.6417	5.55986	3.10803	5.35330	11.00	53.00	0.36	2.368418	0.962
Y	31C	1.2d	61.3	1.7302	2.800	4.00	3.88	5.00	8.50	4.25	1.5149	5.75899	3.4047	5.89712	13.50	52.50	0.25	1.530865	0.977

5.4 PRESSURE FLOW RESULTS

After careful evaluation, Experiments 2 and 12 were selected from the data analysis portion for a pressure flow condition. These experiments were selected by examining many factors, including their relativity low downstream velocities (4 to 6 fps), high total hydraulic head losses, and hydraulic jump efficiency. It was found that these experiments yielded results most applicable to modifying existing culverts with the addition of sills and/or friction blocks. Figure 5.4 and Table 5.12 shows characteristics of the hydraulic jump for Experiment 2. Figure 5.5 and Table 5.13 shows characteristics for Experiment 12.

Table 5.12 Selected factors for Experiment 2.

Experiment 2A For 0.8d	**Experiment 2B For 1.0d**	**Experiment 2C For 1.2d**
Y_2 = 4.90 in	Y_2 = 5.90 in	Y_2 = 6.00 in
$V_{d/s}$ = 4.88 fps	$V_{d/s}$ = 5.59 fps	$V_{d/s}$ = 5.90 fps
THL = 2.22 in.	THL = 1.89 in.	THL = 2.38 in.
E_1/E_2 = 0.87	E_1/E_2 = 0.91	E_1/E_2 = 0.93
Channel reduction = none	Channel reduction = none	Channel reduction = none

Table 5.13 Selected factors for Experiment 12.

Experiment 12A For 0.8d	**Experiment 12B For 1.0d**	**Experiment 12C For 1.2d**
Y_2 = 5.5 in	Y_2 = 5.5 in	Y_2 = 6 in (under pressure)
$V_{d/s}$ = 4.61 fps	$V_{d/s}$ = 5.32 fps	$V_{d/s}$ = 6.06 fps
THL = 3.10 inches	THL = 2.43 inches	THL = 1.67 inches
E_1/E_2 = 0.86	E_1/E_2 = 0.93	E_1/E_2 = 0.93
Channel reduction = 24 in (40 ft)	Channel reduction = 12 in (20 ft)	Channel reduction = none

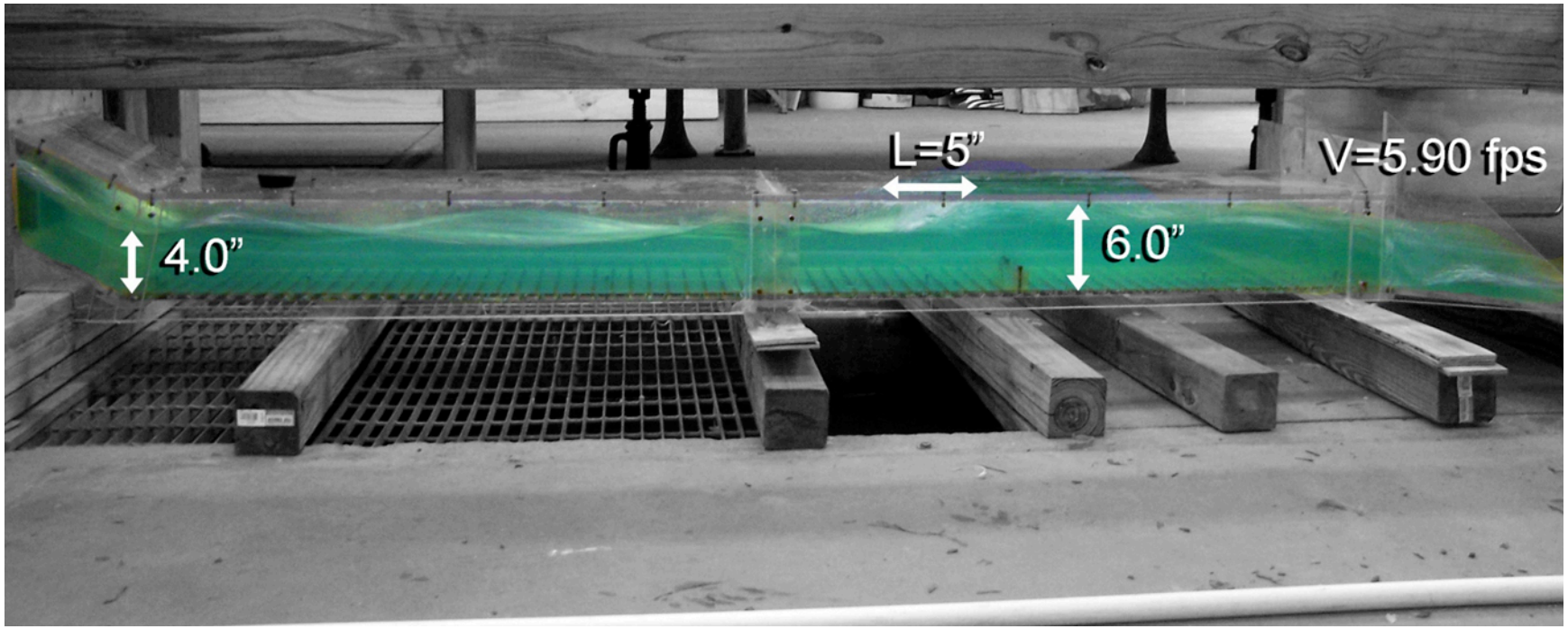

Figure 5.4 Characteristics of hydraulic jump for Experiment 2C under pressure flow condition.

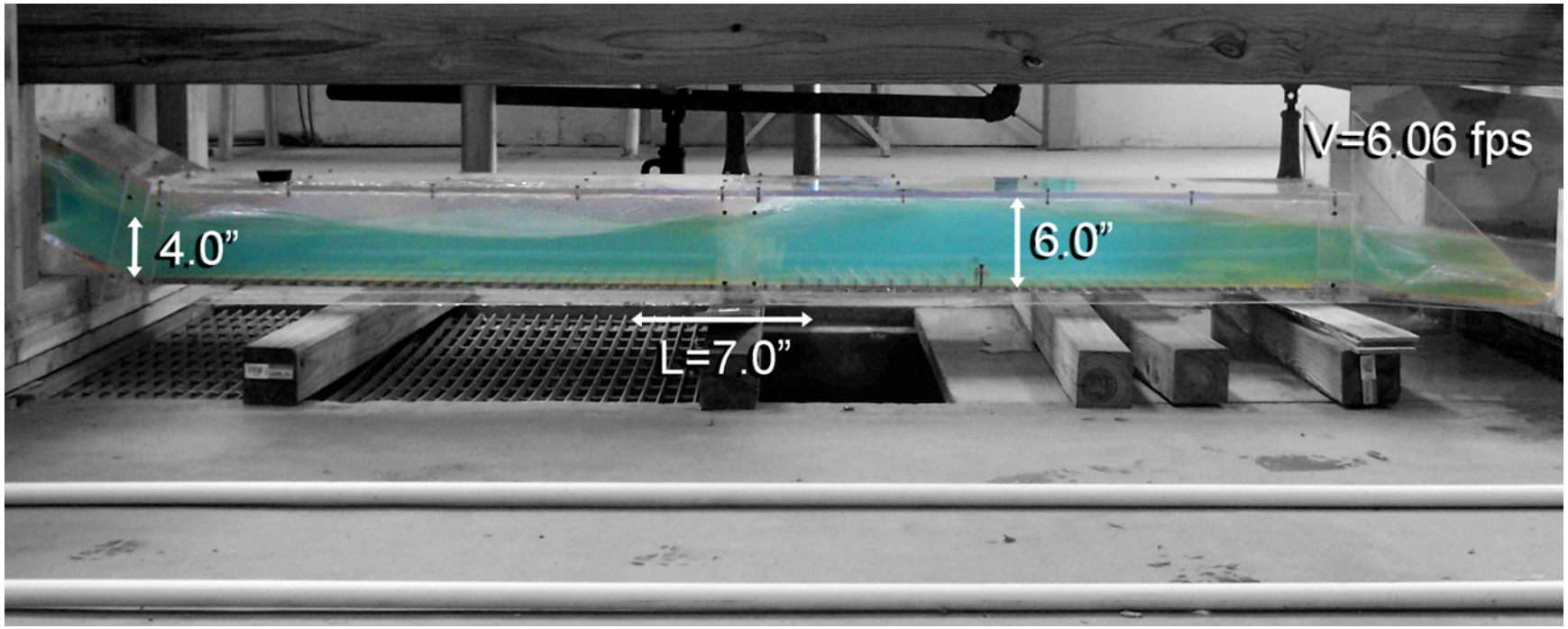

Figure 5.5 Characteristics of hydraulic jump for Experiment 12C under pressure flow condition.

5.5 OPEN CHANNEL RESULTS

After careful evaluation, Experiments 22 and 26 were selected from the data analysis portion for an open channel flow condition. These experiments were selected by examining many factors, including their relativity low downstream velocities, high total hydraulic head losses, acceptable hydraulic jump efficient, and possible reduction in channel length. Experiments 22 and 26 have the similar sill arrangements, with friction blocks added to the horizontal channel barrel in Experiment 31. It was found that these experiments yielded results most applicable to the new construction of culverts due to the increased ceiling height of the culvert. The culvert barrel could be reduced by reducing a section at the end of the channel where the water surface profile is more uniform. Figure 5.6 and Table 5.14 shows characteristics of the hydraulic jump for Experiment 22. Figure 5.7 and Table 5.15 shows characteristics for Experiment 26.

Table 5.14 Selected factors for Experiment 22.

Experiment 22A For 0.8d	**Experiment 22B For 1.0d**	**Experiment 22C For 1.2d**
Y_2 = 6.38 in	Y_2 = 7.5 in	Y_2 = 8.36 in
$V_{d/s}$ = 4.88 fps	$V_{d/s}$ = 5.50 fps	$V_{d/s}$ = 5.95 fps
THL = 2.37 inches	THL = 1.64 inches	THL = 1.66 inches
E_1/E_2 = 0.92	E_1/E_2 = 0.94	E_1/E_2 = 0.96
Channel reduction = 34 in (56.0 ft)	Channel reduction = 34 in (56.0 ft)	Channel reduction = 25 in (42.0 ft)

Table 5.15 Selected factors for Experiment 26.

Experiment 26A For 0.8d	**Experiment 26B For 1.0d**	**Experiment 26C For 1.2d**
Y_2 = 6.38 in	Y_2 = 7.5 in	Y_2 = 8.38 in
$V_{d/s}$ = 5.01 fps	$V_{d/s}$ = 5.38 fps	$V_{d/s}$ = 5.90 fps
THL = 2.23 inches	THL = 2.14 inches	THL = 2.11 inches
E_1/E_2 = 0.89	E_1/E_2 = 0.95	E_1/E_2 = 0.96
Channel reduction = 20 in (33.3 ft)	Channel reduction = 20 in (33.3 ft)	Channel reduction = 12 in (20 ft)

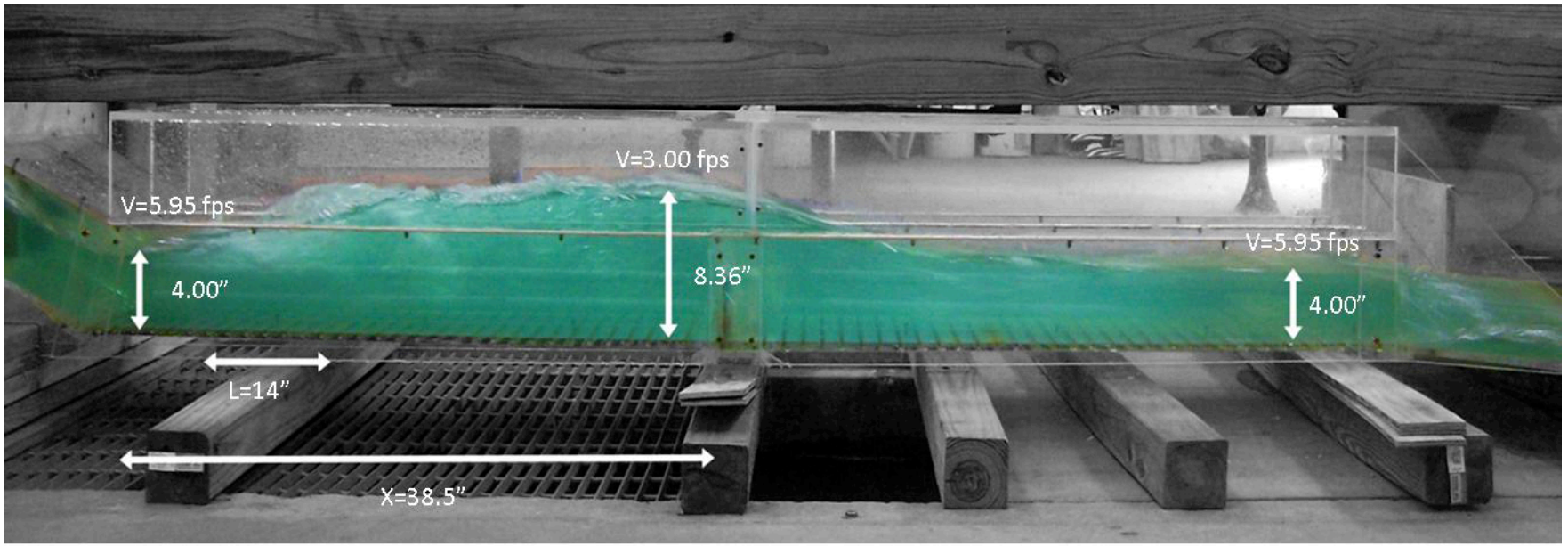

Figure 5.6 Characteristics of hydraulic jump for Experiment 22C under open channel flow condition

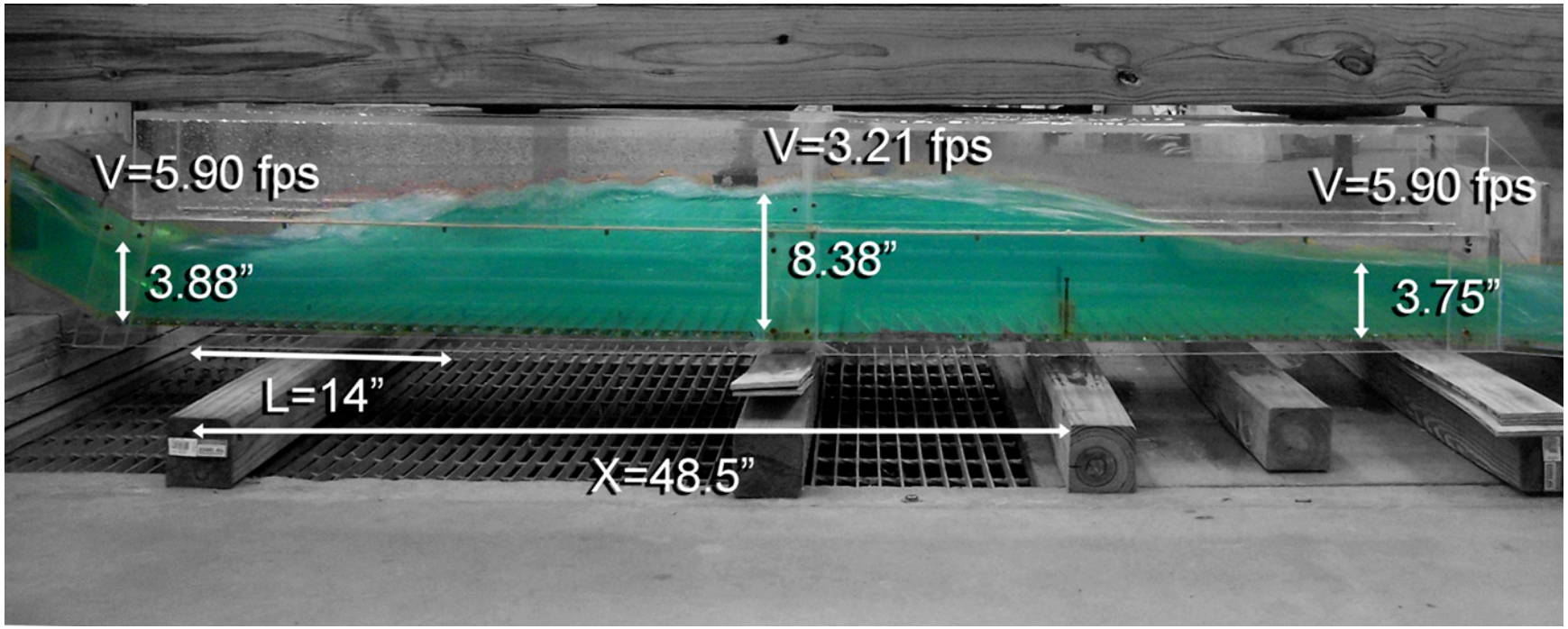

Figure 5.7 Characteristics of hydraulic jump for Experiment 26C under open channel flow condition.

CHAPTER VI

CONCLUSIONS

6.1 OVERVIEW

A laboratory model was constructed to represent a broken-back culvert. The idealized prototype contains a 1 (vertical) to 2 (horizontal) slope, a 12-foot horizontal length of slanted part of culvert continuing down to a 138-foot flat culvert with a 1 percent slope. The model was made to 1:20 scale. The following dimensions are in terms of the prototype culvert. It was noted that the current practice of not using any energy dissipators (as in Experiment 1) allowed all the energy to flow through the culvert instead of reducing or dissipating it.

6.2 GENERAL CONCLUSIONS

The following conclusions can be drawn based on the laboratory experiments for pressure flow conditions and open channel flow conditions:

Pressure Flow Conditions

1. For retrofitting an existing culvert, Experiment 2 is the best option for pressure flow condition. It consists of three flow conditions: 0.8, 1.0 and 1.2 times the

upstream culvert depth of 10 feet. This scenario uses one sill with two small orifices at the bottom, so that water can be completely drained from the culvert. The sill is located 42 feet from the outlet face of the culvert.

2. Optimal placement of one sill, 2.1 ft. (1.25 inches) high, resulted in 91 percent energy dissipation as noted in Experiment 2C.
3. If one sill, 2.1 feet high, and 30 flat faced friction blocks are placed in the flat part of the culvert starting at formation of the hydraulic jump, energy dissipation of 93 percent occurs as noted in Experiment 12C.
4. The reduction of energy due to the region of friction blocks is marginal.
5. Experiment 2 offers similar performance to friction block experiments without the additional cost.
6. For Experiment 2, no reduction in culvert length can be made due to the full flow at the end of the culvert, as can be seen in Table 5.3.
7. For Experiment 12, reduction in culvert length can be made at the end of the culvert for 12A and 12B. No reduction in culvert length can be made for 12C, as can be seen in Table 5.5.

Open Channel Flow Condition

1. For new culvert construction, Experiment 22 is the best option for an open channel flow condition. This option includes one sill with two small orifices at the bottom for draining the culvert completely. The sill is located 69 feet from the end of the culvert. The height of the culvert should be 14 feet to allow open channel condition in the culvert.

2. If one sill 3.0 feet high is placed in the flat part of the culvert, it results in 94 percent of energy loss as seen in Experiment 22C.
3. If one sill 3.0 feet high with 30 flat faced friction blocks are placed in the flat part of the culvert starting at initiation of hydraulic jump, energy dissipation of 96 percent occurs as seen in Experiment 26C.
4. The reduction of energy due to 30 friction blocks is marginal. The optimal 3.0 foot sill is the most economical option.
5. Experiment 22 shows an opportunity to reduce the culvert length at the end in the range of 42 to 56 feet. The 42-foot reduction was determined by eliminating the downstream segment of the culvert where the water surface is no longer uniform after the jump. The 56-foot reduction results from removing a portion of the downstream culvert from the sill to the beginning of the downstream wing-wall section. This option is important if there are problems with the right-of-way.

REFERENCES

Alikhani, A. Behrozi-Red, R. and Fathi-Moghadam, M. (2010). Hydraulic jump in stilling basin with vertical end sill. International Journal of Physical Sciences. 5(1), 25-29. http://www.academicjournals.org/IJPS.

Bhutto, H., Mirani, S. and Chandio, S. (1989). Characteristics of free hydraulic jump in rectangular channel. *Mehran University Research Journal of Engineering and Technology*, 8(2), 34 – 44.

Chadwick, A., Morfett, J., and Borthwick, M. (2004). Hydraulics in Civil and Environmental Engineering, 4th Ed. Spon Press, London.

Chanson, H. (2008). Acoustic Doppler velocimetery (ADV) in the field and in laboratory: practical experiences. *International Meeting on Measurements and Hydraulics of Sewers*, 49-66.

Chanson, H. (2009). Current knowledge in hydraulic jumps and related phenomena. European Journal of Mechanics B/Fluid. 29(2009), 191-210.

Caric, D. M. (1977). "Flow in Circular Conduits." Water Power and Dam Construction, 29(11), 29-33.

Chow, V.T. (1959). Open-channel Hydraulics. McGraw-Hill, New York, NY, 680 pages.

Eloubaidy, A., Al-Baidiani, J., and Ghazali, A. (1999). Dissipation of hydraulic energy by curved baffle Blocks. Pertanika Journal Science Technology. 7 (1), 69-77 (1999).

Federal Highway Administration (2011). The Hydraulic Design of Energy Dissipaters for Culverts and Channels.

Federal Highway Administration (1998). Hydraulic Design of Highway Culverts.

Finnemore, J. E., and Franzini, B. J., (2002) Fluid mechanics with engineering applications. McGraw-Hill, New York, NY, 790.

Forster, J.W. and R.A. Skrinde. (1950) Control of Hydraulic Jump by sills. *Transactions of the American Society of Civil Engineers*, 115, 973-987.

Gary M. Haderlie and Blake P. Tullis (2008) Hydraulics of Multibarrel Culverts under Inlet Control. *Journal Irrigation and Drainage Engineering.* 134, 507; doi:10.1061/(ASCE)0733-9437(2008)134:4(507).

Gharanglk, A. and Chaudhry, M. (1991). Numerical simulation of hydraulic jump. *Journal of Hydraulic Engineering. 117(9),* 1195 – 1211.

Goring, D., Nikora, V. (2002). Despiking ascoustic doppler velocimeter data. *Journal Of Hydraulic Engineering, 128(1),* 117-128.

Gunal, Mustafa and Rangaswami Narayanan. (1996) Hydraulic Jump in Sloping Channels. Journal of Hydraulic Engineering. 122(8): 436-442.

H.Abida and R.D. Townsend (1991) Local Scour Downstream of Box-Culvert outlet. *Journal of Irrigation and Drainage Engineering*, 117 (3), 425-440.

Hager, W. H. (1999). Wastewater Hydraulics. Springer-Verlag, Berlin.

Hager, W.H. and D. Li. (1992) Sill-controlled energy dissipator. *Journal of Hydraulic Research*, 30(2), 165-181.

Haindl, K., and Sotornik, V. (1957). "Quantity of air drawn into a conduit by the hydraulic jump and its measurement by gamma-radiation." Proceedings of the International Association for Hydraulics Research, Vol. 2, Lisbon, Spain, D31.1- D31.7.

Harleman, D. R. F. (1959). "Discussion to Rouse, et al." Transactions of the American Society of Civil Engineers, 124 959-962.

Hotchkiss, R. and Donahoo, K. (2001). Hydraulic design of broken-back culvert. *Urban Drainage Modeling,* American Society of Civil Engineers, 51 – 60.

Hotchkiss, R. and Larson, E. (2005). Simple Methods for Energy Dissipation at Culvert Outlets. *Impact of Global Climate Change*. World Water and Environmental Resources Congress.

Hotchkiss, R., Flanagan, P. and Donahoo, K. (2003). Hydraulic jumps in broken-back culvert. *Transportation Research Record* (1851), 35 – 44.

Hotchkiss, R., Thiele, E., Nelson, J., and Thompson, P. (2008). Culvert Hydraulics: Comparison of Current Computer Models and Recommended Improvements. *Journal of the Transportation Research Board*, No. 2060, Transportation Research Board of the National Academies, Washington, D.C, 2008, pp. 141-149.

Hughes, W. C., and Flack, J. E. (1984). "Hydraulic Jump Properties Over a Rough Bed." Journal of Hydraulic Engineering, 110(12), 1755-1771.

Husain, D., Negm, Abdel-Azim M., and A.A. Alhamid. (1994) Length and depth of hydraulic jump in sloping channels. *Journal of Hydraulic Research.* 32(6): 899-910.

Hydraulic Design of Energy Dissipators for Culverts and Channels Hydraulic Engineering Circular Number 14, Third Edition.

Kalinske, A. A., and Robertson, J. M. (1943). "Closed Conduit Flow." Transactions of the American Society of Civil Engineers, 108 1435-1447.

Kandaswamy, P.K. and H. Rouse. (1957) Characteristics of flow over terminal weirs and sills. *Proceedings of ASCE Journal Hydraulics Division.* 83 (HY4), pp.1345.

Lane, E. W., and Kinsvatar, C. E. (1938). "Hydraulic Jump in Enclosed Conduits." Engineering News-Record, Dec. 29 815-817.

Larson, E. (2004). “Energy dissipation in culverts by forcing a hydraulic jump at the outlet.” M.S. thesis, Washington State University.

Lowe, N.J. (2008) "Theoretical determination of subcritical sequent depths for complete and incomplete hydraulic jumps in closed conduits of any shape." M.S. thesis, Brigham Young Univ. Provo, UT.

Lowe, N.J., Hotchkiss, R.H., and Nelson, E.J. (2011) Theoretical Determination of Sequent Depths in Closed Conduits. *Journal of Irrigation and Drainage Engineering,* 137(12), pp. 801-810.

Montes, S. (1998). *Hydraulics of Open-Channel Flow.* ASCE Press, Reston, VA.

Mignot, E. and Cienfuegos, R. (2010). Energy dissipation and turbulent production in weak hydraulic jumps. *Journal of Hydraulic Engineering*, ASCE, 136 (2), 116-121.

Mori, N. Suzuki, T., and Kakuno, S. (2007). Noise of acoustic doppler velocimeter data in bubbly flows. *Journal of Engineering Mechanics*, *133(1),* 122-125.

Ohtsu I, Yasuda, Y., and Hashiba, H. (1996). Incipient jump conditions for flows over a verticle sill. *Journal of Hydraulic Engineering*, ASCE. 122(8) 465-469. doi: 10.1061/(ASCE)0733-29(1996)122:8(465).

Ohtsu, I et al. (2001). Hydraulic condition for undular jump formation. Journal of Hydraulic Research. 39(2), 203-209. http://cat.inist.fr/?aModele=afficheN&cpsidt=1054107.

Ohtsu, I., Yasuda, Y., Yamanaka, Y. (1991) Drag on vertical sill of forced jump. *Journal of Hydraulic Research.* 29(1), pp. 29-47.

Narayanan, R. and L.S. Schizas. (1980) Force on sill of forced jump. *Proceedings of ASCE Journal Hydraulics Division.* 106(HW4), pp. 15368.

Pagliara, S., Lotti, I., Palermo, M. (2008). Hydraulic jump on rough bed of stream rehabilitation structures. *Journal of Hydro-environment Research* 2(1), 29-38.

Peterka, A. J. (1964) Hydraulic Design of Stilling Basins and Energy Dissipators A Water Resources Technical Publication, Engineering Monograph No. 25. U.S. Department of the Interior and U.S. Bureau of Reclamation.

Rajaratnam, N. and V. Murahari. (1971) A contribution to forced hydraulic jumps. *Journal of Hydraulic Research.* 9(2), pp. 217-240.

Rajaratnam, N. (1964) The Forced Hydraulic Jump. *Water Power* pp. 14-19 and 61-65.

Rajaratnam, N. and Subramany, K. (1968) Hydraulic jumps below abrupt symmetrical expansions. *Proceedings of ASCE Journal Hydraulics Division.* 94(HY2) paper 5860.

Rand, Walter. (1957) An approach to generalized design of stilling basins. The New York Academy of Sciences. pp. 173-191.

Rand, Walter. (1965) Flow over a vertical sill in an open channel. *Proceedings of ASCE Journal Hydraulics Division.* 91(HY4), pp. 4408.

Rand, Walter. (1970) Sill-controlled flow transitions and extent of erosion. *Proceedings of ASCE Journal Hydraulics Division.* 96(HY4), pp. 7212.

Rusch, R. (2008) Personal communication, Oklahoma Department of Transportation.

Sharp, J. J. Hydraulic modeling London; Boston: Butterworths 1981, 242 pgs. 25 cm. TC 163 .S33 Engineering Library OU.

SonTek/YSI, Inc. *ADVField/Hydra System Manual* (2001).

Sturm, T. W. (2001). Open Channel Hydraulics. McGraw-Hill, New York.

Thompson, P. L., and Kilgore, R. T. (2006). "Hydraulic Jump." Hydraulic Engineering Series No. 14, 3rd. Ed. - Hydraulic Design of Energy Dissipators for Culverts and Channels, Federal Highway Administration, Washington, D. C., 6-1 to 6-14.

Tyagi, A. K. and Schwarz, B. (2002). A Prioritizing Methodology for Scour-critical Culverts in Oklahoma. Oklahoma Transportation Center.

Tyagi, A.K. et al., (2010a). Energy Dissipation in Broken-back Culverts under Open Channel Flow Conditions. ASCE International Perspective on Current and Future State of Water Resources, 10.

Tyagi, A.K., Al-Madnhich, A., and Brown, J. (2010b). Energy Dissipation in Broken-back Culverts under Pressure Flow Conditions. J. Hyd. Eng. (submitted for peer review).

Tyagi, A.K., et al., (2009)a, "Laboratory Modeling of Energy Dissipation in Broken-back Culverts – Phase I," Oklahoma Transportation Center, Oklahoma, 82 pp.

Tyagi, A.K., et al., (2009)b, "Laboratory Modeling of Energy Dissipation in Broken-back Culverts – Phase II," Oklahoma Transportation Center, Oklahoma, 84 pp.

Utah Department of Transportation (2004.) *Manual of Instruction – Roadway Drainage and Culverts*.

Varol, F., Cevik, E., and Yuksel, Y. (2009). The effect of water jet on the hydraulic jump. Thirteenth International Water Technology Conference, IWTC. 13 (2009), 895-910, Hurghada, Egypt.

Wahl, T. (2000). Analyzing ADV data using WinADV. *2000 joint water resources engineering and water resources planning and management,* July 30- August 2, 2000-Minneapolis, Minnesota.

Wahl, T. (2003). Discussion of "Despiking acoustic Doppler velocimeter data" by Goring, D. and Nikora, V. *Journal of Hydraulic En*gineering,129(6), 484-487.

Zhu, D. W. (2008). "A study of the techniques of railway bridge and culvert construction in perennially frozen soil zone." M.S. thesis, Tianjin University (People's Republic of China)).

APPENDIX A

LABORATORY DATA OF HYDRAULIC JUMP EXPERIMENTS

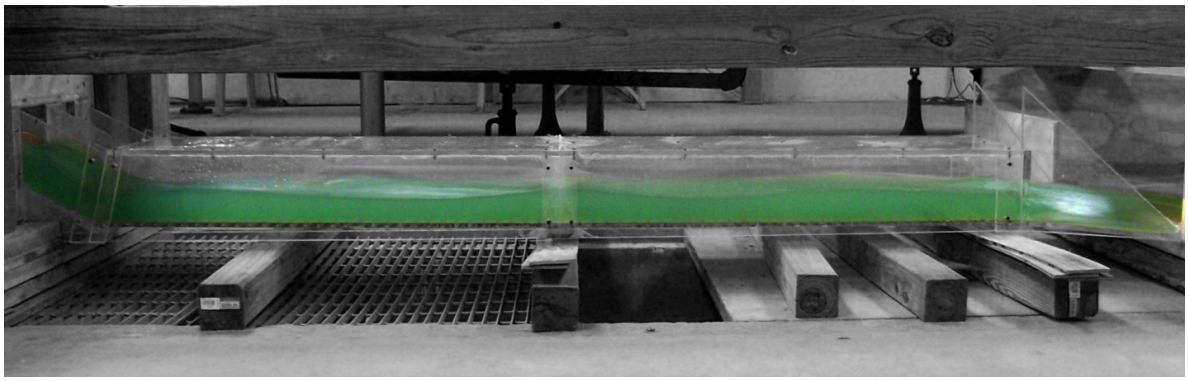

Figure A1. Experiment 1A

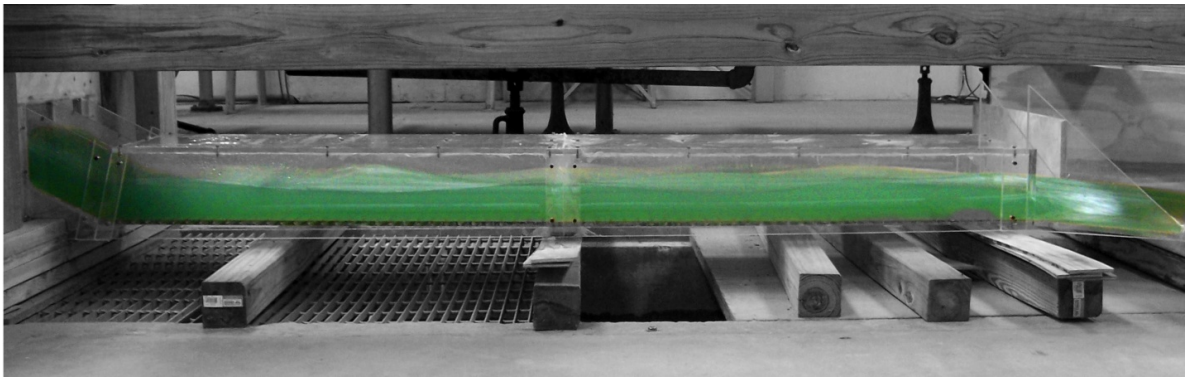

Figure A2. Experiment 1B

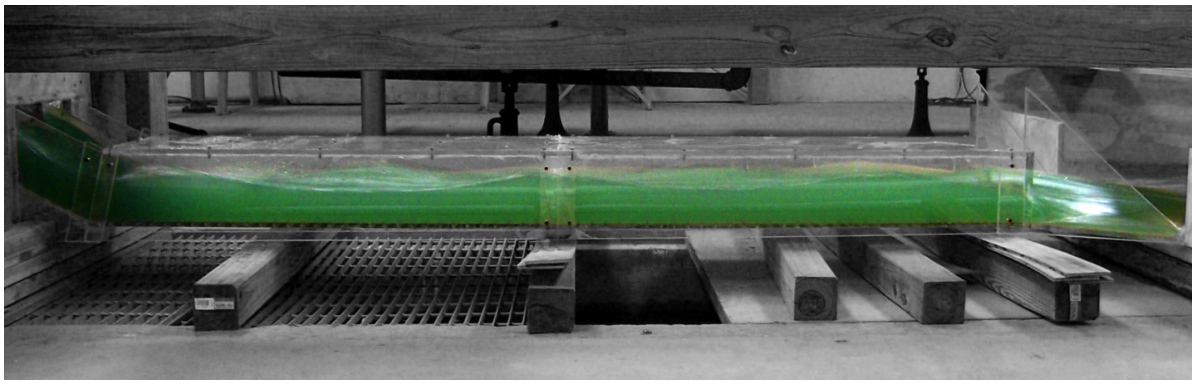

Figure A3. Experiment 1C

Table A1. Experiment 1 using Pressure Flow Condition with no sill in the culvert.

H.J.	Run	H	W_{temp}	Q	$V_{u/s}$	Y_s	Y_{toe}	Y_1	Y_2	$Y_{d/s}$	Fr1	V_1	V_2	$V_{d/s}$	L	X	ΔE	THL	E_2/E_1
N	1A	0.8d	-	1.0092	2.500	2.50	2.50	-	-	2.13	2.2343	5.78698	-	6.00533	-	-	-	0.714598	-
N	1B	1.0d	-	1.3145	2.700	2.83	3.37	-	-	2.63	1.9791	5.95147	-	6.419968	-	-	-	0.648387	-
N	1C	1.2d	-	1.7117	2.800	4.13	4.00	-	-	3.13	1.8330	6.00533	-	6.61755	-	-	-	0.970876	-

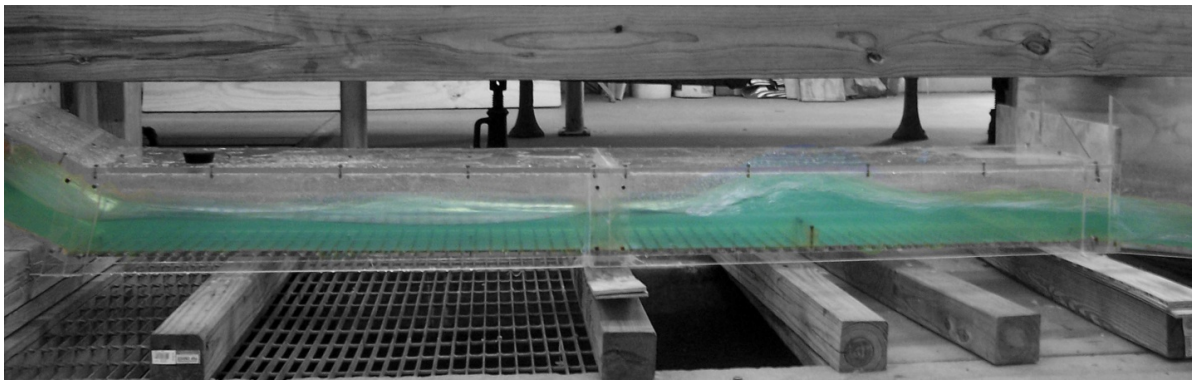

Figure A4. Experiment 2A

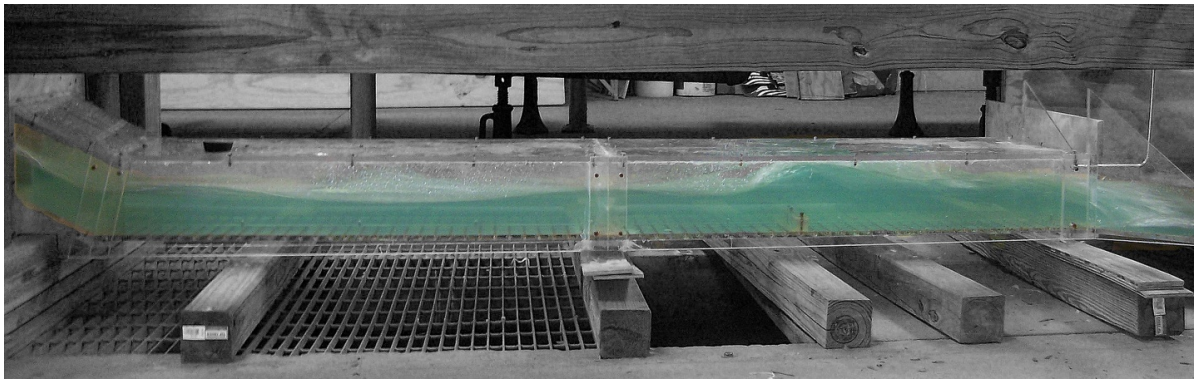

Figure A5. Experiment 2B

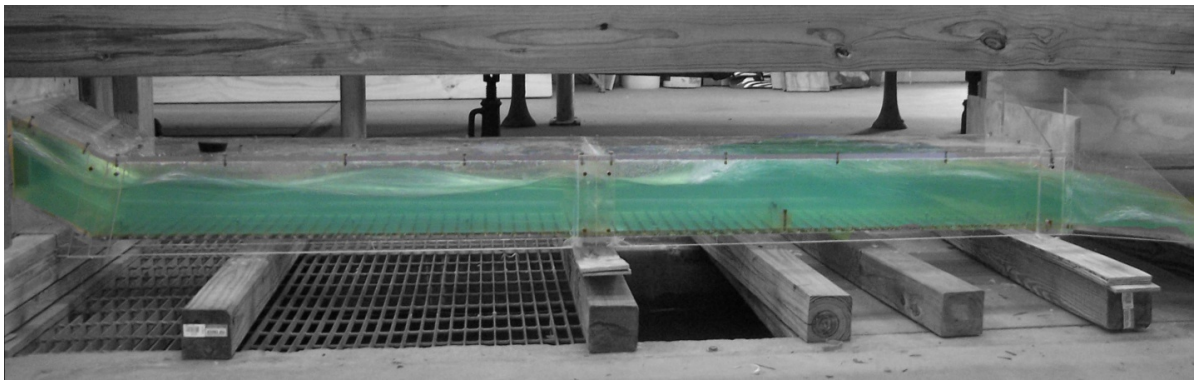

Figure A6. Experiment 2C

Table A2. Experiment 2 using Pressure Flow Condition with a 1.25 inch sill at 25 inches from the end of the culvert.

H.J.	Run	H	W_{temp}	Q	$V_{u/s}$	Y_s	Y_{toe}	Y_1	Y_2	$Y_{d/s}$	Fr1	V_1	V_2	$V_{d/s}$	L	X	ΔE	THL	E_2/E_1
Y	2A	0.8d	-	0.9893	2.500	2.50	2.40	2.55	4.90	2.90	2.2123	5.78688 P-tube	-	4.88139 P-tube	5.00	-	0.26	2.224602	0.874
Y	2B	1.0d	-	1.3853	2.700	2.88	3.38	3.25	5.90	3.25	2.0153	5.95147 P-tube	-	5.58874 P-tube	4.00	-	0.24	1.888382	0.907
Y	2C	1.2d	-	1.6930	2.800	4.25	4.00	3.90	6.00	3.40	1.8729	6.05871 P-tube	-	5.89712 P-tube	4.50	-	0.10	2.380865	0.929

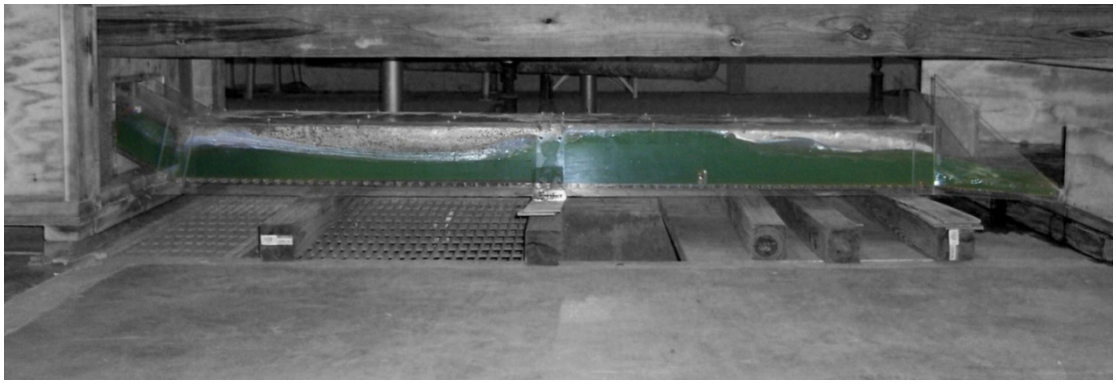

Figure A7. Experiment 3A

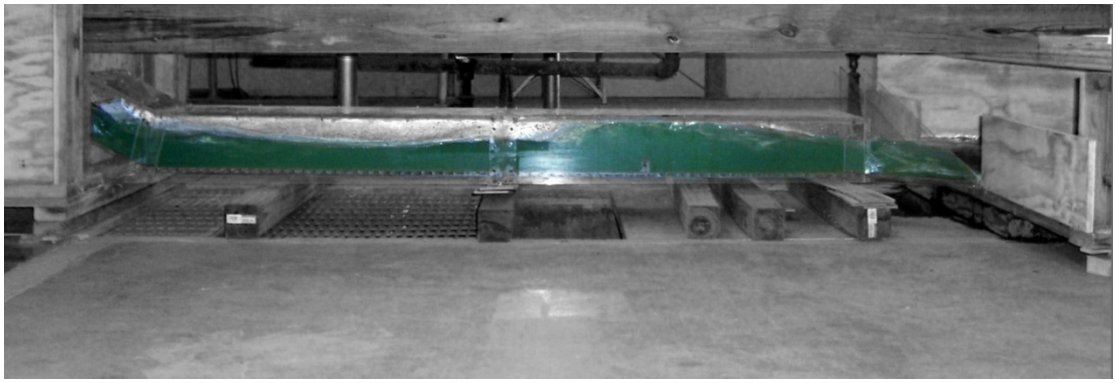

Figure A8. Experiment 3B

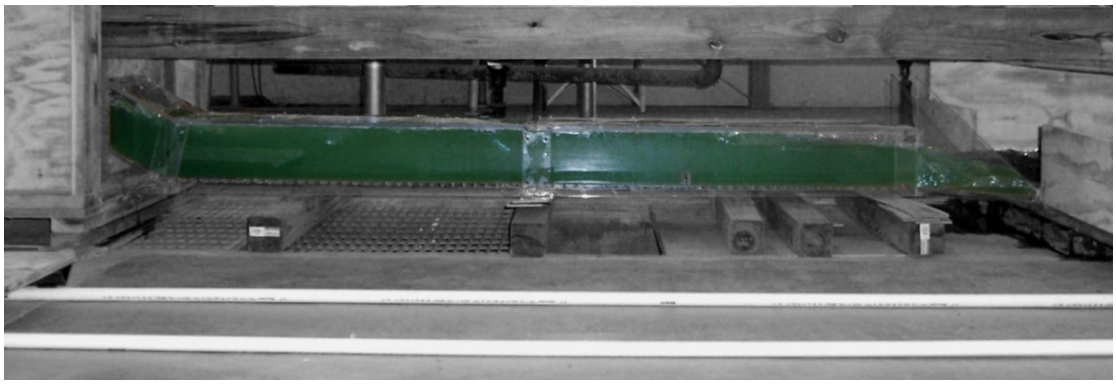

Figure A9. Experiment 3C

Table A3. Experiment 3 using Pressure Flow Condition with a 1.5 inch sill at 25 inches from the end of the culvert.

H.J.	Run	H	W_{temp}	Q	$V_{u/s}$	Y_s	Y_{toe}	Y_1	Y_2	$Y_{d/s}$	Fr1	V_1	V_2	$V_{d/s}$	L	X	ΔE	THL	E_2/E_1
Y	3A	0.8 d	53.5	1.0092	2.500	2.75	2.50	2.00	5.25	2.87	2.2127	5.73097 P-tube	-	4.81498 P-tube	9.50	-	0.82	2.374590	0.874
Y	3B	1.0 d	53.5	1.3255	2.700	4.38	3.50	3.50	6 (u.p.)	3.00	1.9420	5.95147 P-tube	-	5.41313 P-tube	8.50	-	0.19	2.498389	0.919
Y (Drown	3C	1.2 d	53.5	1.6598	2.800	4.65	6.00	4.65 (slope)	6 (u.p.)	4.50	1.2443	4.39545 P-tube	-	6.216108	2.50	-	0.02	0.560870	0.996

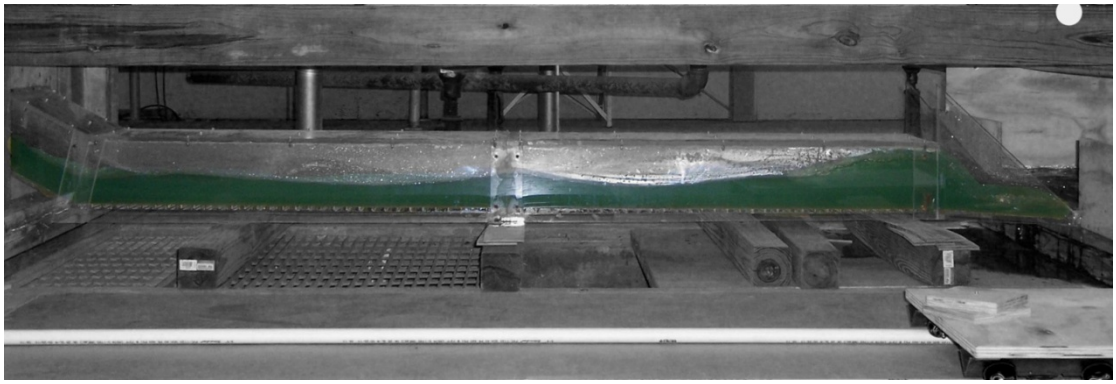

Figure A10. Experiment 4A

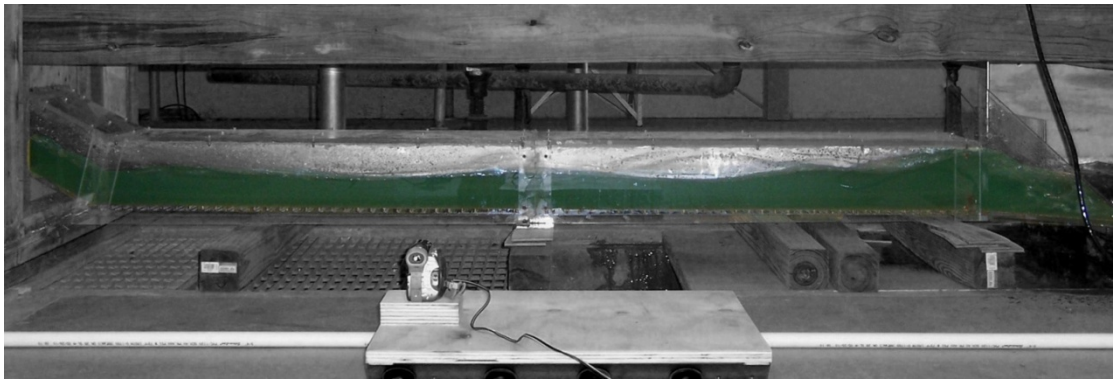

Figure A11. Experiment 4B

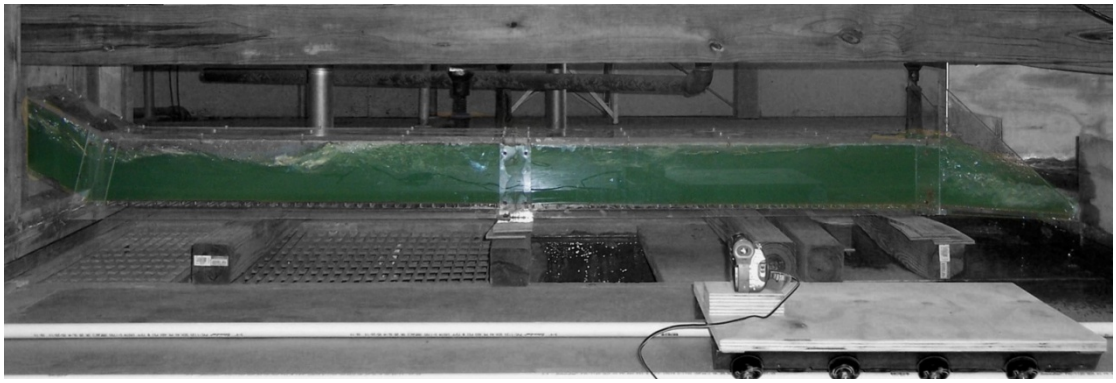

Figure A12. Experiment 4C

Table A4. Experiment 4 using Pressure Flow Condition with a 1.5 inch sill at the end of the culvert.

H.J.	Run	H	W_{temp}	Q	$V_{u/s}$	Y_s	Y_{toe}	Y_1	Y_2	$Y_{d/s}$	Fr1	V_1	V_2	$V_{d/s}$	L	X	ΔE	THL	E_2/E_1
Y	4A	0.8d	-	1.0132	2.500	2.25	2.13	2.13	4.75	4.75	2.4234	5.78688 P-tube	-	5.501636 P-tube	8.50	-	0.45	-0.825403	0.838
N	4B	1.0d	-	1.2962	2.700	2.87	2.38	2.25	5.50	5.50	2.4221	5.95147 P-tube	-	5.6831 corr = 80%	-	-	0.69	-0.559806	0.838
Y	4C	1.2d	-	1.7024	2.800	3.87	3.75	3.75	6 (u.p.)	6 (u.p.)	1.7158	5.442793 P-tube	-	5.7316 corr = 78%	5 (slope)	-	0.13	0.139521	0.952

Table A5. Experiment 5 using Pressure Flow Condition with a 2 inch sill at the end of the culvert.

H.J.	Run	H	W_{temp}	Q	$V_{u/s}$	Y_s	Y_{toe}	Y_1	Y_2	$Y_{d/s}$	Fr1	V_1	V_2	$V_{d/s}$	L	X	ΔE	THL	E_2/E_1
Y	5A	0.8d	57.4	1.0210	2.500	2.50	2.38*	2.38	6 (u.p.)	6 (u.p.)	2.3118	5.8423	-	4.6099	15.50	-	0.83	-0.395	0.857
Y	5B	1.0d	57.4	1.3266	2.700	3.00	3.00*	3.00	6 (u.p.)	6 (u.p.)	1.6248	4.609989	-	5.7309	8.00	-	0.38	-1.161	0.964
Y (Drown)	5C	1.2d	56.8	1.5912	2.800	6.00	6.00*	5.25	6 (u.p.)	6 (u.p.)	1.2442	4.669892	-	6.666	3.00	-	0.00	-2.019	0.996

Table A7. Experiment 7 using Pressure Flow Condition with a 1.75 inch sill at the end of the culvert.

H.J.	Run	H	W_{temp}	Q	$V_{u/s}$	Y_s	Y_{toe}	Y_1	Y_2	$Y_{d/s}$	Fr1	V_1	V_2	$V_{d/s}$	L	X	ΔE	THL	E_2/E_1
Y	7A	0.8d	-	0.9933	2.500	2.88	2.38	2.25	6.00	6.00	2.3551	5.7869	-	4.24641	10.00	-	0.98	0.204597	0.849
Y	7B	1.0d	-	1.3084	2.700	2.88	3.25	2.75	6 (u.p.)	6.00	1.7725	4.81498	-	5.95147	7.00	-	0.52	-1.641614	0.944
Y (Drown)	7C	1.2d	49.7	1.6717	2.800	5.00	6 (u.p.)	6 (u.p.)	6 (u.p.)	6 (u.p.)	1.0954	4.39545	-	6.216101	2.00	-	0.00	-0.939114	1.000

Table A8. Experiment 8 using Pressure Flow Condition with a 1.25 inch sill at 25 inches from the end of the culvert and a 1.5 inch sill at the end of the culvert.

H.J.	Run	H	W_{temp}	Q	$V_{u/s}$	Y_s	Y_{toe}	Y_1	Y_2	$Y_{d/s}$	Fr1	V_1	V_2	$V_{d/s}$	L	X	ΔE	THL	E_2/E_1
Y	8A	0.8d	50.8	0.9973	2.500	2.25	2.50	3.00	5.25	5.00	2.0976	5.9515	-	4.5396	6.00	-	0.18	0.724602	0.893
Y	8B	1.0d	50.9	1.3650	2.700	3.00	3.50	3.25	6 (u.p.)	6 (u.p.)	1.9969	5.8971	-	5.2008	7.00	-	0.27	-0.081675	0.910
Y	8C	1.2d	51.1	1.6788	2.800	4.25	4.50	4.50	6 (u.p.)	6 (u.p.)	1.4236	4.9469	-	5.9515	4.00	-	0.03	-0.339196	0.985

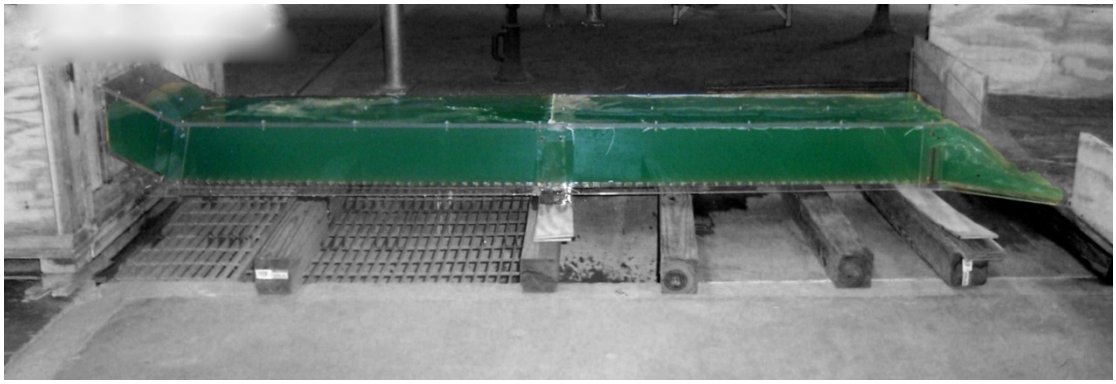

Figure A13. Experiment 6A

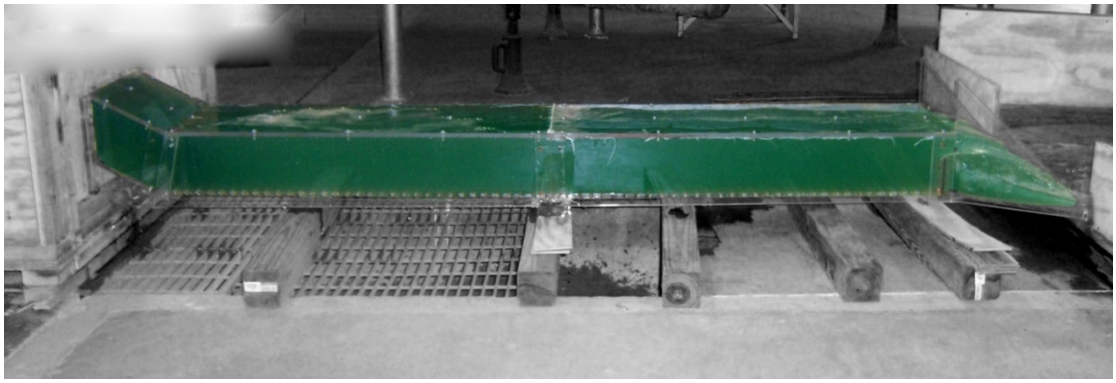

Figure A14. Experiment 6B

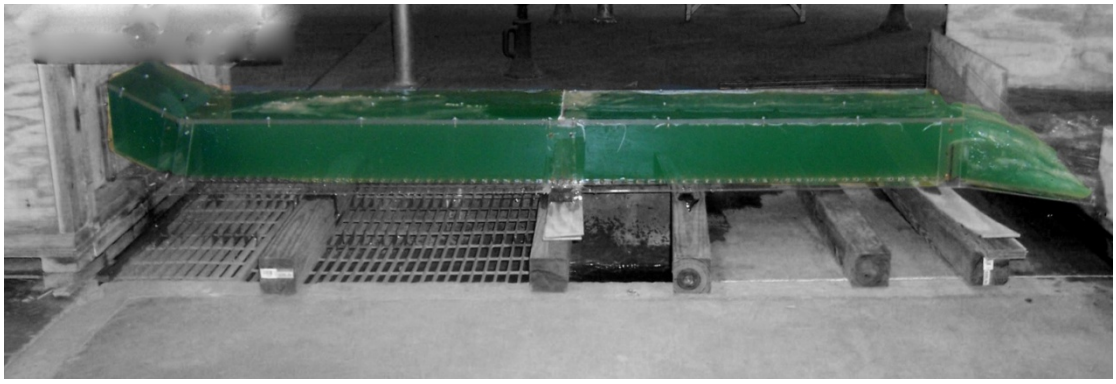

Figure A15. Experiment 6C

Table A6. Experiment 6 using Pressure Flow Condition with a 1.25 inch sill at the end of the culvert.

H.J.	Run	H	W_{temp}	Q	$V_{u/s}$	Y_s	Y_{toe}	Y_1	Y_2	$Y_{d/s}$	Fr1	V_1	V_2	$V_{d/s}$	L	X	ΔE	THL	E_2/E_1
N	6A	0.8d	-	0.9893	2.500	2.75	2.50	2.25	4.50	4.50	2.3777	5.84226	-	5.73096	-	-	0.28	-1.055386	0.846
N	6B	1.0d	-	1.3145	2.700	2.87	3.25	2.13	4.50	4.50	2.9263	6.9959 P-tube	-	6.1116 P-tube	-	-	0.35	-0.501551	0.755
N	6C	1.2d	-	1.7117	2.800	4.13	3.87	3.13	5.00	5.00	2.0906	6.0587 P-tube	-	6.41997	-	-	0.10	-0.419133	0.894

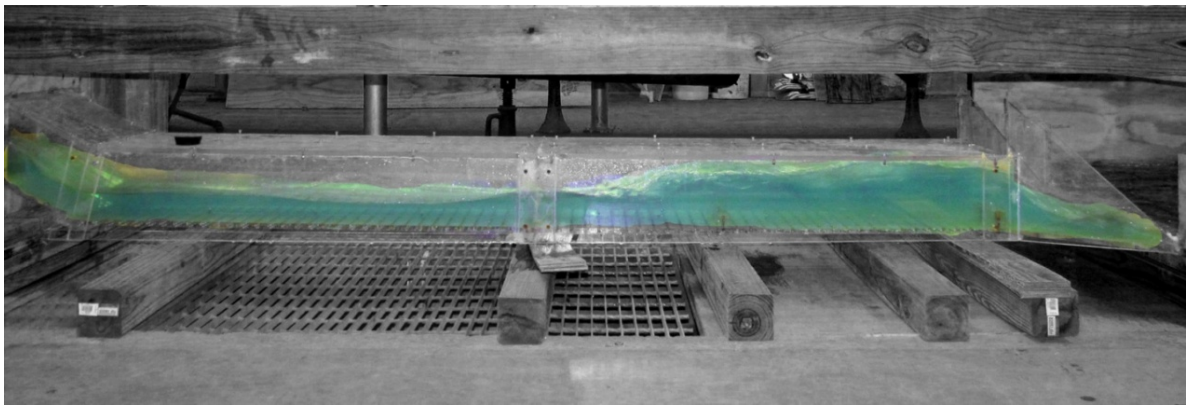

Figure A16. Experiment 9A

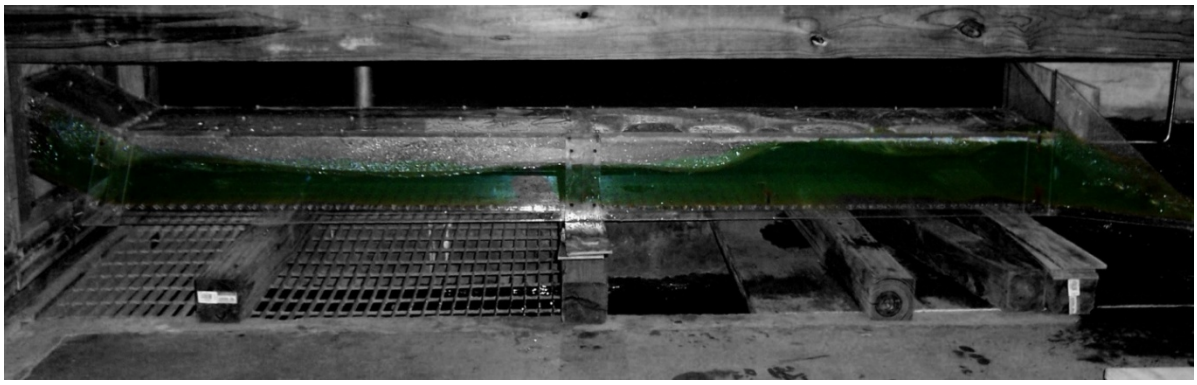

Figure A17. Experiment 9B

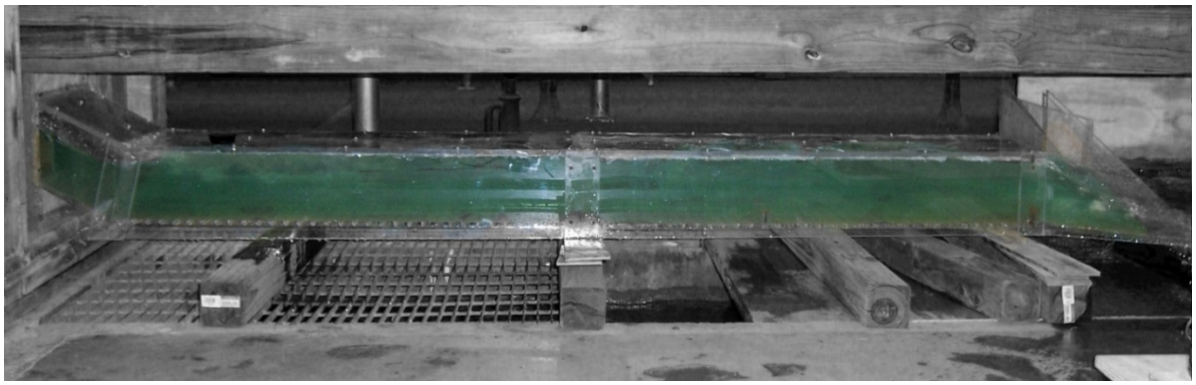

Figure A18. Experiment 9C

Table A9. Experiment 9 using Pressure Flow Condition with a 1 inch sill 25 inches from the end of the culvert and a 1.5 inch sill at the end of the culvert.

H.J.	Run	H	W_{temp}	Q	$V_{u/s}$	Y_s	Y_{toe}	Y_1	Y_2	$Y_{d/s}$	Fr1	V_1	V_2	$V_{d/s}$	L	X	ΔE	THL	E_2/E_1
Y	9A	0.8d	50.8	1.0053	2.513	2.50	2.50	2.50	5.00	5.50	2.2127	5.73097 P-tube	-	4.5396 P-tube	4.00	-	0.31	0.236980	0.874
Y	9B	1.0d	48.5	1.3084	2.617	2.75	3.00	3.00	5.50	6 (u.p.)	2.1354	6.0587 P-tube	-	4.60999 P-tube	3.50	-	0.24	0.915957	0.887
Y	9C	1.2d	48.4	1.7047	2.841	4.25	4.63	4.63	6 (u.p.)	6.00	1.4035	4.94692 P-tube	-	5.01158 P-tube	2.50	-	0.02*	1.624154	0.987

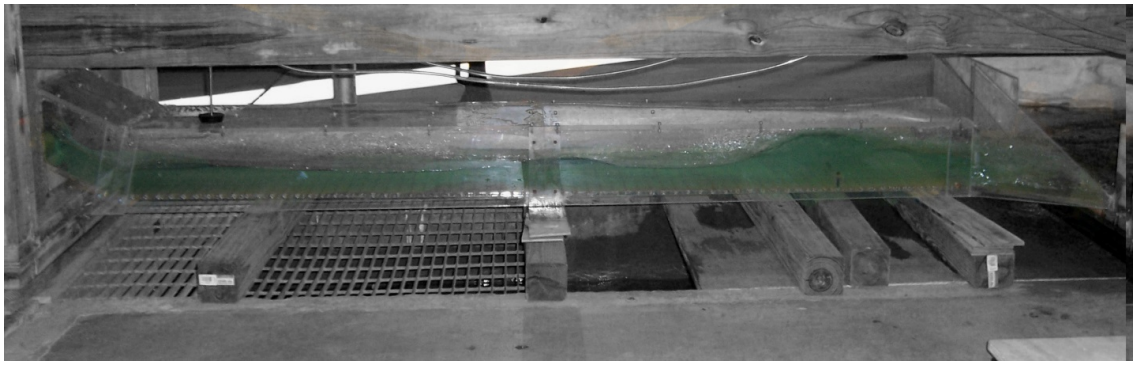

Figure A19. Experiment 10A

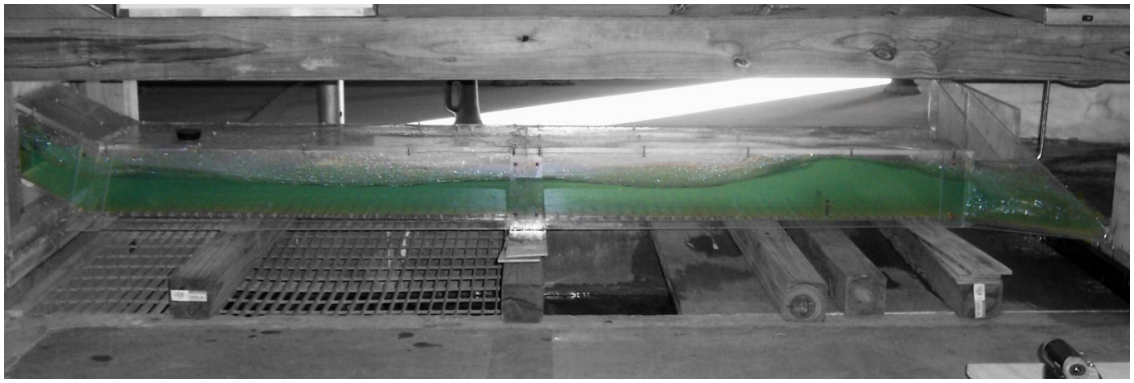

Figure A20. Experiment 10B

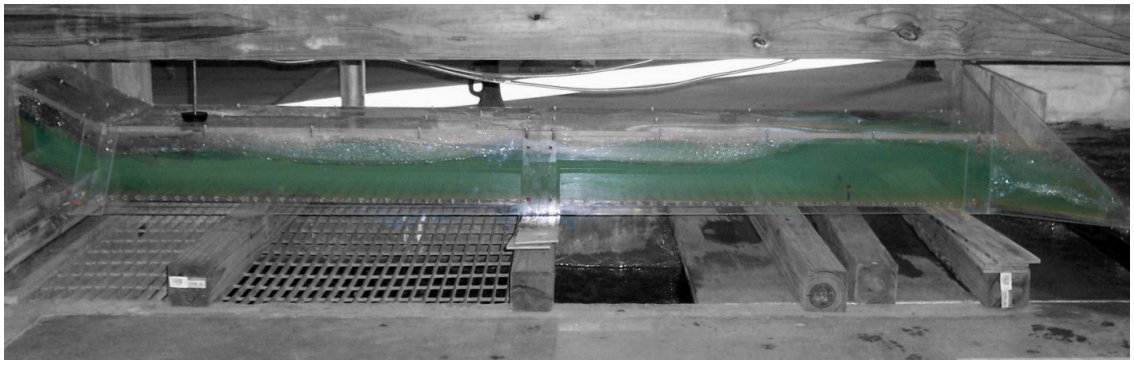

Figure A21. Experiment 10C

Table A10. Experiment 10 using Pressure Flow Condition with a 1.25 inch sill 13 inches from the end of the culvert.

H.J.	Run	H	W_{temp}	Q	$V_{u/s}$	Y_s	Y_{toe}	Y_1	Y_2	$Y_{d/s}$	Fr1	V_1	V_2	$V_{d/s}$	L	X	ΔE	THL	E_2/E_1
Y	10A	0.8d	49.0	0.9933	2.483	2.25	2.50	2.25	5.00	2.83	2.3094	5.6745	-	4.74763	4.50	-	0.46	2.519045	0.857
Y	10B	1.0d	48.9	1.3355	2.671	3.00	3.37	2.75	5.63	3.75	2.1507	5.84226	-	5.26232	2.50	-	0.39	2.019359	0.884
Y	10C	1.2d	49.1	1.6930	2.822	4.00	3.88	3.38	6 (u.p.)	4.00	1.9762	5.9515	-	6.05871	5.00	-	0.22	1.443572	0.913

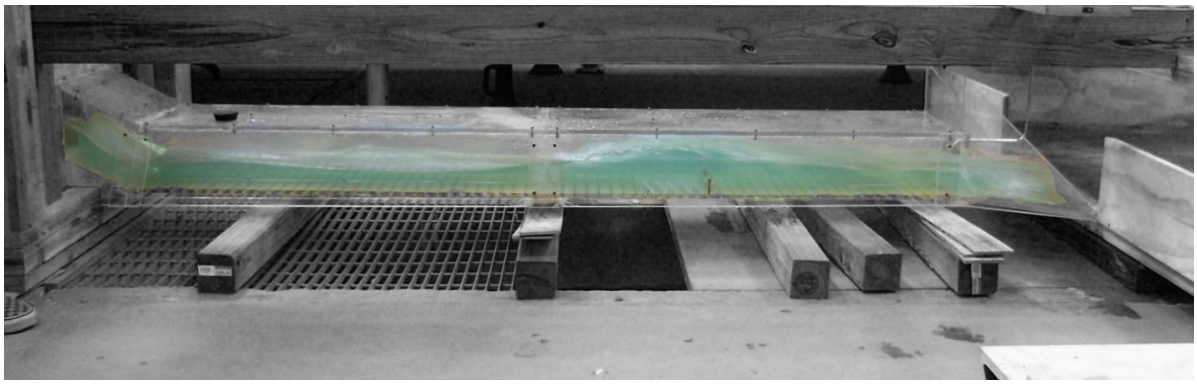

Figure A22. Experiment 11A

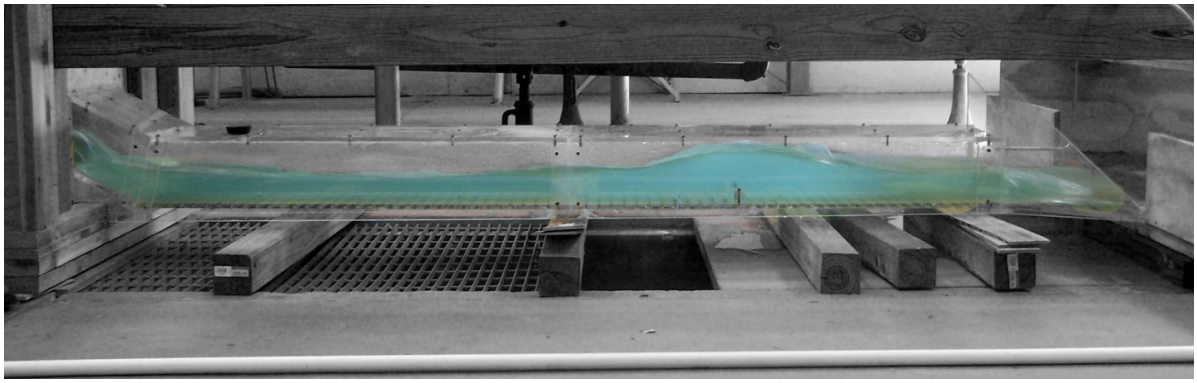

Figure A23. Experiment 11B

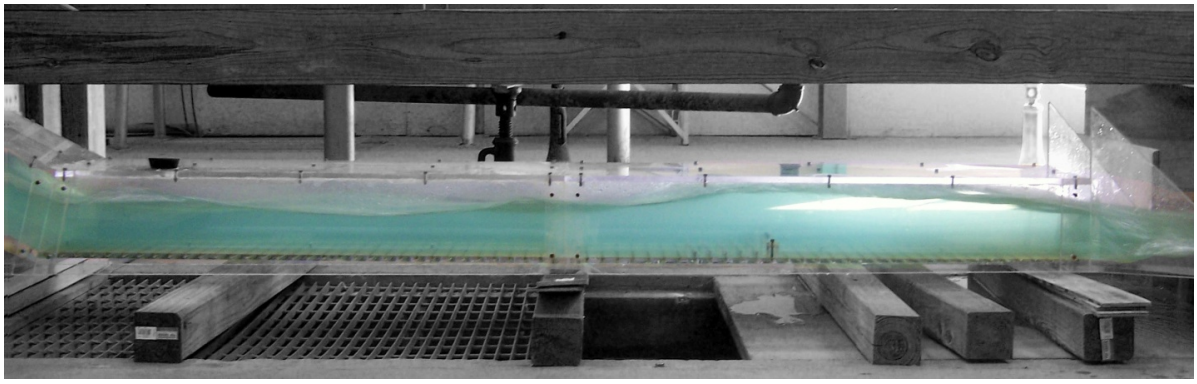

Figure A24. Experiment 11C

Table A11. Experiment 11 using Pressure Flow Condition with a 1.25 inch sill 25 inches from the end of the culvert and 15 flat-faced friction blocks in front of the sill.

H.J.	Run	H	W_{temp}	Q	$V_{u/s}$	Y_s	Y_{toe}	Y_1	Y_2	$Y_{d/s}$	Fr1	V_1	V_2	$V_{d/s}$	L	X	ΔE	THL	E_2/E_1
Y	11A	0.8d	49.3	0.9893	2.500	2.75	2.38	3.00	5.00	2.50	2.0199	5.73100	-	4.67932	5.75	-	0.13	2.984590	0.906
Y (?)	11B	1.0d	49.7	1.3205	2.700	2.75	3.50	3.50	5.00	3.00	1.9243	5.89710	-	5.73097	4.50	-	0.05	-1.161615	0.921
Y (?)	11C	1.2d	49.8	1.7302	2.800	4.25	4.00	4.25	5.38	4.00	1.7624	5.95150	-	6.11163	4.00	-	0.02	1.300866	0.946

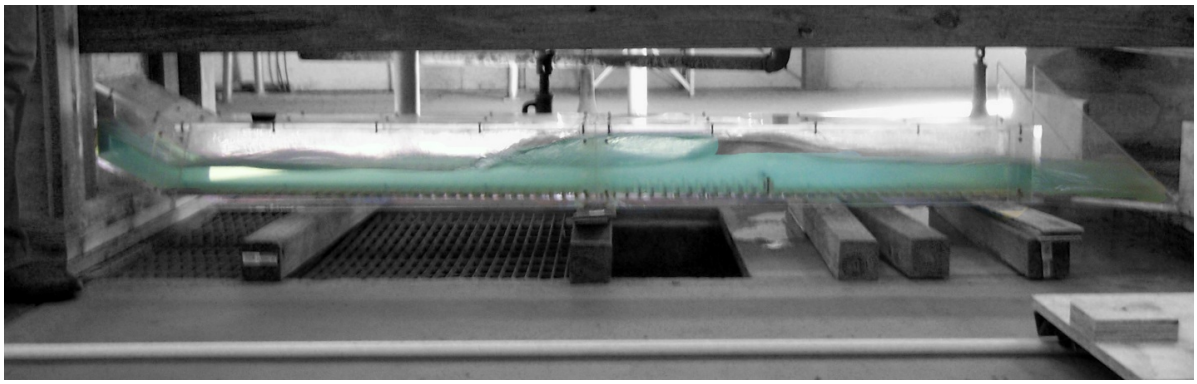

Figure A25. Experiment 12A

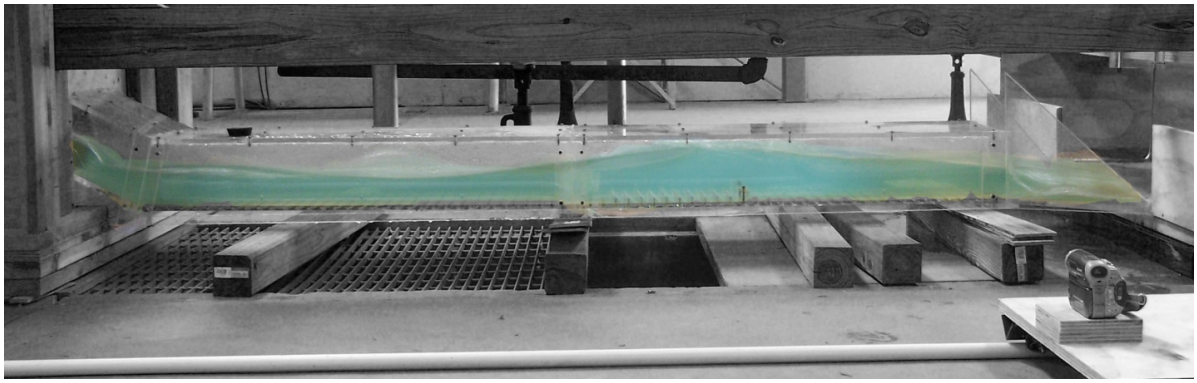

Figure A26. Experiment 12B

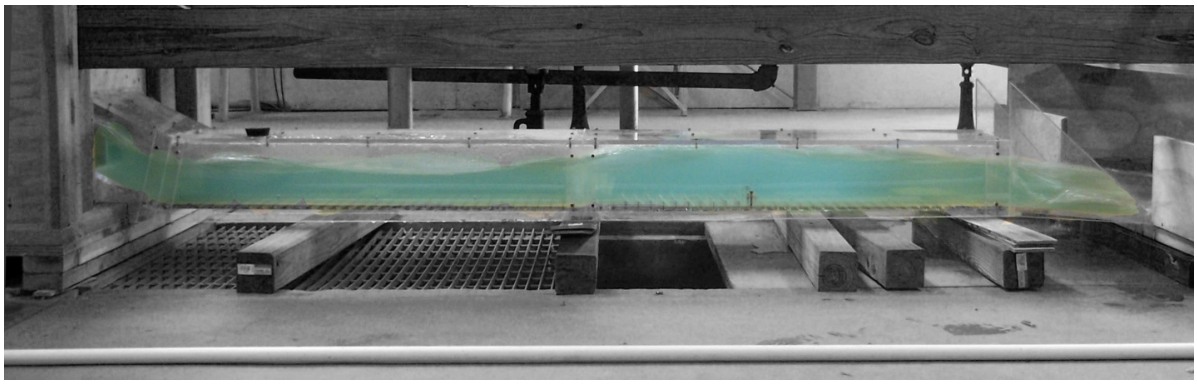

Figure A27. Experiment 12C

Table A12. Experiment 12 using Pressure Flow Condition with a 1.25 inch sill at 25 inches from the end of the culvert with 30 flat-faced friction blocks in front of the sill.

H.J.	Run	H	W_{temp}	Q	$V_{u/s}$	Y_s	Y_{toe}	Y_1	Y_2	$Y_{d/s}$	Fr1	V_1	V_2	$V_{d/s}$	L	X	ΔE	THL	E_2/E_1
Y	12A	0.8d	50.3	0.9812	2.500	2.50	2.38	2.00	5.50	2.50	2.4739	5.73096	-	4.609989	8.00	-	0.97	3.104597	0.829
Y	12B	1.0d	50.4	1.3621	2.700	3.50	3.75	4.13	5.50	3.25	1.8040	6.00533	-	5.3232	3.50	-	0.03	2.428300	0.940
Y	12C	1.2d	50.3	1.6883	2.800	3.88	4.00	3.88	6 (u.p.)	3.75	1.8777	6.05871	-	6.05871	7.00	-	0.10	1.670876	0.929

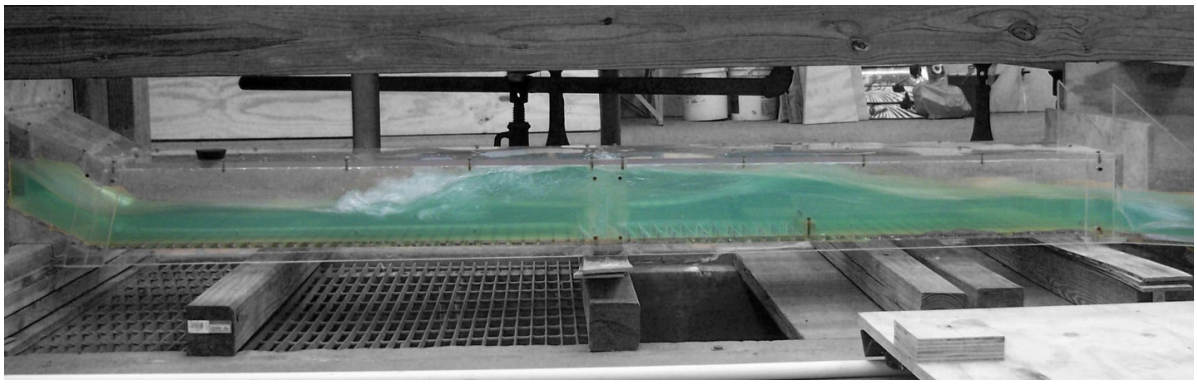

Figure A28. Experiment 13A

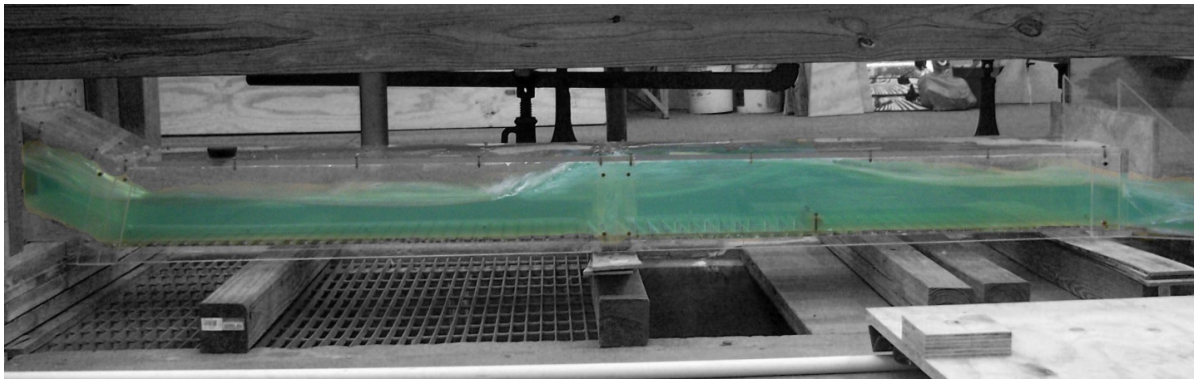

Figure A29. Experiment 13B

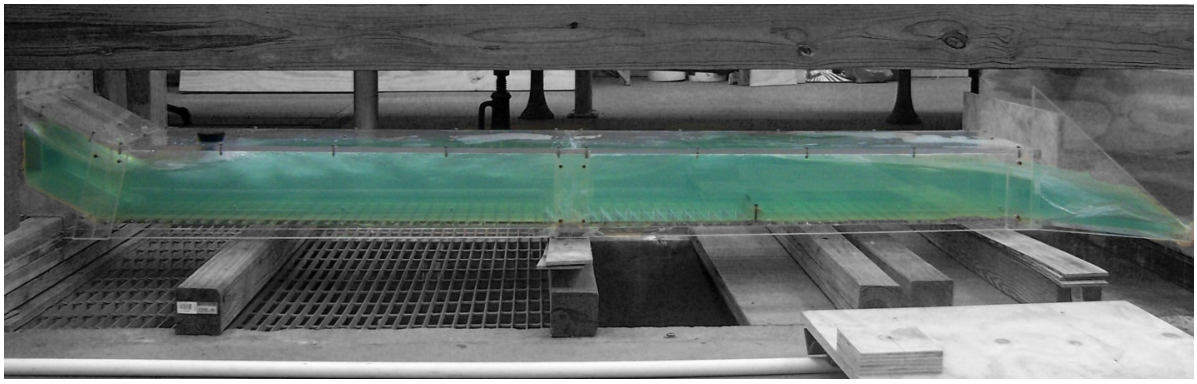

Figure A30. Experiment 13C

Table A13. Experiment 13 using Pressure Flow Condition with a 1.25 inch sill at 25 inches from the end of the culvert with 45 flat-faced friction blocks in front of the sill.

H.J.	Run	H	W_{temp}	Q	$V_{u/s}$	Y_s	Y_{toe}	Y_1	Y_2	$Y_{d/s}$	Fr1	V_1	V_2	$V_{d/s}$	L	X	ΔE	THL	E_2/E_1
Y	13A	0.8d	50.5	0.9933	2.500	2.63	2.50	2.38	6.00	2.63	2.2454	5.67450	-	4.74763	10.00	-	0.83	2.734598	0.868
Y	13B	1.0d	50.5	1.3145	2.700	2.88	2.38	3.13	6 (u.p.)	3.38	2.0348	5.89710	-	5.32316	8.00	-	0.31	-0.321621	0.904
Y	13C	1.2d	50.6	1.7187	2.800	4.25	4.13	4.13	6 (u.p.)	4.25	1.7878	5.95150	-	5.89710	7.00	-	0.07	1.530909	0.942

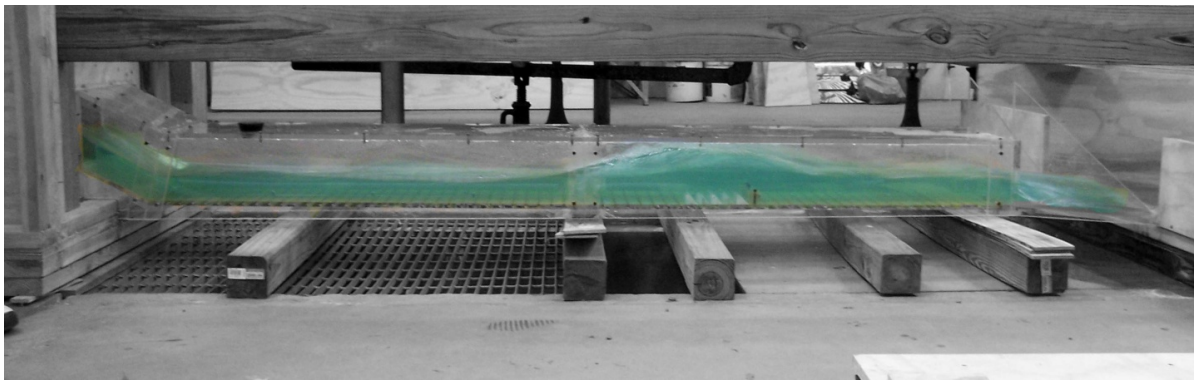

Figure A31. Experiment 14A

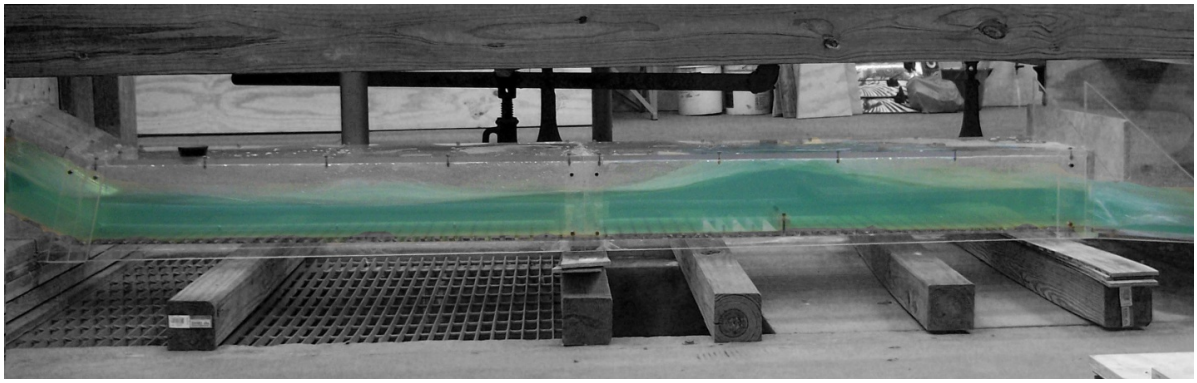

Figure A32. Experiment 14B

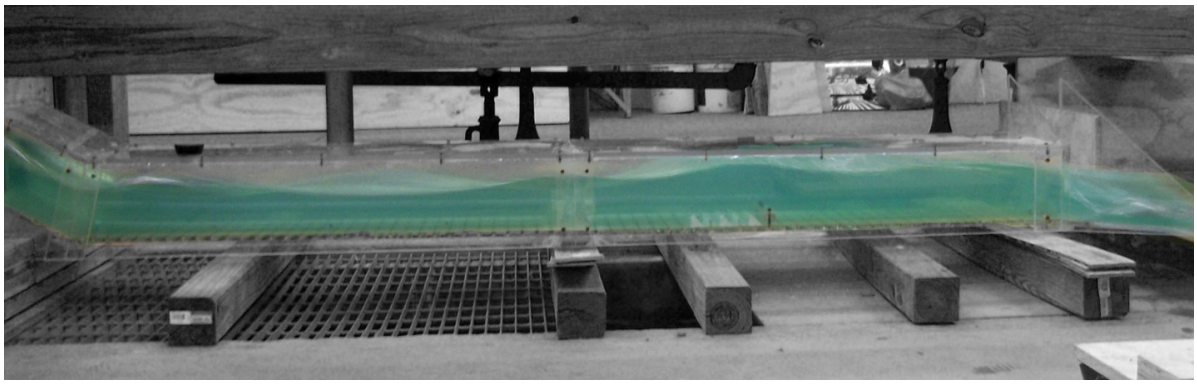

Figure A33. Experiment 14C

Table A14. Experiment 14 using Pressure Flow Condition with a 1.25 inch sill at 25 inches from the end of the culvert with 15 curved-face friction blocks in front of the sill.

H.J.	Run	H	W_{temp}	Q	$V_{u/s}$	Y_s	Y_{toe}	Y_1	Y_2	$Y_{d/s}$	Fr1	V_1	V_2	$V_{d/s}$	L	X	ΔE	THL	E_2/E_1
Y	14A	0.8d	48.2	0.9933	2.500	2.50	2.38	2.88	5.25	3.75	2.0616	5.730968	-	4.81498	7.00	-	0.22	1.494590	0.899
Y (?)	14B	1.0d	48.3	1.3084	2.700	3.00	3.38	3.50	5.00	3.00	1.9243	5.897118	-	5.559856	4.00	-	0.05	2.198385	0.921
Y (?)	14C	1.2d	48.1	1.7047	2.800	4.20	4.00	4.25	5.50	3.50	1.7783	6.00533	-	6.05871	5.00	-	0.02	1.920876	0.943

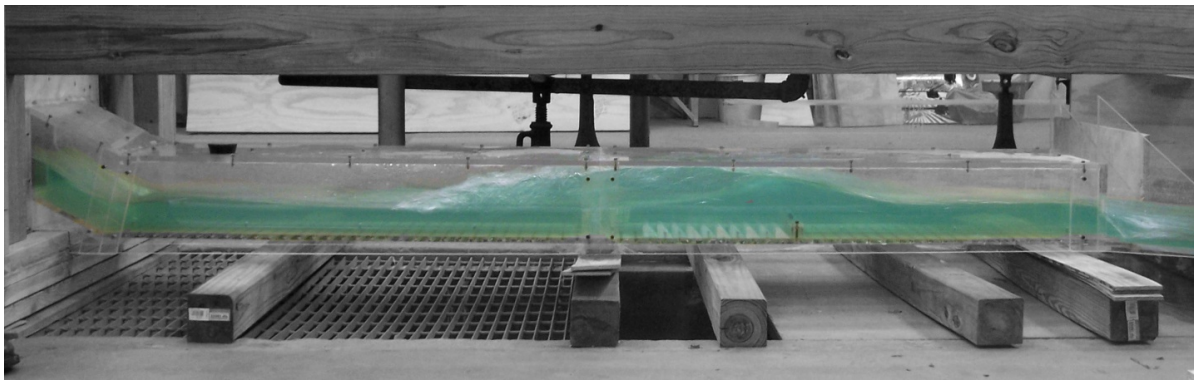

Figure A34. Experiment 15A

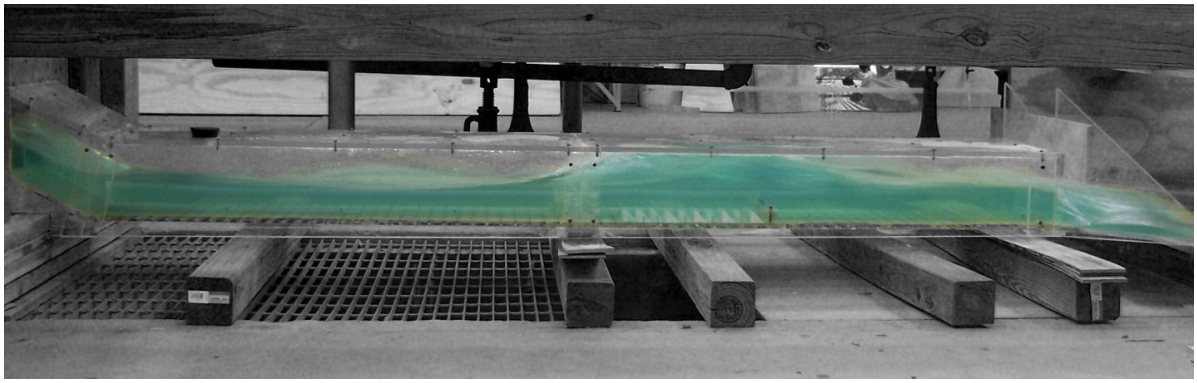

Figure A35. Experiment 15B

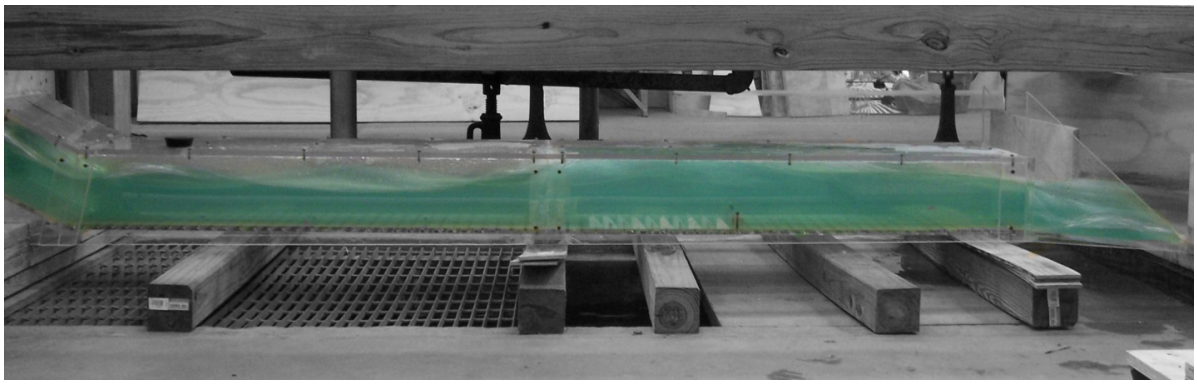

Figure A36. Experiment 15C

Table A15. Experiment 15 using Pressure Flow Condition with a 1.25 inch sill at 25 inches from the end of the culvert with 30 curved-face friction blocks in front of the sill.

H.J.	Run	H	W_{temp}	Q	$V_{u/s}$	Y_s	Y_{toe}	Y_1	Y_2	$Y_{d/s}$	Fr1	V_1	V_2	$V_{d/s}$	L	X	ΔE	THL	E_2/E_1
Y	15A	0.8d	48.2	1.0132	2.500	2.50	2.63	2.38	6 (u.p.)	2.88	2.2678	5.73097	-	4.88139	12.00	-	0.83	2.244597	0.864
Y	15B	1.0d	47.0	1.3084	2.700	3.00	3.38	3.50	6 (u.p.)	3.25	1.8701	5.73097	-	5.50164	7.50	-	0.19	-0.681615	0.930
Y	15C	1.2d	47.1	1.7325	2.800	4.38	4.00	4.50	6 (u.p.)	4.25	1.7282	6.00530	-	5.95147	5.00	-	0.03	1.410870	0.951

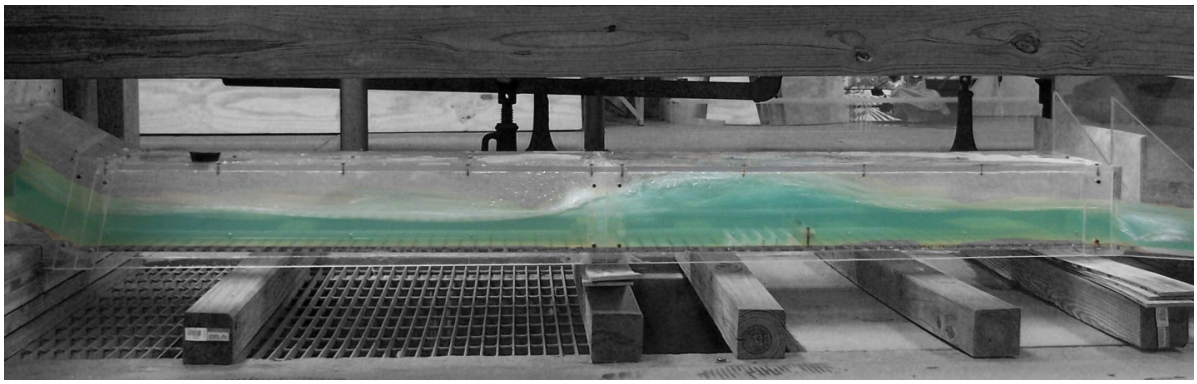

Figure A37. Experiment 16A

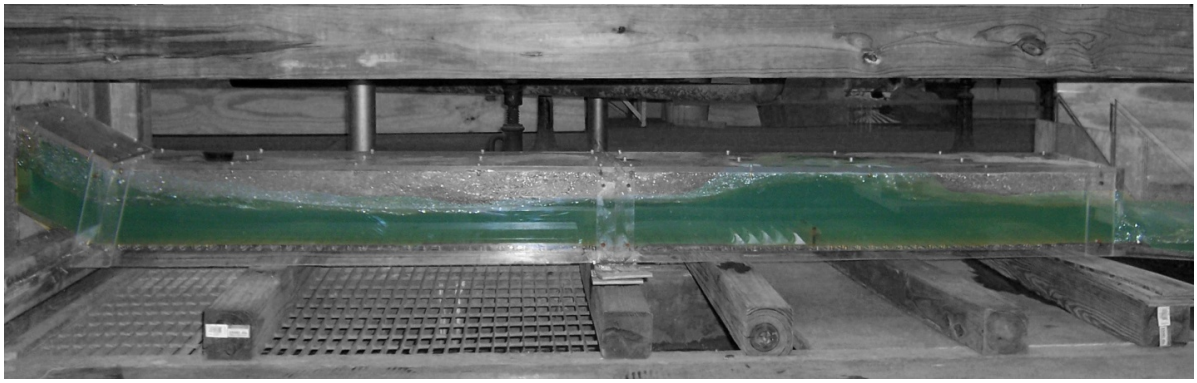

Figure A38. Experiment 16B

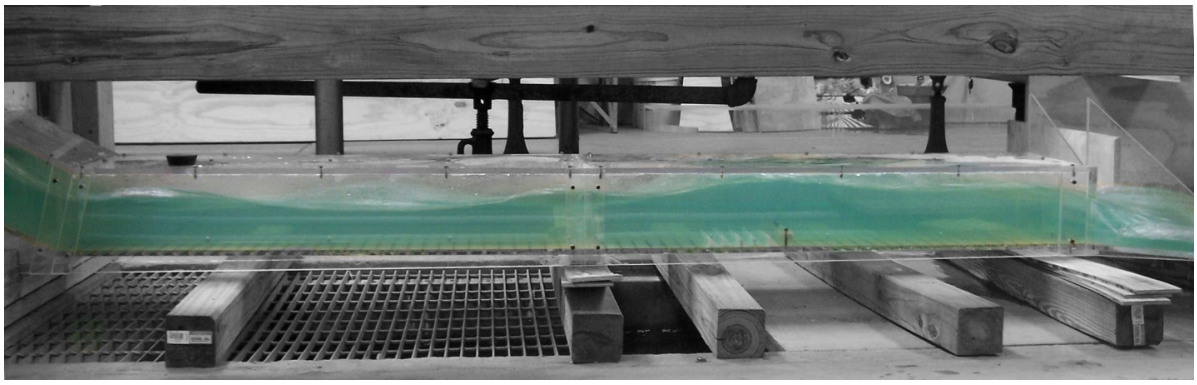

Figure A39. Experiment 16C

Table A16. Experiment 16 using Pressure Flow Condition with a 1.25 inch sill at 25 inches from the end of the culvert with 15 C-shaped friction blocks in front of the sill.

H.J.	Run	H	W_{temp}	Q	$V_{u/s}$	Y_s	Y_{toe}	Y_1	Y_2	$Y_{d/s}$	Fr1	V_1	V_2	$V_{d/s}$	L	X	ΔE	THL	E_2/E_1
Y	16A	0.8d	47.0	1.0013	2.500	2.63	2.38	3.13	4.88	2.63	1.9775	5.730969	-	4.747631	7.00	-	0.09	2.734596	0.913
Y (?)	16B	1.0d	46.9	1.3355	2.700	3.00	3.38	3.50	5.00	3.00	1.9243	5.897118	-	5.674504	4.00	-	0.05	1.958385	0.921
Y (?)	16C	1.2d	47.0	1.7256	2.800	4.20	4.00	4.25	5.50	3.50	1.7941	6.058713	-	6.058713	5.00	-	0.02	1.920870	0.941

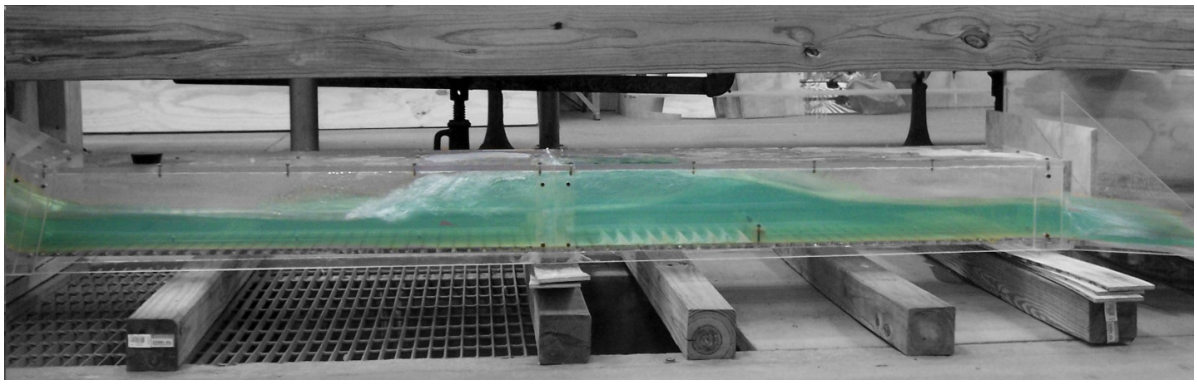

Figure A40. Experiment 17A

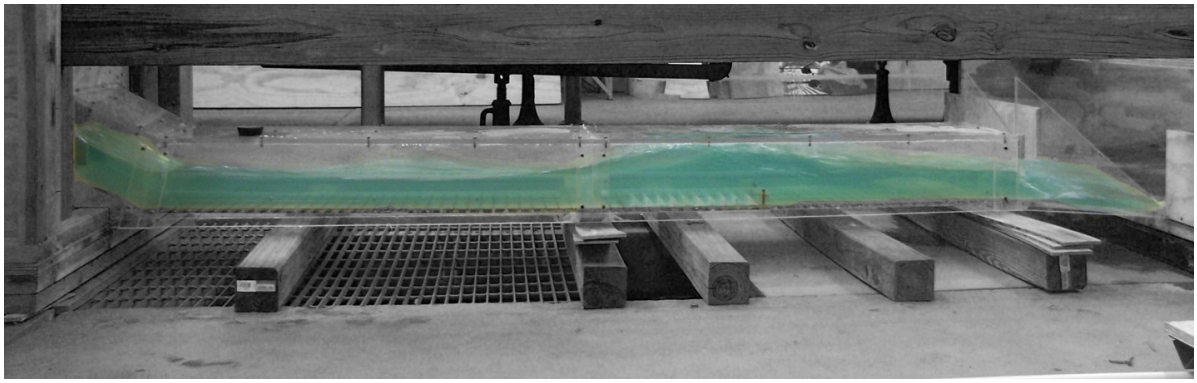

Figure A41. Experiment 17B

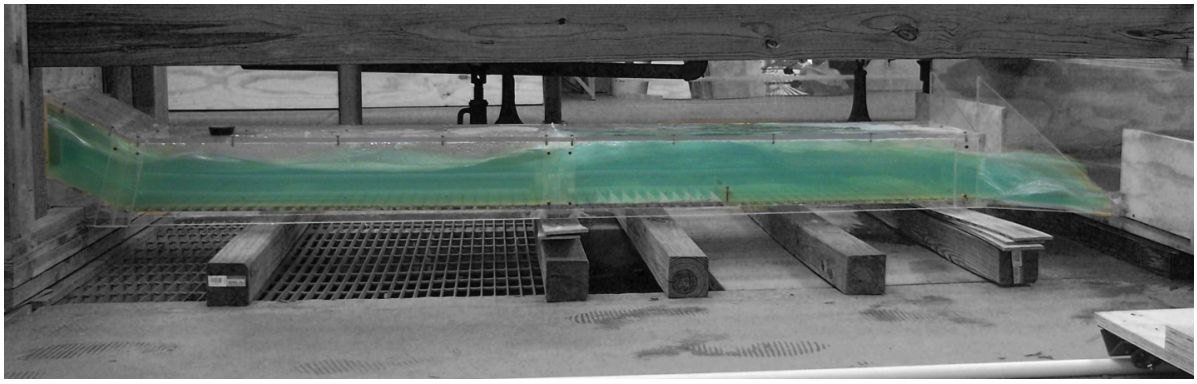

Figure A42. Experiment 17C

Table A17. Experiment 17 using Pressure Flow Condition with a 1.25 inch sill at 25 inches from the end of the culvert with 30 C-shaped friction blocks in front of the sill.

H.J.	Run	H	W_{temp}	Q	$V_{u/s}$	Y_s	Y_{toe}	Y_1	Y_2	$Y_{d/s}$	Fr1	V_1	V_2	$V_{d/s}$	L	X	ΔE	THL	E_2/E_1
Y	17A	0.8d	47.8	1.0092	2.500	2.25	2.63	2.38	6.00	2.75	2.3118	5.84226	-	4.88139	12.50	-	0.83	2.374596	0.876
Y (?)	17B	1.0d	47.8	1.3325	2.700	3.00	3.38	4.13	6 (u.p.)	2.83	1.7714	5.89712	-	5.50164	3.50	-	0.07	-0.681615	0.916
Y	17C	1.2d	48.0	1.7348	2.800	4.38	4.00	3.88	6 (u.p.)	4.38	1.8941	6.11163	-	6.05871	6.50	-	0.10	1.040870	0.930

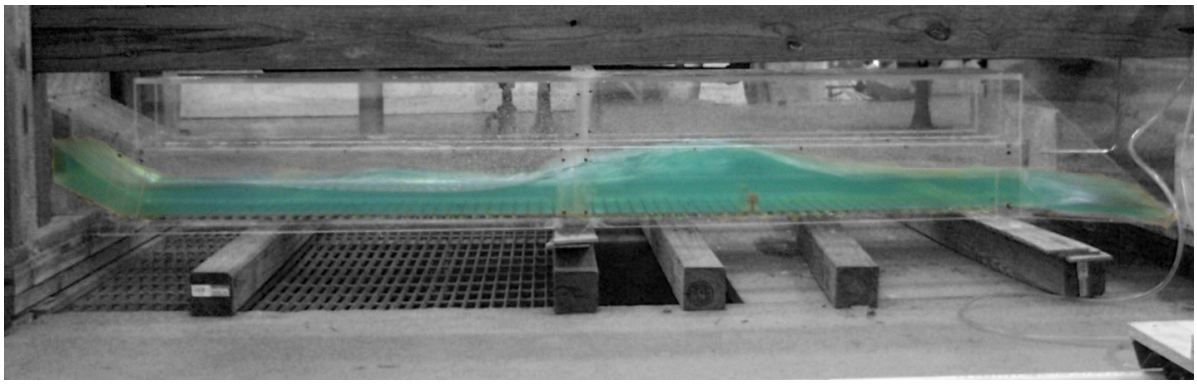

Figure A43. Experiment 18A

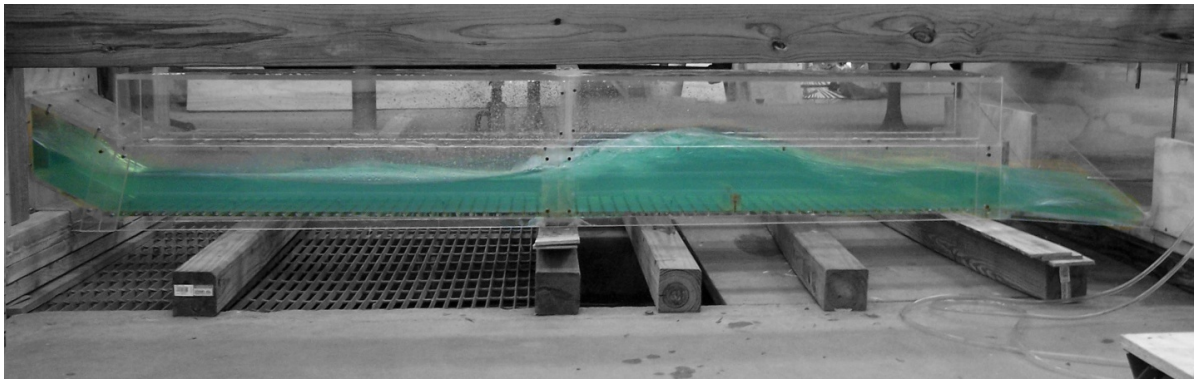

Figure A44. Experiment 18B

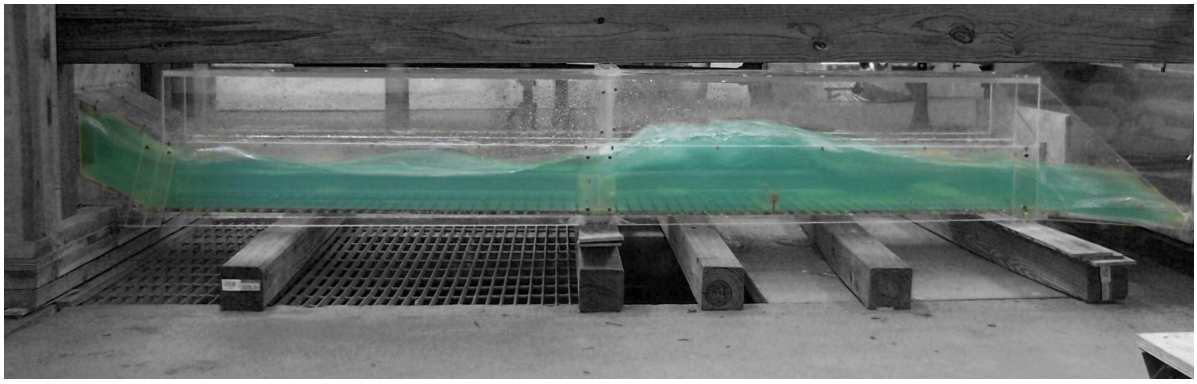

Figure A45. Experiment 18C

Table A18. Experiment 18 using Open Channel Condition with a 1.5 inch sill at 25 inches from the end of the culvert.

H.J.	Run	H	W_{temp}	Q	$V_{u/s}$	Y_s	Y_{toe}	Y_1	Y_2	$Y_{d/s}$	Fr1	V_1	V_2	$V_{d/s}$	L	X	ΔE	THL	E_2/E_1
Y	18A	0.8d	49.6	1.0053	2.500	2.50	2.63	2.38	5.63	2.75	1.9952	5.786882	3.49799	4.946918	9.00	24.75	0.64	2.254597	0.910
Y	18B	1.0d	50.2	1.3145	2.700	2.88	3.38	3.38	6.38	3.25	1.6508	6.00533	4.09194	5.323157	8.00	19.75	0.31	2.428385	0.961
Y	18C	1.2d	50.6	1.7163	2.800	4.38	3.88	5.00	7.25	3.75	1.3328	6.41997	3.6775	5.730968	8.50	17.50	0.08	2.390871	0.992

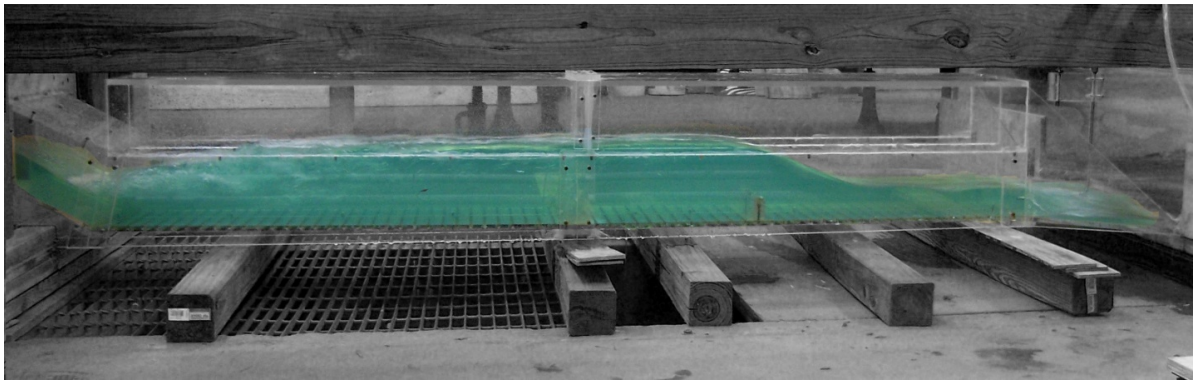

Figure A46. Experiment 19A

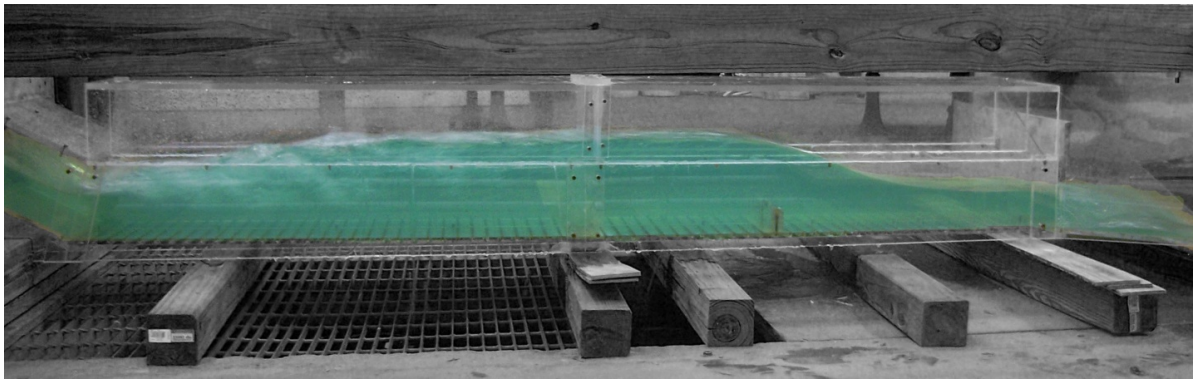

Figure A47. Experiment 19B

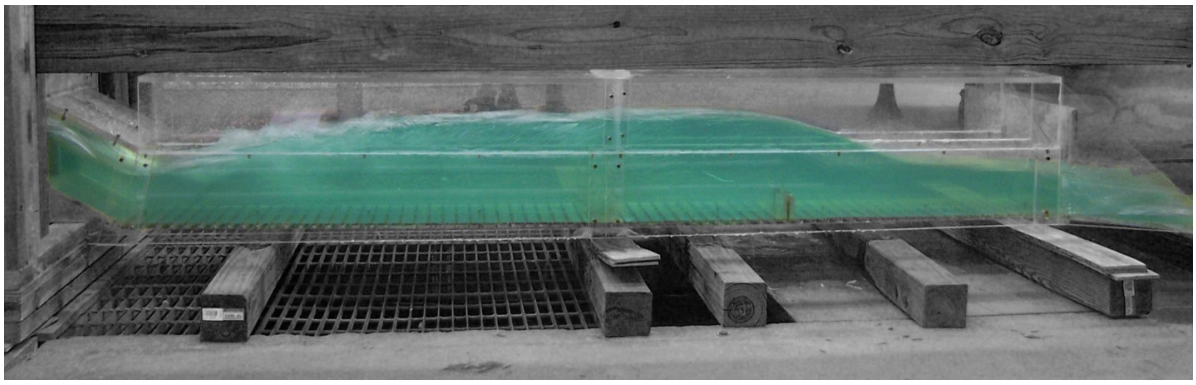

Figure A48. Experiment 19C

Table A19. Experiment 19 using Open Channel Condition with a 2 inch sill at 25 inches from the end of the culvert.

H.J.	Run	H	W_{temp}	Q	$V_{u/s}$	Y_s	Y_{toe}	Y_1	Y_2	$Y_{d/s}$	Fr1	V_1	V_2	$V_{d/s}$	L	X	ΔE	THL	E_2/E_1
Y	19A	0.8d	52.2	0.9933	2.500	2.25	N/A	2.00 (toe)	5.88	2.50	2.4066	4.78142	1.9657	5.13848	6.50	-	1.24	2.144601	0.841
Y	19B	1.0d	52.5	1.3385	2.700	3.00	3.63	3.63	7.50	3.00	1.7797	5.38331	2.53772	5.55986	10.00	54.00	0.53	-0.801615	0.943
Y	19C	1.2d	52.8	1.7094	2.800	4.25	4.13	4.13	8.75	3.75	1.8176	5.38331	2.8934	6.11163	12.00	55.00	0.68	1.550870	0.938

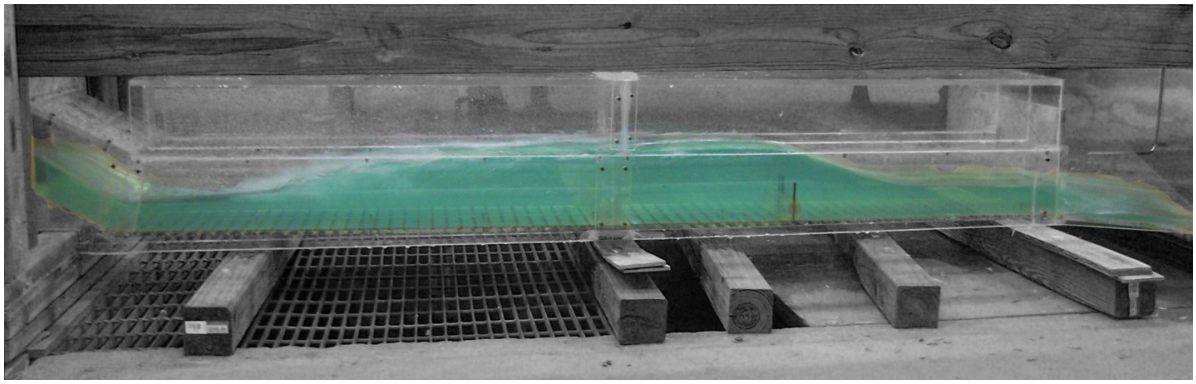

Figure A49. Experiment 20A

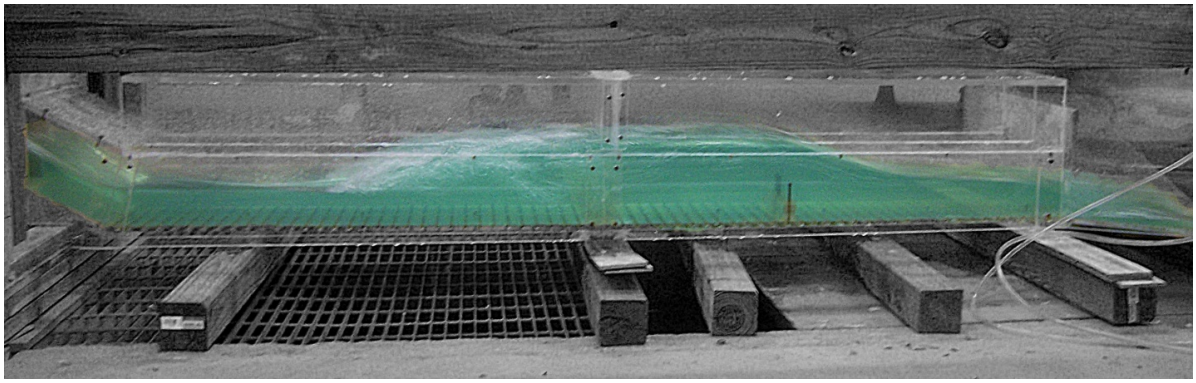

Figure A50. Experiment 20B

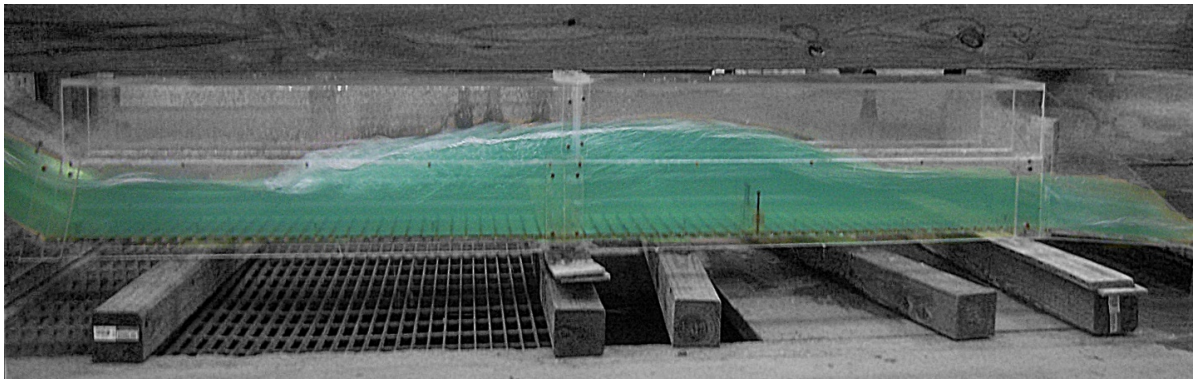

Figure A51. Experiment 20C

Table A20. Experiment 20 using Open Channel Condition with a 1.75 inch sill at 25 inches from the end of the culvert.

H.J.	Run	H	W_{temp}	Q	$V_{u/s}$	Y_s	Y_{toe}	Y_1	Y_2	$Y_{d/s}$	Fr1	V_1	V_2	$V_{d/s}$	L	X	ΔE	THL	E_2/E_1
Y	20A	0.8d	53.2	1.0013	2.500	2.75	2.50	3.00	6.38	2.75	1.8234	5.786882	2.53772	4.88139	10.00	44.75	0.50	2.374602	0.937
Y	20B	1.0d	53.3	1.2931	2.700	3.00	3.25	3.00	7.25	3.25	2.0319	5.95147	2.89344	5.38331	11.00	43.50	0.88	2.308380	0.904
Y	20C	1.2d	52.8	1.7302	2.800	4.50	3.88	3.75	8.38	3.88	1.9011	5.897118	2.77995	5.92435 6	15.00	46.25	0.79	1.840871	0.925

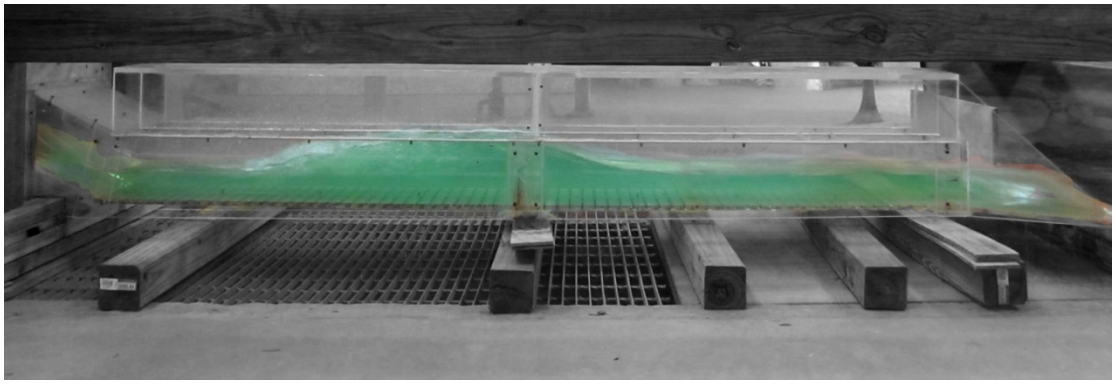

Figure A52. Experiment 21A

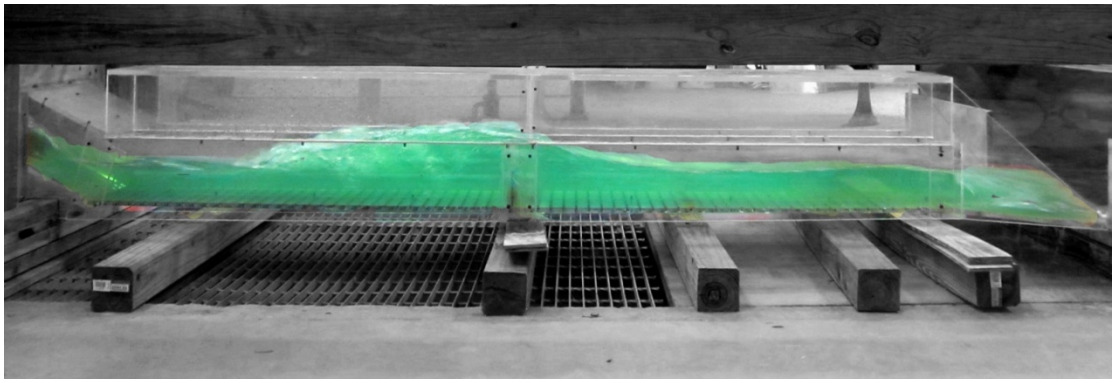

Figure A53. Experiment 21B

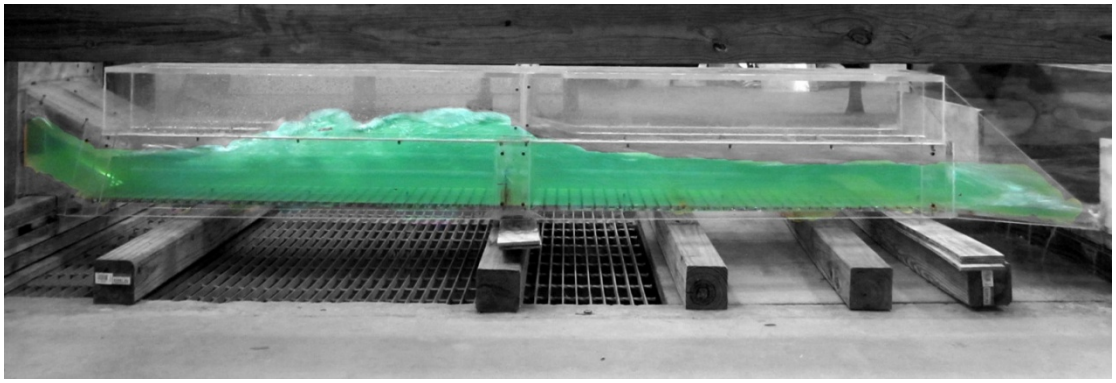

Figure A54. Experiment 21C

Table A21. Experiment 21 using Open Channel Condition with a 1.5 inch sill at the middle of the culvert.

H.J.	Run	H	W_{temp}	Q	$V_{u/s}$	Y_s	Y_{toe}	Y_1	Y_2	$Y_{d/s}$	Fr1	V_1	V_2	$V_{d/s}$	L	X	ΔE	THL	E_2/E_1
Y	21A	0.8d	53.9	1.0092	2.500	2.63	2.38	2.38	5.75	2.75	2.0314	5.55985	3.20998	4.81498	10.00	-	0.70	2.494596	0.904
Y	21B	1.0d	54.8	1.3504	2.700	3.65	3.65	3.00	6.88	3.50	1.9433	6.31886	3.20998	5.38330	11.00	-	0.71	-0.441600	0.918
Y	21C	1.2d	55.4	1.7394	2.800	4.50	4.00	3.75	7.88	4.00	1.8051	6.2677	4.0125	5.89710	11.50	-	0.60	1.780909	0.940

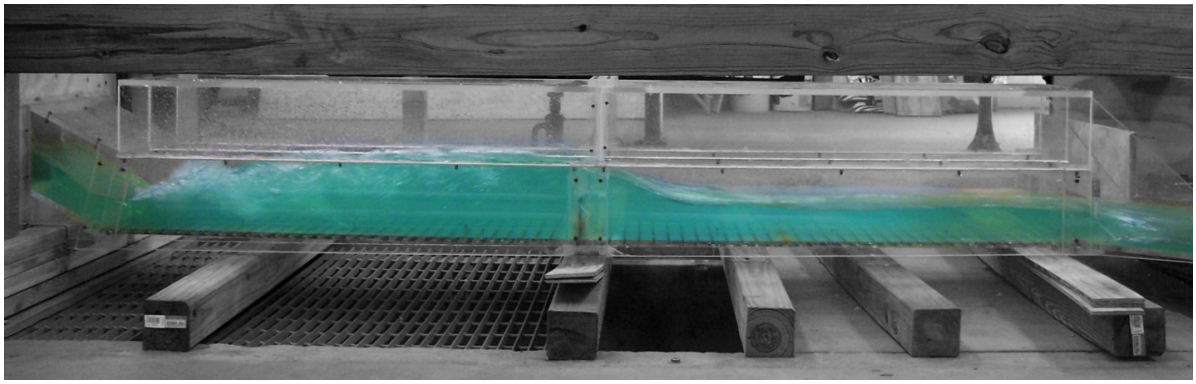

Figure A55. Experiment 22A

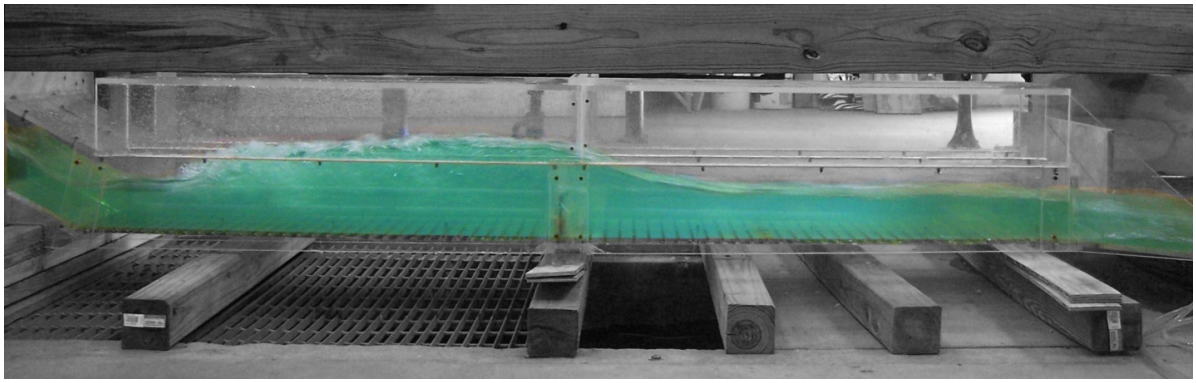

Figure A56. Experiment 22B

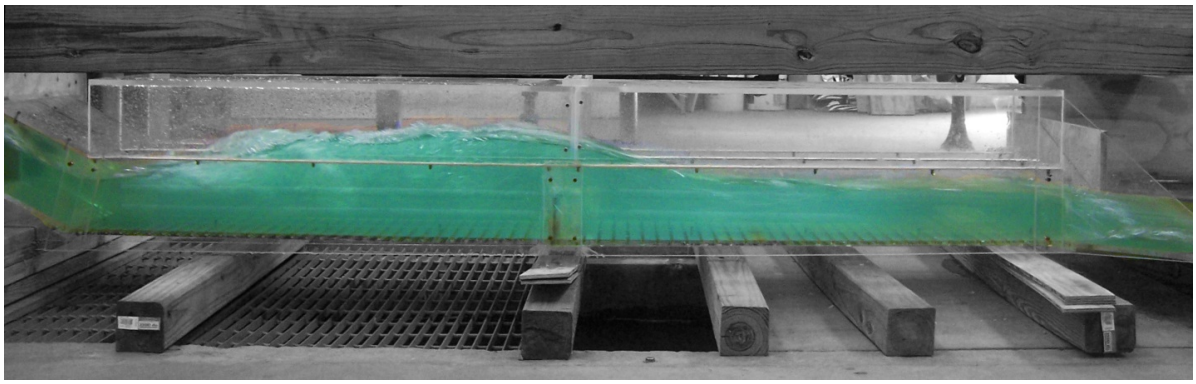

Figure A57. Experiment 22C

Table A22. Experiment 22 using Open Channel Condition with a 1.75 inch sill at the middle of the culvert.

H.J.	Run	H	W_{temp}	Q	$V_{u/s}$	Y_s	Y_{toe}	Y_1	Y_2	$Y_{d/s}$	Fr1	V_1	V_2	$V_{d/s}$	L	X	ΔE	THL	E_2/E_1
Y	22A	0.8d	56.3	0.9893	2.500	2.63	2.50	2.50	6.38	2.75	2.1289	4.94692	2.40749	4.88139	8.50	38.50	0.92	2.374602	0.888
Y	22B	1.0d	56.8	1.3385	2.700	3.00	3.38	3.50	7.50	3.63	1.8350	5.4428	3.10805	5.50164	12.00	-	0.61	1.688377	0.935
Y	22C	1.2d	57.4	1.6954	2.800	4.36	4.00	4.00	8.36	4.00	1.7970	5.5599	3.0027	5.95147	14.00	-	0.62	1.660870	0.941

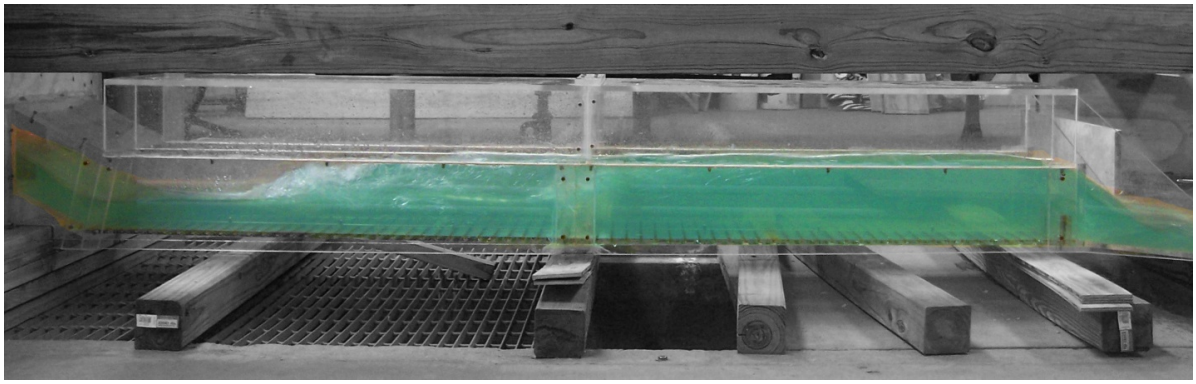

Figure A58. Experiment 23A

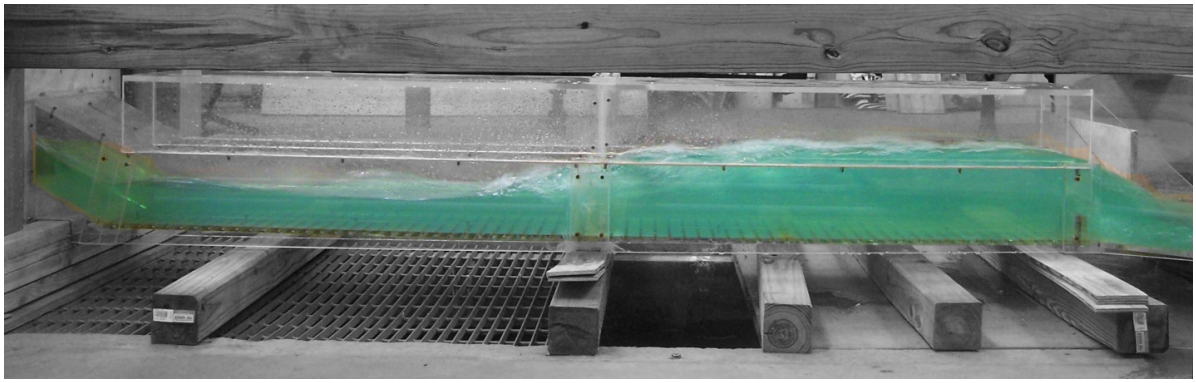

Figure A59. Experiment 23B

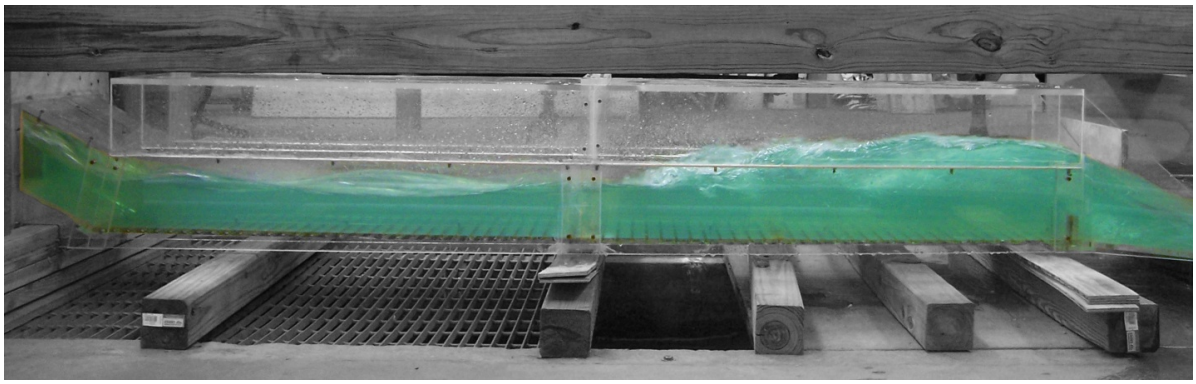

Figure A60. Experiment 23C

Table A23. Experiment 23 using Open Channel Condition with a 2 inch sill at the end of the culvert.

H.J.	Run	H	W_{temp}	Q	$V_{u/s}$	Y_s	Y_{toe}	Y_1	Y_2	$Y_{d/s}$	Fr1	V_1	V_2	$V_{d/s}$	L	X	E	THL	E_2/E_1
Y	23A	0.8d	57.4	0.9973	2.500	2.63	2.38	2.88	6.13	6.50	1.8247	5.7869	2.6004	4.81498	13.00	-	0.49	-1.25541	0.937
Y	23B	1.0d	57.5	1.3205	2.700	3.00	3.38	2.88	7.13	6.75	2.0742	6.13791	3.498	5.32316	12.00	-	0.93	-0.321621	0.897
Y	23C	1.2d	57.8	1.7279	2.800	4.36	3.88	4.25	7.88	7.25	1.6266	6.3696	3.2099	5.53082	10.50	-	0.36	-0.689130	0.964

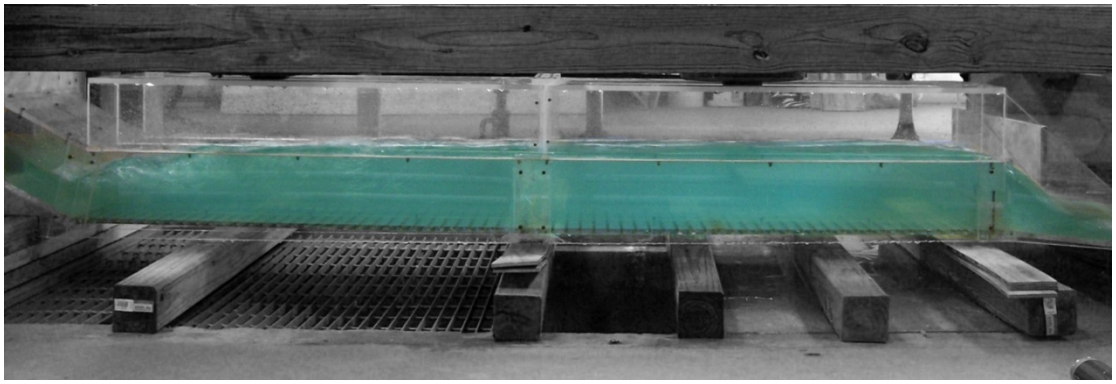

Figure A61. Experiment 24A

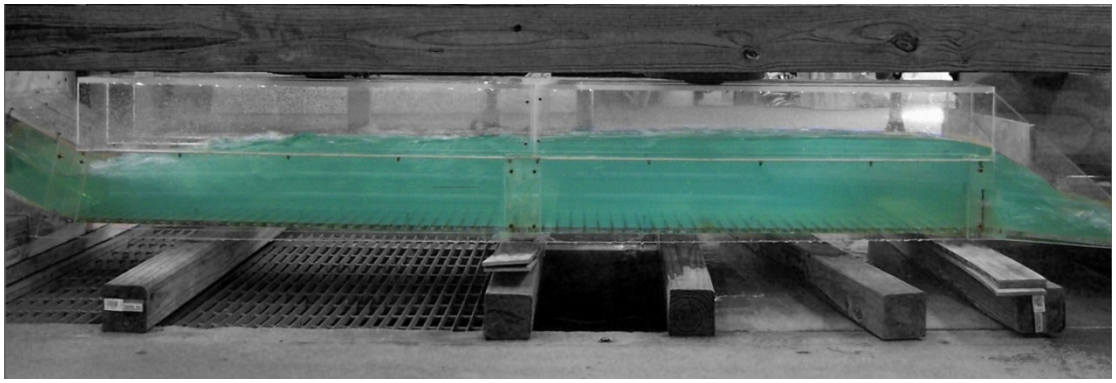

Figure A62. Experiment 24B

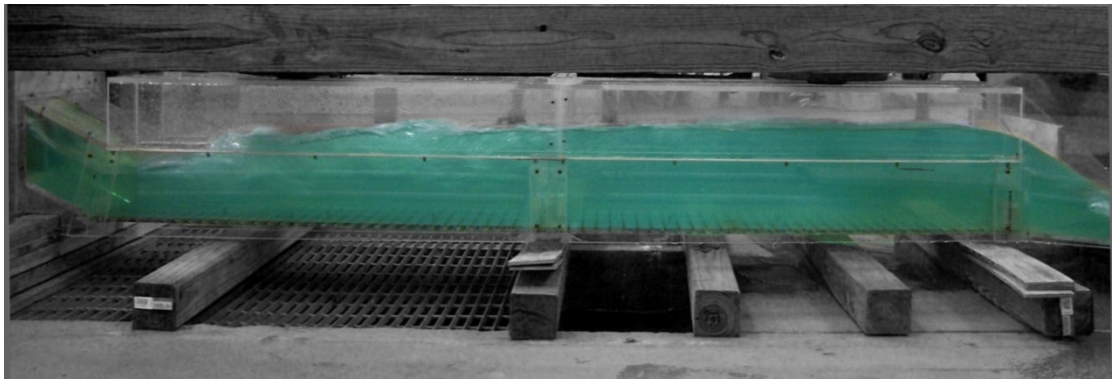

Figure A63. Experiment 24C

Table A24. Experiment 24 using Open Channel Condition with a 2.5 inch sill at the end of the culvert.

H.J.	Run	H	W_{temp}	Q	$V_{u/s}$	Y_s	Y_{toe}	Y_1	Y_2	$Y_{d/s}$	Fr1	V_1	V_2	$V_{d/s}$	L	X	ΔE	THL	E_2/E_1
Y (slope)	24A	0.8d	57.8	0.9812	2.500	2.63	4.50	2.63	6.63	6.38	2.1066	4.4687	2.2698	4.5396	10.00	-	0.92	-0.655398	0.892
Y (toe)	24B	1.0d	58.0	1.3266	2.700	3.00	3.25	3.38	7.25	6.63	1.8366	5.3833	2.8934	5.1385	13.00	82.50	0.59	-0.591649	0.935
Y	24C	1.2d	57.8	1.7210	2.800	4.36	4.00	4.25	8.63	8.13	1.7541	5.6745	3.1080	5.2623	15.00	78.50	0.57	-1.029093	0.947

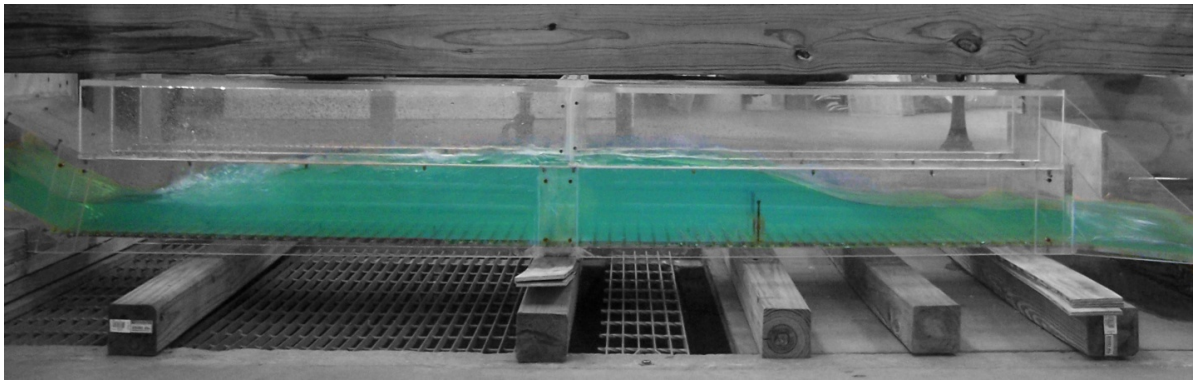

Figure A64. Experiment 25A

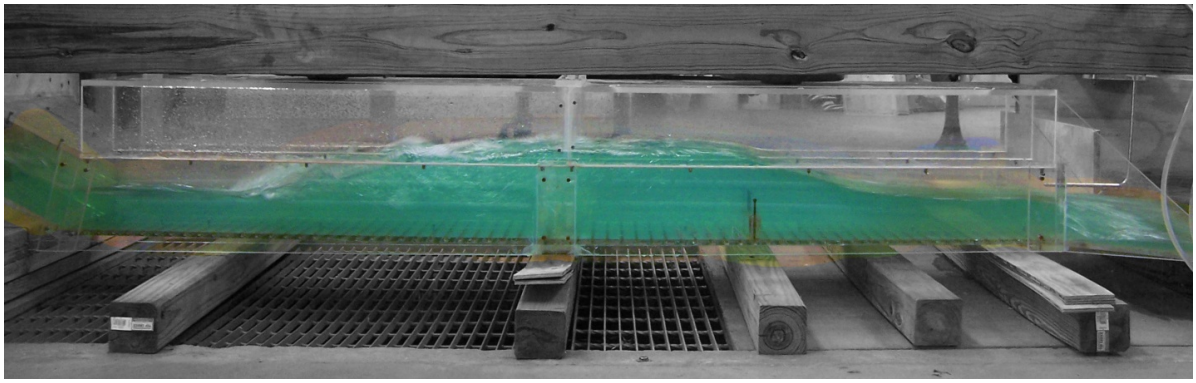

Figure A65. Experiment 25B

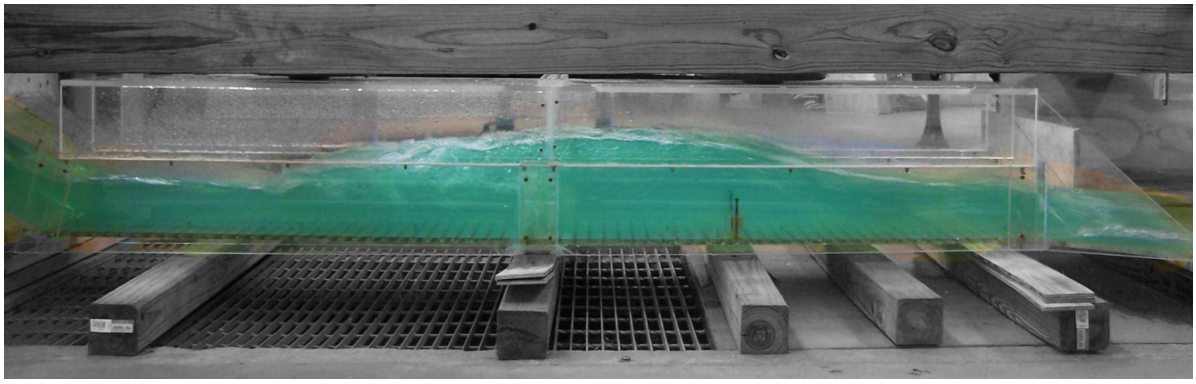

Figure A66. Experiment 25C

Table A25. Experiment 25 using Open Channel Condition with a 1.75 inch sill at 25 inches from the end of the culvert with 15 flat-faced friction blocks in front of the sill.

H.J.	Run	H	W_{temp}	Q	$V_{u/s}$	Y_s	Y_{toe}	Y_1	Y_2	$Y_{d/s}$	Fr1	V_1	V_2	$V_{d/s}$	L	X	ΔE	THL	E_2/E_1
Y	25A	0.8d	56.1	1.0053	2.500	2.63	2.38	3.00	6.50	2.75	1.8522	5.5598	2.5377	5.01159	12.00	49.75	0.55	2.134597	0.905
Y	25B	1.0d	56.2	1.3205	2.700	3.13	3.38	3.25	7.38	3.25	1.9271	5.73097	2.7799	5.44279	11.00	41.25	0.73	-0.561608	0.907
Y	25C	1.2d	56.4	1.7371	2.800	4.25	3.88	3.88	8.38	3.88	1.8472	5.9515	2.83725	5.84226	13.00	40.50	0.70	2.020869	0.920

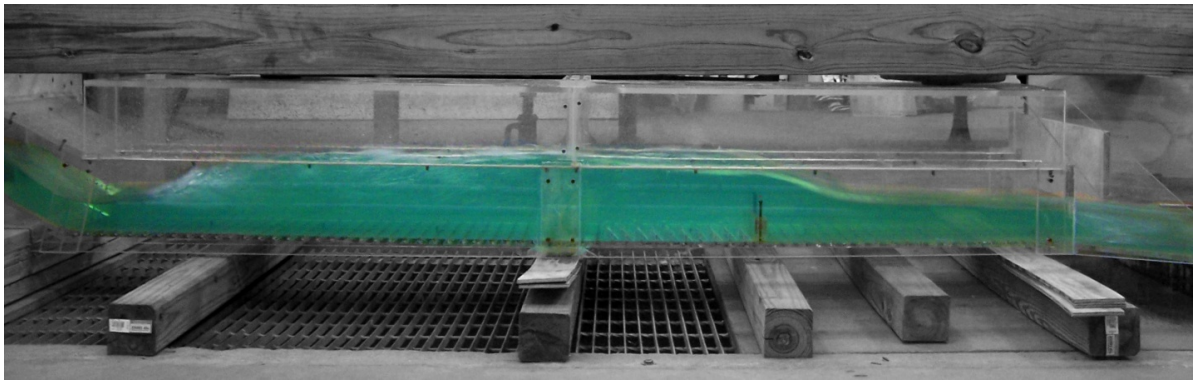

Figure A67. Experiment 26A

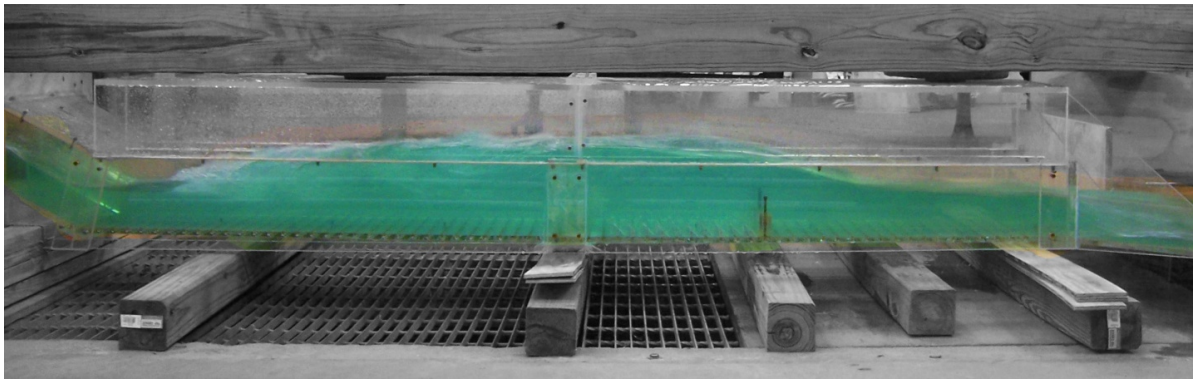

Figure A68. Experiment 26B

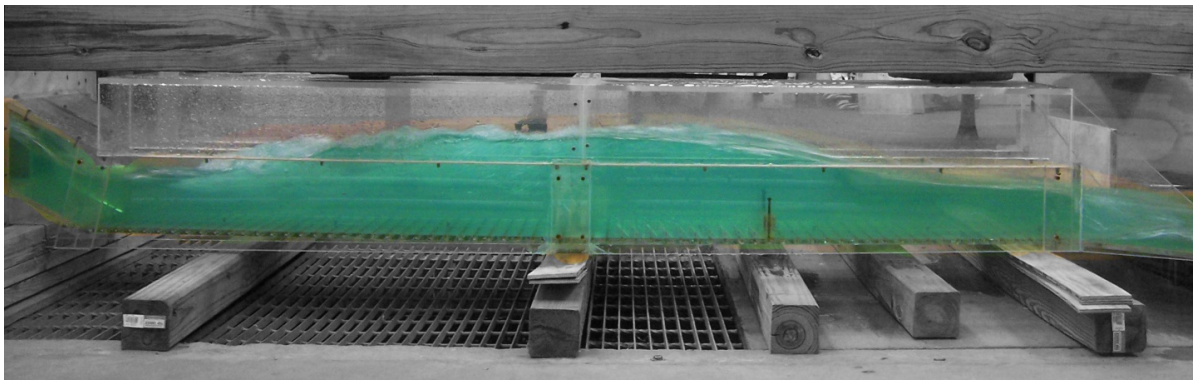

Figure A69. Experiment 26C

Table A26. Experiment 26 using Open Channel Condition with a 1.75 inch sill at 25 inches from the end of the culvert with 30 flat-faced friction blocks in front of the sill.

H.J.	Run	H	W_{temp}	Q	$V_{u/s}$	Y_s	Y_{toe}	Y_1	Y_2	$Y_{d/s}$	Fr1	V_1	V_2	$V_{d/s}$	L	X	ΔE	THL	E_2/E_1
Y	26A	0.8d	56.8	0.9893	2.473	2.38	2.38	2.38	6.38	2.63	2.2211	5.32316	2.7799	5.011586	14.00	54.00	1.05	2.229808	0.892
Y	26B	1.0d	56.8	1.3296	2.659	3.00	3.50	4.13	7.50	3.38	1.5990	5.6745	3.30877	5.3833	13.00	51.00	0.31	2.137657	0.954
Y	26C	1.2d	57.1	1.7279	2.880	4.38	3.88	4.88	8.38	3.75	1.5274	5.89712	3.20998	5.89712	14.00	48.50	0.26	2.115357	0.963

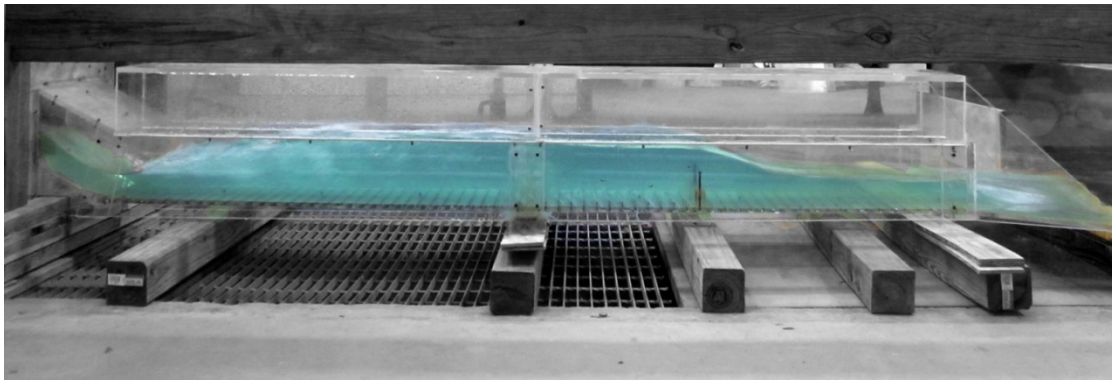

Figure A70. Experiment 27A

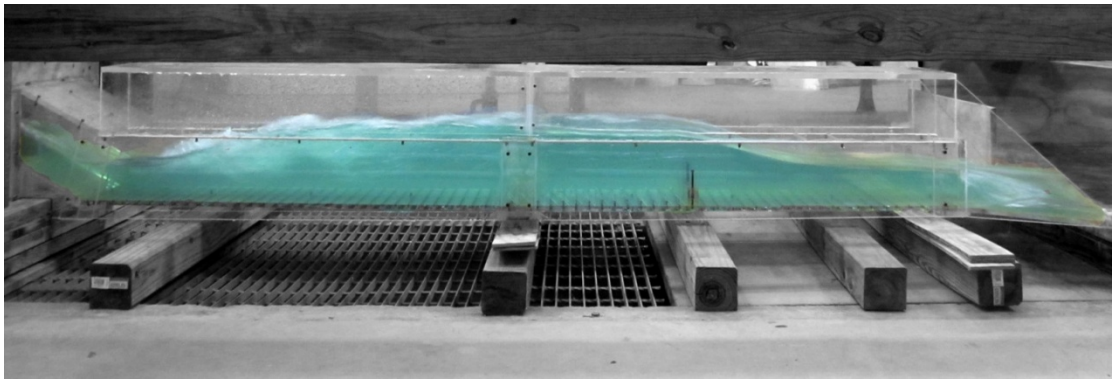

Figure A71. Experiment 27B

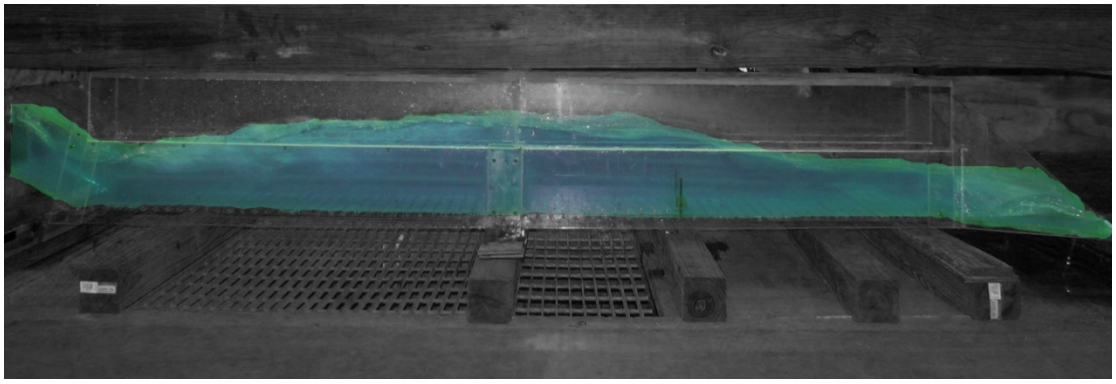

Figure A72. Experiment 27C

Table A27. Experiment 27 using Open Channel Condition with a 1.75 inch sill at 25 inches from the end of the culvert with 45 flat-faced friction blocks in front of the sill.

H.J.	Run	H	W_{temp}	Q	$V_{u/s}$	Y_s	Y_{toe}	Y_1	Y_2	$Y_{d/s}$	Fr1	V_1	V_2	$V_{d/s}$	L	X	ΔE	THL	E_2/E_1
Y	27A	0.8d	57.0	0.9893	2.473	2.63	2.38	2.38	6.50	2.75	2.2572	5.3833	2.8934	5.01159	13.00	54.00	1.13	2.109801	0.888
Y	27B	1.0d	57.1	1.3355	2.671	3.00	3.50	3.50	7.38	3.25	1.8103	5.61747	3.49799	5.44280	13.00	52.50	0.57	2.159348	0.935
Y	27C	1.2d	57.2	1.7094	2.849	3.88	4.00	4.38	8.25	3.75	1.6479	5.78688	3.8486	5.84230	14.00	52.25	0.40	2.202360	0.956

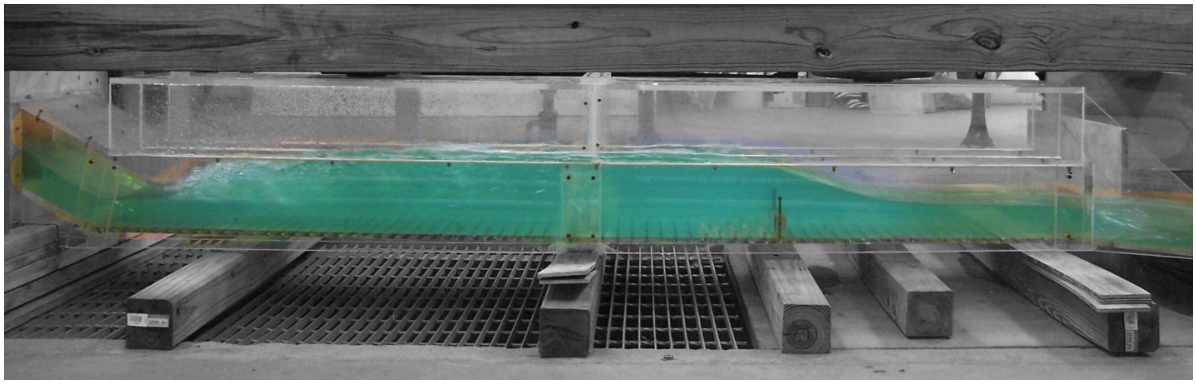

Figure A73. Experiment 28A

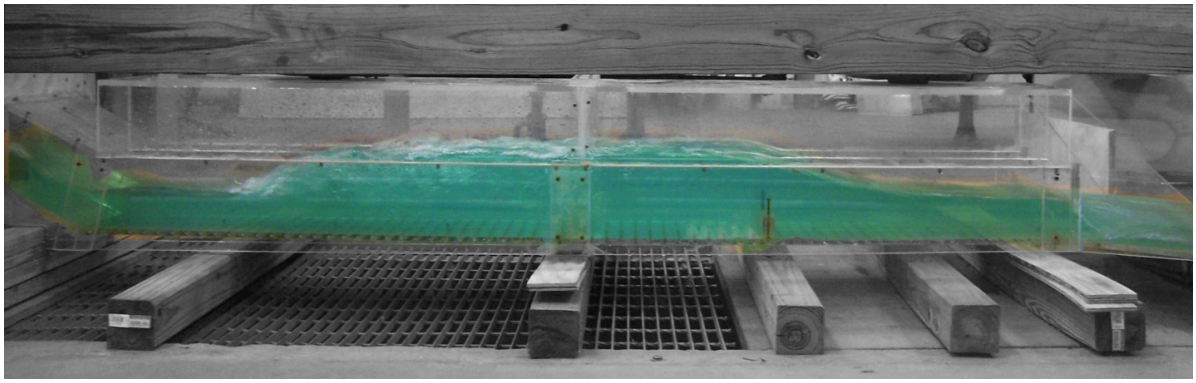

Figure A74. Experiment 28B

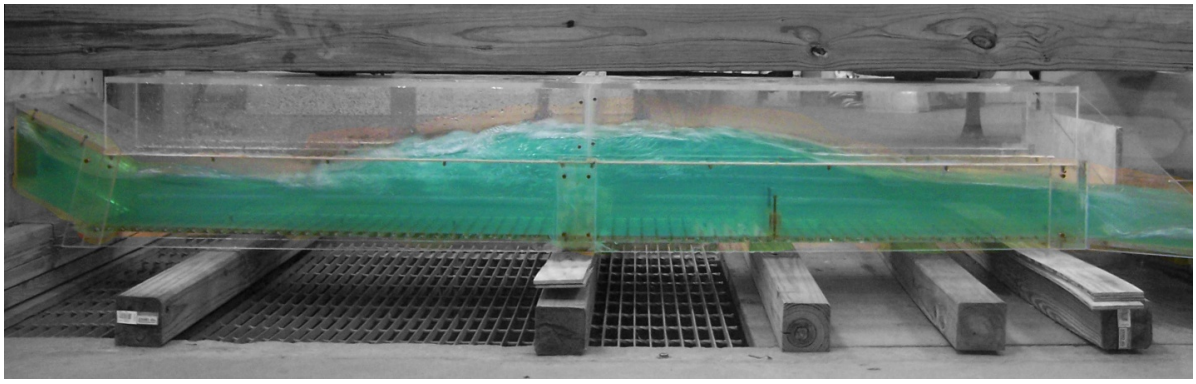

Figure A75. Experiment 28C

Table A28. Experiment 28 using Open Channel Condition with a 1.75 inch sill at 25 inches from the end of the culvert with 15 curved-face friction blocks in front of the sill.

H.J.	Run	H	W_{temp}	Q	$V_{u/s}$	Y_s	Y_{toe}	Y_1	Y_2	$Y_{d/s}$	Fr1	V_1	V_2	$V_{d/s}$	L	X	ΔE	THL	E_2/E_1
Y	28A	0.8d	57.7	0.9893	2.500	2.50	2.38	2.38	6.50	2.75	2.2572	5.2623	2.4075	5.0754	10.00	51.50	1.13	2.014655	0.866
Y	28B	1.0d	58.0	1.3325	2.700	2.88	3.38	3.50	7.13	3.38	1.7588	5.32316	3.10808	5.44279	13.00	44.00	0.48	2.058392	0.946
Y	28C	1.2d	58.6	1.7047	2.800	4.00	3.85	3.88	8.25	2.88	1.8231	5.73097	2.89345	5.89712	13.50	39.00	0.65	2.900865	0.937

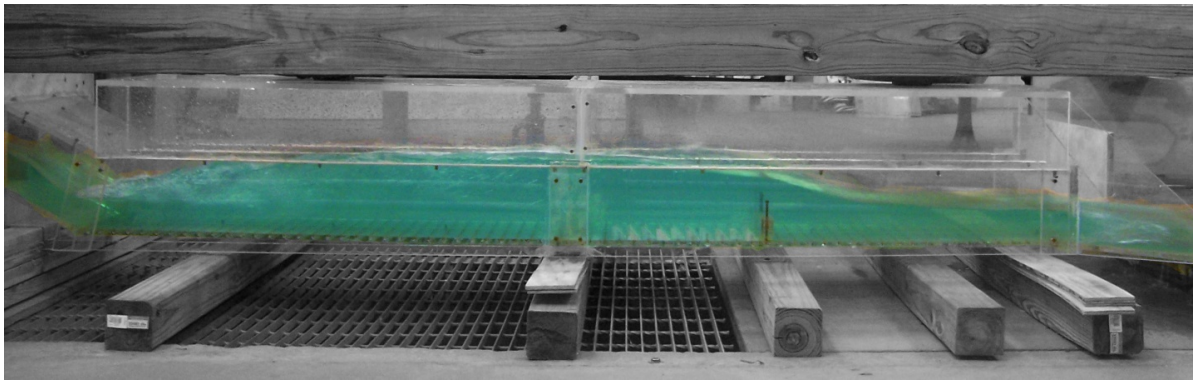

Figure A76. Experiment 29A

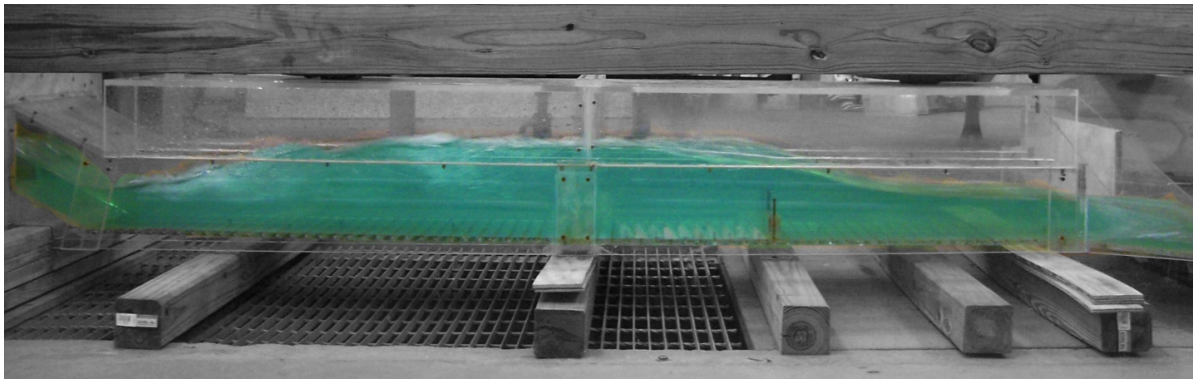

Figure A77. Experiment 29B

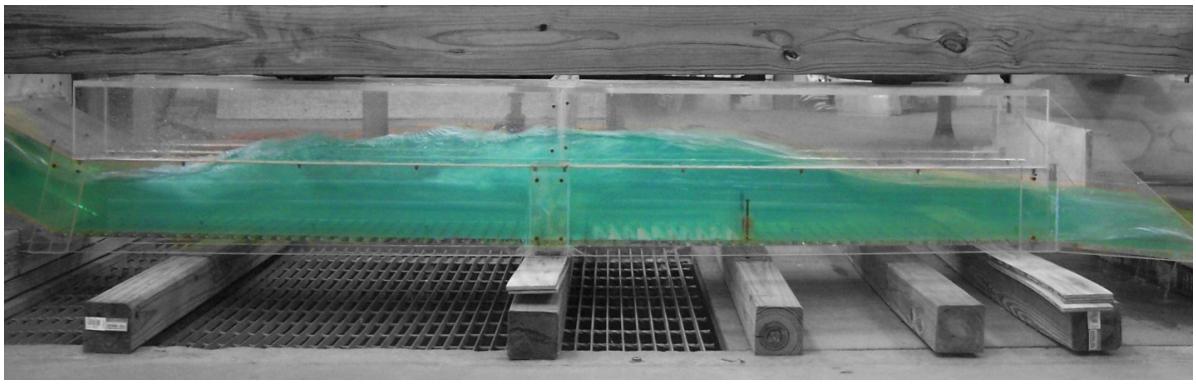

Figure A78. Experiment 29C

Table A29. Experiment 29 using Open Channel Condition with a 1.75 inch sill at 25 inches from the end of the culvert with 30 curved-face friction blocks in front of the sill.

H.J.	Run	H	W_{temp}	Q	$V_{u/s}$	Y_s	Y_{toe}	Y_1	Y_2	$Y_{d/s}$	Fr1	V_1	V_2	$V_{d/s}$	L	X	ΔE	THL	E_2/E_1
Y	29A	0.8d	59.1	0.9973	2.500	2.38	2.50	2.50	6.50	2.75	2.1633	5.01159	2.53715	4.94692	10.00	56.00	0.98	2.254593	0.882
Y	29B	1.0d	59.7	1.3084	2.700	2.88	3.25	3.25	7.50	3.38	1.9536	5.55986	2.89344	5.32316	12.00	53.00	0.79	-0.321621	0.917
Y	29C	1.2d	59.8	1.7140	2.800	4.13	4.00	4.13	8.38	4.13	1.7530	5.78688	3.10805	5.95147	12.00	49.00	0.55	1.530870	0.947

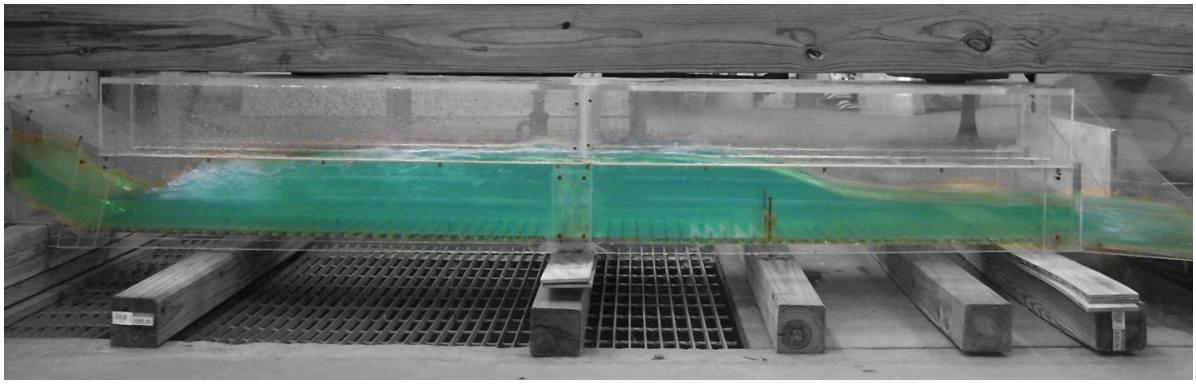

Figure A79. Experiment 30A

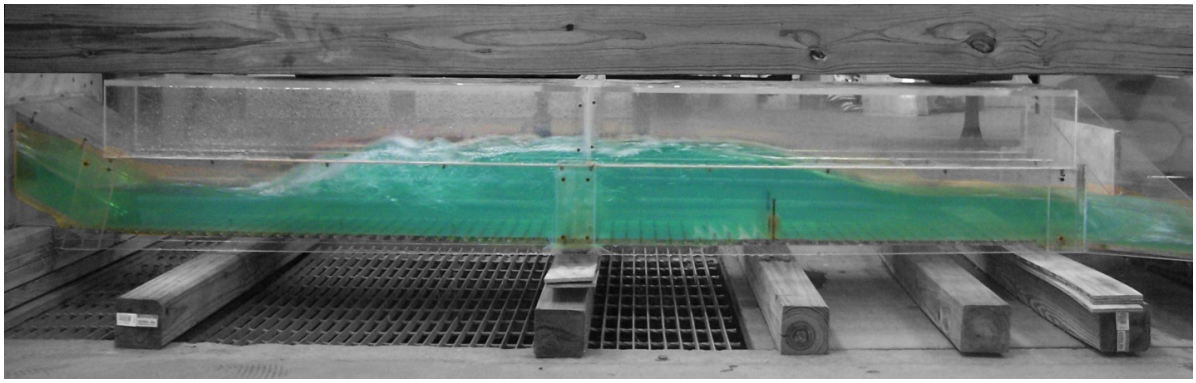

Figure A80. Experiment 30B

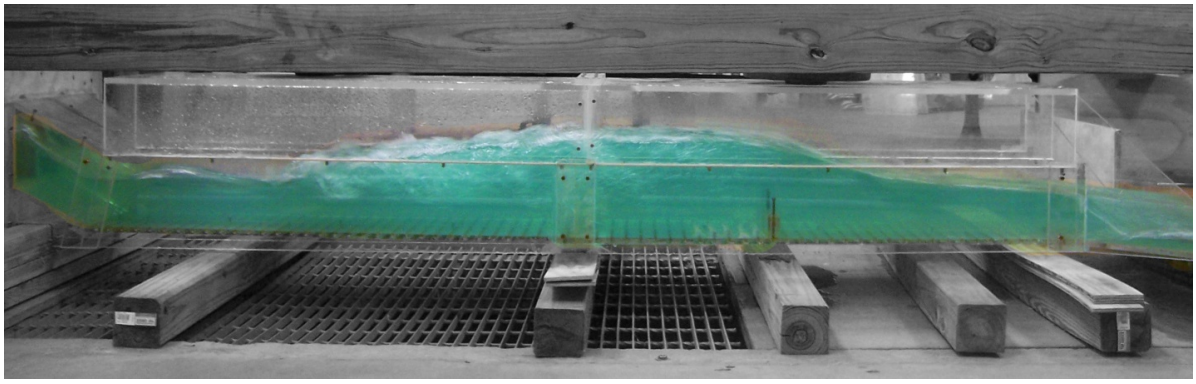

Figure A81. Experiment 30C

Table A30. Experiment 30 using Open Channel Condition with a 1.75 inch sill at 25 inches from the end of the culvert with 15 C-shaped friction blocks in front of the sill.

H.J.	Run	H	W_{temp}	Q	$V_{u/s}$	Y_s	Y_{toe}	Y_1	Y_2	$Y_{d/s}$	Fr1	V_1	V_2	$V_{d/s}$	L	X	ΔE	THL	E_2/E_1
Y	30A	0.8d	59.6	0.9933	2.500	2.63	2.38	2.50	6.63	2.75	2.2006	5.4723	2.4075	5.01159	14.00	53.00	1.06	2.134590	0.876
Y	30B	1.0d	59.9	1.3175	2.700	3.00	3.80	3.50	7.38	3.25	1.8103	5.9515	2.7799	5.3533	13.00	44.25	0.57	2.368418	0.939
Y	30C	1.2d	60.2	1.7071	2.800	4.50	3.88	4.00	8.25	4.00	1.7771	6.2161	2.66158	5.8971	10.00	41.50	0.58	1.780909	0.944

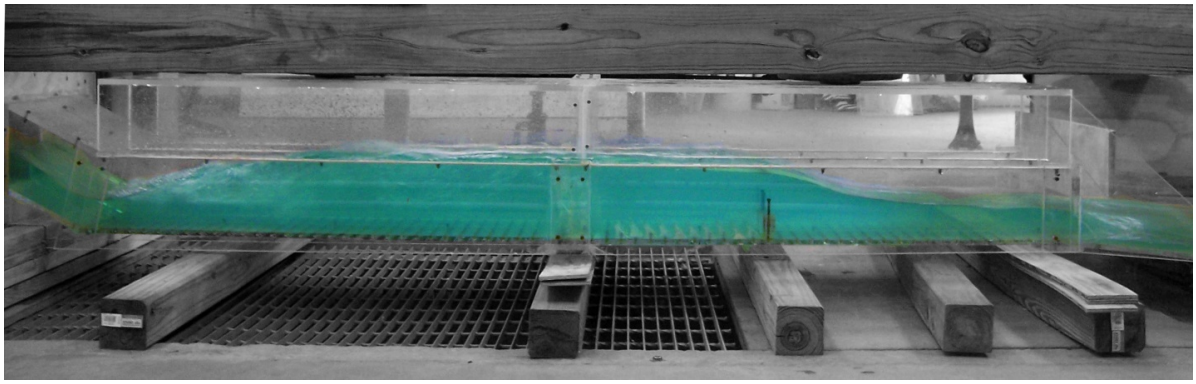

Figure A82. Experiment 31A

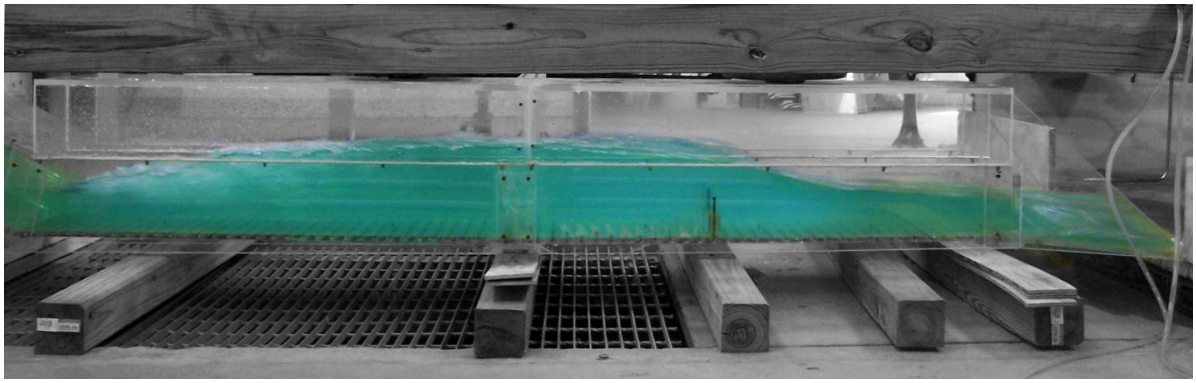

Figure A83. Experiment 31B

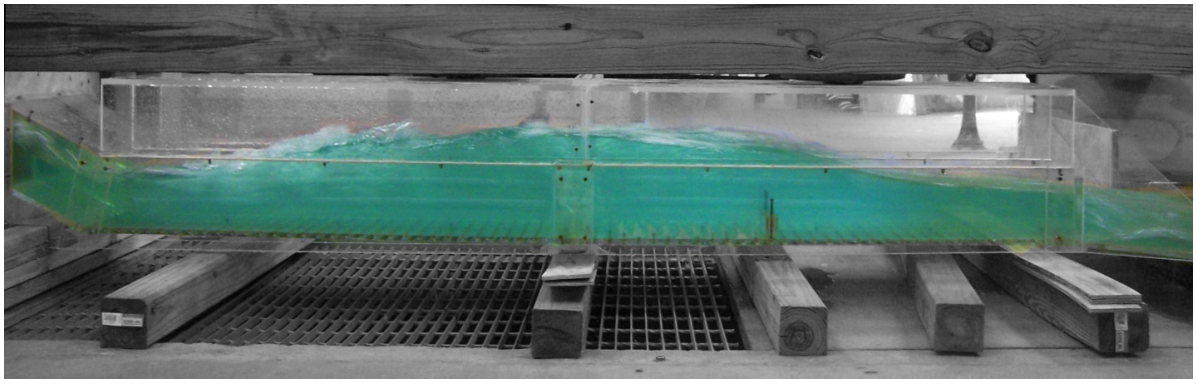

Figure A84. Experiment 31C

Table A31. Experiment 31 using Open Channel Condition with a 1.75 inch sill at 25 inches from the end of the culvert with 15 C-shaped friction blocks in front of the sill.

H.J.	Run	H	W_{temp}	Q	$V_{u/s}$	Y_s	Y_{toe}	Y_1	Y_2	$Y_{d/s}$	Fr1	V_1	V_2	$V_{d/s}$	L	X	ΔE	THL	E_2/E_1
Y	31A	0.8d	60.8	0.9937	2.500	2.63	2.50	2.50	6.50	2.88	2.1633	5.07543	2.77992	4.94690	10.00	55.50	0.98	2.12463	0.882
Y	31B	1.0d	61.1	1.3175	2.700	3.00	3.38	4.00	7.50	3.25	1.6417	5.55986	3.10803	5.35330	11.00	53.00	0.36	2.368418	0.962
Y	31C	1.2d	61.3	1.7302	2.800	4.00	3.88	5.00	8.50	4.25	1.5149	5.75899	3.4047	5.89712	13.50	52.50	0.25	1.530865	0.977

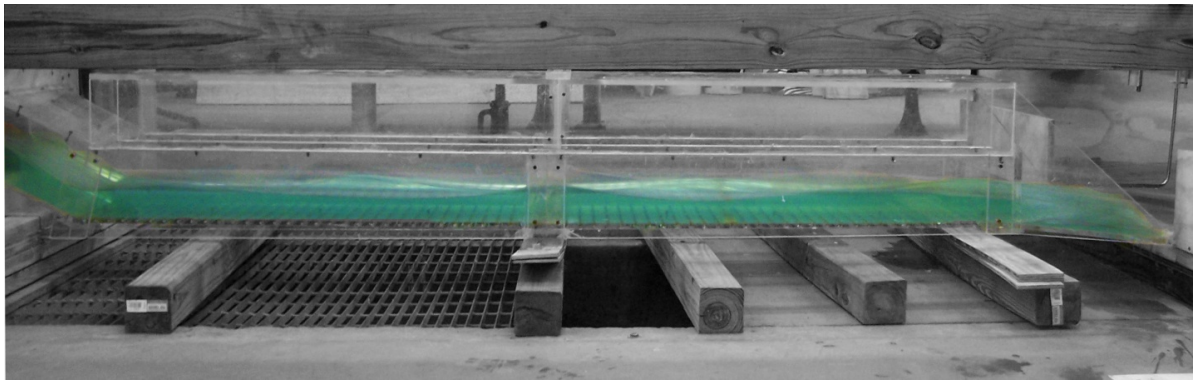

Figure A85. Experiment 32A

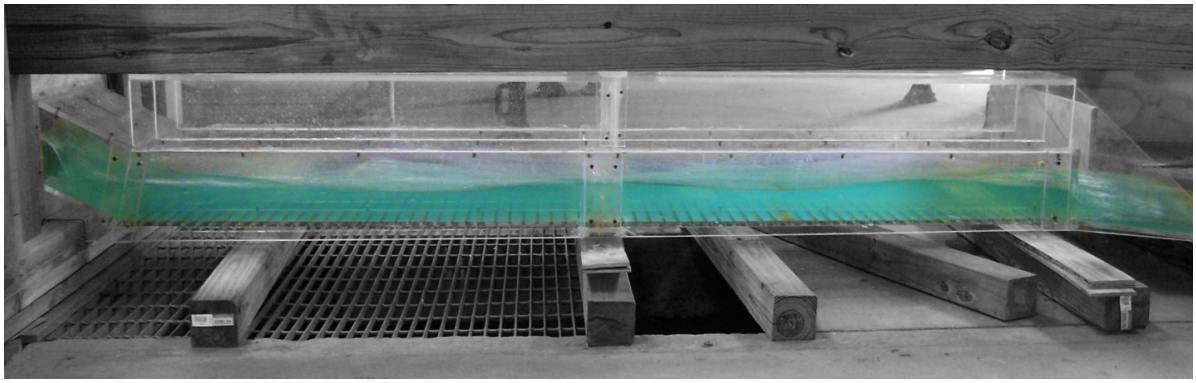

Figure A86. Experiment 32B

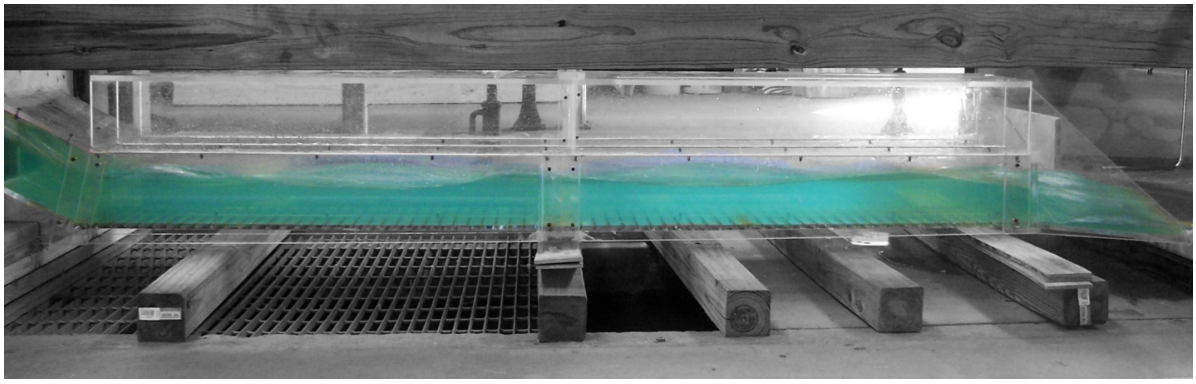

Figure A87. Experiment 32C

Table A32. Experiment 32 using Open Channel Condition with no sill in the culvert.

H.J.	Run	H	W_{temp}	Q	$V_{u/s}$	Y_s	Y_{toe}	Y_1	Y_2	$Y_{d/s}$	Fr1	V_1	V_2	$V_{d/s}$	L	X	ΔE	THL	E_2/E_1
N	32A	0.8d	53.4	0.9852	2.500	2.75	2.38	-	-	2.00	2.3118	5.8423	-	6.0587	-	-	-	0.724625	-
N	32B	1.0d	53.3	1.3444	2.700	2.50	3.25	-	-	2.63	1.9969	5.8971	-	6.34429	-	-	-	0.828382	-
N	32C	1.2d	53.6	1.7348	2.800	3.78	4.00	-	-	3.25	1.8412	6.03208	-	6.444998	-	-	-	1.270870	-

APPENDIX B

CALCULATIONS

B.1 Incomplete Jump calculations (excepts from Lowe 2008)

Momentum background and assumptions

Complete and incomplete hydraulic jumps are ideal candidates for the application of momentum theory, because a "precise mathematical description of the internal flow pattern is not possible" due to its complexity (Sturm 2001), and the stability of a jump depends entirely upon the equilibrium between the momentum flux across the jump, and the external forces acting upon it (Chadwick et al. 2004). Figure B1 depicts the forces typically considered when applying momentum theory to a hydraulic jump.

To simplify the momentum problem several assumptions are commonly made. First, generally the channel is assumed to be straight and prismatic. This precludes any corrections needed for longitudinal anomalies, such as abrupt expansions or steps. Although, there is an expansion at the downstream wingwall in this study the assumption is still valid because the expansion is gradual. Second, the slope is assumed to be horizontal. This assumption eliminates the weight term, and is justifiable for slopes up to 5% (Hager 1999). In this study the slope there the jump is occurring is within that limit, at 1%. Third, the channel is assumed to be relatively smooth, such that the effects of friction within the control volume may be considered negligible when compared to the other forces involved. The length of the jump is typically short enough for this to be a valid assumption (Montes 1998). Fourth, the pressure distributions at sections (1) and (2) are assumed to be hydrostatic, such that the pressure forces may be expressed in terms of the cross-sectional area of flow, A, and the distance from the water surface to the centroid of the cross-sectional area. This assumption may be unrealistic, but correcting for it

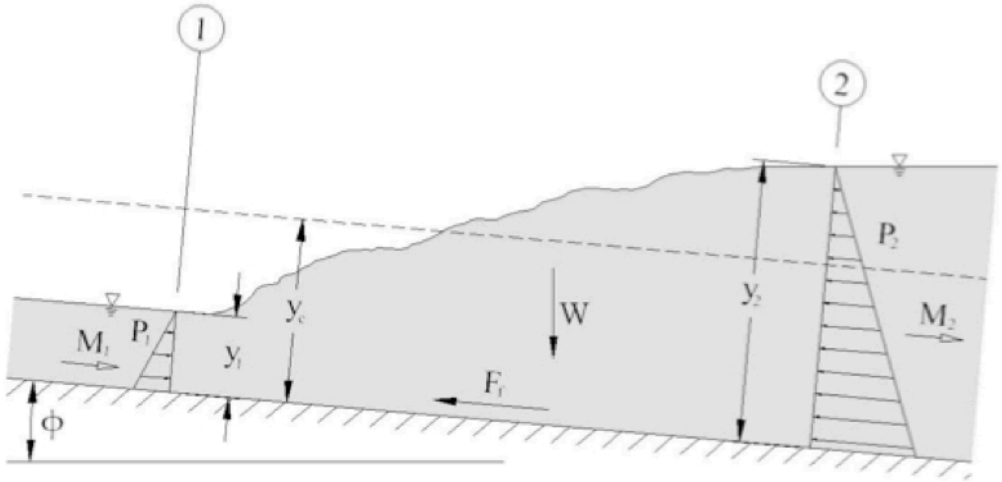

Figure B1 Typical forces acting on a hydraulic jump y1, y2 = flow depth; yc = critical depth; M1, M2 = momentum forces; P1, P2 =pressure forces; W = weight; F1 = friction; ϕ = bed slope angle.

appears to make little difference (Hughes and Flack 1984). Fifth, the velocity distributions at sections (1) and (2) are assumed to be uniform, which allows for the use of average velocity. This is also hardly accurate, but it produces acceptable results nonetheless, since the effects of turbulence flux appear to counteract the effects of velocity distribution (Harleman 1959). Sixth, air entrainment is assumed in this study to be negligible, such that section (2) may still be considered one-phase flow. The effects of air entrainment increase exponentially with the upstream Froude number (Kalinske and Robertson 1943; Haindl and Sotornik 1957), but in relatively flat conduits such as those considered in this study, Froude numbers are typically small enough (i.e. less than 5) to have little effect on the solution. And seventh, the effects of viscosity are assumed to be negligible, typically justified by the large Reynolds numbers involved (Rajaratnam 1968b).

Most research on hydraulic jumps has dealt with open channel rather than closed conduit flow (Montes 1998), although researchers have been studying the latter since 1938, beginning with Lane and Kinsvatar (1938). Since the focus of this study is on hydraulic jumps in closed conduits, open-channel jumps are not discussed here.

Hydraulic jumps in closed conduits behave similarly to open-channel jumps, as long as a free surface remains and sufficient air is supplied above the flow. What makes closed-conduit jumps different is that they potentially can, due to downstream submergence, fill the conduit completely, resulting in pressure flow conditions within the barrel (Caric 1977; Hager 1999). This phenomenon is known as an incomplete or pressure jump, as opposed to a complete or free-surface jump (Hotchkiss et al. 2003; Montes 1998), and because of the inherent dissimilarities between the two, each must be

approached differently.

One example of closed-conduit jump behavior occurs within culvert barrels. Under inlet control conditions, in which flow through a culvert becomes supercritical, high flow velocities at the outlet can potentially scour the streambed and undercut the culvert barrel. Oftentimes to prevent this from happening, culvert designers will install energy dissipaters at the outlet or within the culvert itself, but these devices can be costly. A significantly less-expensive alternative is to force a hydraulic jump to occur within the culvert barrel by controlling the tailwater. The culvert itself protects the channel against erosion, while the hydraulic jump dissipates energy, thereby reducing the need for further dissipaters downstream (Hotchkiss et al. 2005). If the outlet of the culvert is not submerged, a complete hydraulic jump can form within the culvert barrel; otherwise the jump must be incomplete.

Figure 2.2 depicts typical profiles for complete and incomplete closed-conduit jumps. In the case of complete jumps, the subcritical sequent depth is less than the rise (ft, m) of the conduit (i.e. $y2 < D$), whereas in the case of incomplete jumps, it is greater (i.e. $y2 > D$). Since the flow depth in incomplete jumps cannot reach the expected sequent depth, the deficit is supplemented by the hydrostatic pressure head (ft, m) against the top of the conduit, symbolized in this figure as H (Montes 1998). It should be noted that the pressure head at section (2) depends only upon the pressure head at the outlet, the slope of the conduit, and the hydraulic grade line, not on the jump itself; H is merely used to solve for y2 when the jump is at equilibrium (Haindl 1957).

Hypothetically, a point should exist at which the conduit becomes “just full” at section (2), or at which the subcritical flow depth exactly meets the crown of the conduit

(i.e. y2 = D). This situation marks the transition between complete and incomplete jumps, and is therefore named here as a "transitional" jump. In practice, this condition is rare if not impossible, because as y approaches D, "choking" occurs, in which the flow abruptly and spontaneously fills the conduit and becomes pressurized (Hager 1999). In theory, however, it is important to determine the conditions under which this transition will occur, so that the appropriate method (i.e. complete or incomplete) may be used to calculate the subcritical sequent depth.

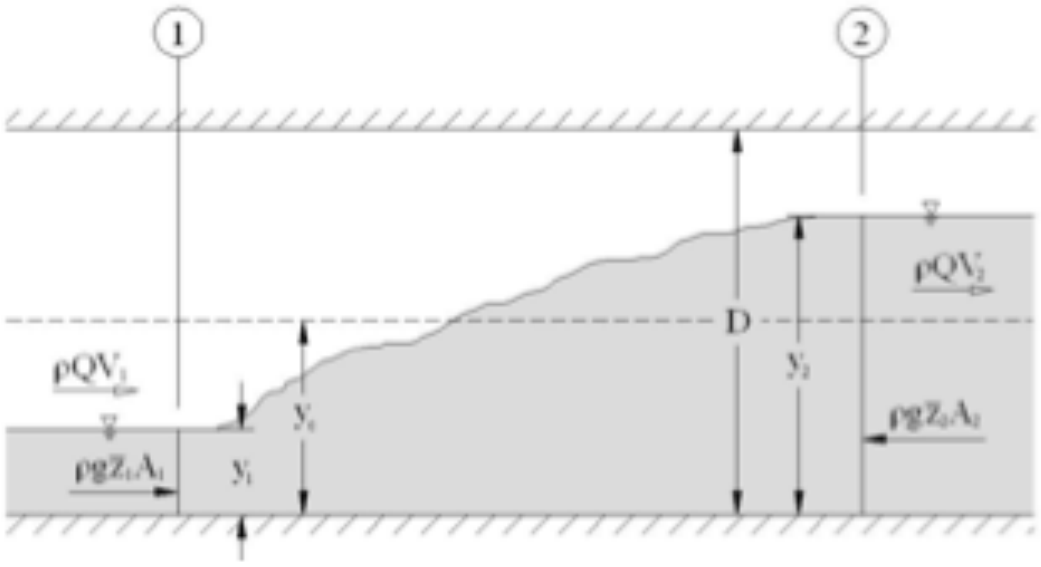

(a)

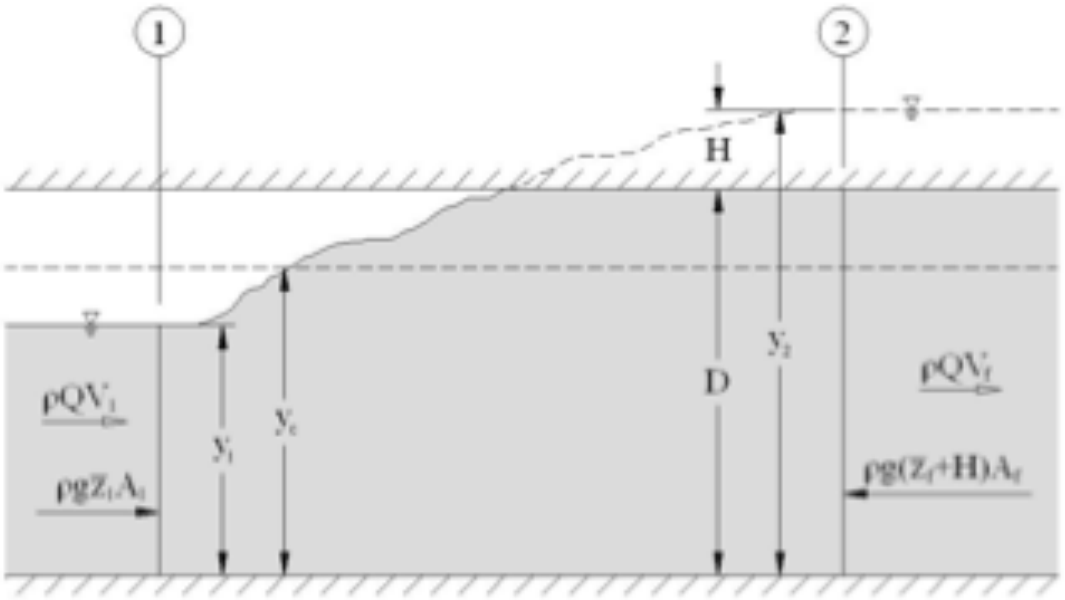

(b)

Figure 2-2 Forces acting on (a) complete and (b) incomplete hydraulic jumps in **closed conduits (ρ = water density; g = acceleration** of gravity; Q = flow rate; V_1, V_2, V_f = average flow velocity; $\bar{Z}_1$, $\bar{Z}_2$, $\bar{Z}_f$ = distance to centroid of flow; A_1, A_2, A_f = area of flow; H = pressure head against top of conduit)

B.2 Rectangular Conduits

B.2.1 Definitions

Figure B-2 below depicts the parameters used for rectangular conduits.

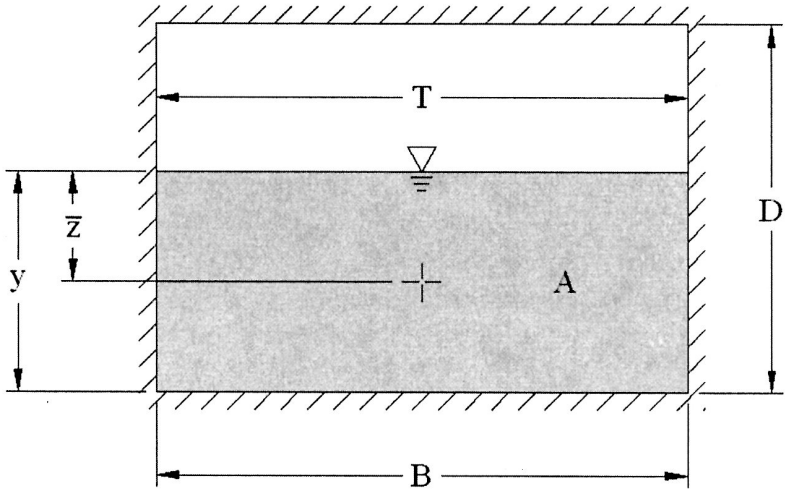

Figure B-2 Cross section for rectangular conduits

The top width (Γ), area (Ω), and centroid-area (Ψ) functions for rectangular conduits are given by the following equations (Sturm 2001):

$$\Gamma(\text{rect},y') = T' = \frac{T}{B} = \frac{B}{B} = 1 \tag{B-26a}$$

$$\Omega(\text{rect},y') = A' = \frac{A}{BD} = \frac{By}{BD} = \frac{y}{D} = y' \tag{B-26b}$$

$$\Psi(\text{rect},y') = (\bar{z}A)' = \frac{\bar{z}A}{BD^2} = \frac{By^2}{2BD^2} = \frac{1}{2}\left(\frac{y}{D}\right)^2 = \frac{1}{2}(y')^2 \tag{B-26c}$$

B.2.2 Solution

B.2.2.1 Complete Jumps

Inserting Equations B-26a through B-26c into Equation B-20 using Equations B-15 through B-18 yields the following equation for complete jumps:

$$Fr_1^{\,2} = \frac{(1)(y'_2)\left[\left(\frac{1}{2}y'^{\,2}_2\right)-\left(\frac{1}{2}y'^{\,2}_1\right)\right]}{(y'_1)^2[(y'_2)-(y'_1)]} = \frac{1}{2}\left(\frac{y'_2}{y'_1}\right)^2 + \frac{1}{2}\left(\frac{y'_2}{y'_1}\right) \tag{B-27}$$

This may be further reduced to a dimensionless form of the well-known Belanger equation, as follows:

$$\frac{1}{2}\left(\frac{y'_2}{y'_1}\right)^2 + \frac{1}{2}\left(\frac{y'_2}{y'_1}\right) - Fr_1^{\,2} = 0 \tag{B-28}$$

$$\frac{y'_2}{y'_1} = \frac{-\left(\frac{1}{2}\right) \pm \sqrt{\left(\frac{1}{2}\right)^2 - 4\left(\frac{1}{2}\right)\left(-Fr_1^{\,2}\right)}}{2\left(\frac{1}{2}\right)} = \frac{1}{2}\left(\sqrt{1+8Fr_1^{\,2}} - 1\right) \tag{B-29}$$

$$y'_2 = \frac{y'_1}{2}\left(\sqrt{1+8Fr_1^{\,2}} - 1\right) \tag{B-30}$$

B.2.2.2 Incomplete Jumps

Inserting Equations B-26a through B-26c into Equation B-24 using Equations B-15 through B-18 yields the following equation:

$$y'_2 = 1 + \frac{1}{(1)(y'_f)^2}\left\{Fr_1^{\,2}(y'_1)^2[(y'_f)-(y'_1)]-(1)(y'_f)\left[\left(\frac{1}{2}y'^{\,2}_f\right)-\left(\frac{1}{2}y'^{\,2}_1\right)\right]\right\} \qquad \text{(B-31)}$$

By combining like terms and rearranging, and noting that y'_f by definition equals 1, the following equation is obtained for incomplete jumps:

$$y'_2 = \frac{1}{2} + \left(Fr_1^{\,2} + \frac{1}{2}\right)y'^{\,2}_1 - Fr_1^{\,2}y'^{\,3}_1 \qquad \text{(B-32)}$$

B.2.2.3 Transitional Jumps

Inserting Equations B-26a through B-26c into Equation B-25 using Equations B-15 through B-18 yields the following equation for the transition between complete and incomplete jumps:

$$(Fr_1)_t^{\,2} = \frac{(1)(y'_f)\left[\left(\frac{1}{2}y'^{\,2}_f\right)-\left(\frac{1}{2}y'^{\,2}_1\right)\right]}{(y'_1)^2[(y'_f)-(y'_1)]} \qquad \text{(B-33)}$$

which reduces to:

$$(Fr_1)_t = \sqrt{\frac{1+y'_1}{2y'^{\,2}_1}} \qquad \text{(B-34)}$$

B.2.3 Sequent Depth Chart

A visual representation of Equations B-30, B-32, and B-34 is shown Figure B-3 on the next page. This is modeled after the format used by Montes (1998), and provides a simple and effective shortcut for finding the sequent depth for any upstream depth and Froude number in rectangular conduits.

Several observations should be made at this point about graphically determining the sequent depth using this type of chart. Note that although the sequent depth is often treated as the dependant variable as in this derivation, y'_2 in Figure B-3 is placed on the abscissa to suggest that hydraulic jumps are induced by downstream conditions, not upstream, although supercritical flow is also a prerequisite for the formation of a hydraulic jump. Note also that for all Fr_1, as y'_1 increases and approaches about 0.67, y'_2 reaches a maximum, and as y'_1 approaches 1, y'_2 also approaches 1, consistent with the observations of Smith and Chen (1989). This suggests that for conduits flowing less than 2/3 full, the downstream depth increases with the upstream depth and Froude number; for conduits flowing more than 2/3 full, the downstream depth still increases with the upstream Froude number, but decreases with the upstream depth; for conduits flowing full, no jump will occur for any upstream Froude number. As the following sections demonstrate, these observations apply to all closed conduit shapes.

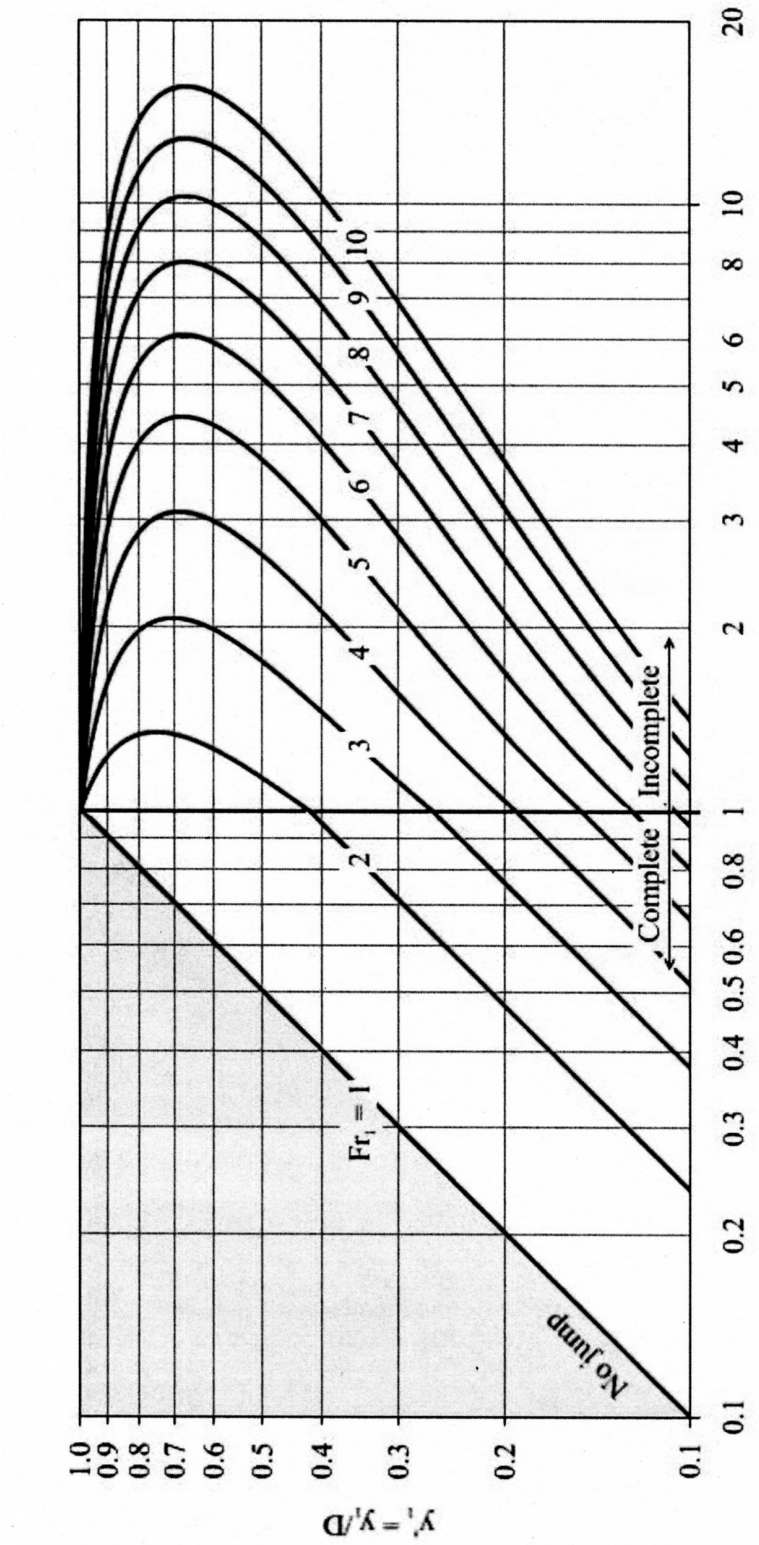

Figure B-3 Sequent depth ratio chart for rectangular conduits

B.3 Specific Momentum Equation Derive (excepts of Lowe 2008)

The nature of the hydraulic jump cannot be accounted for by use of the energy equation, because there is a substantial dissipation of energy owning to the turbulence associated with the jump. However, because momentum is conserved across hydraulic jumps under assumptions discuss later, momentum theory may be applied to determine the jump size and location (Hotchkiss et al. 2003). Momentum theory states that the sum of the external forces acting upon a system equals the change in momentum across that system (Thompson and Kilgore 2006). This principle can successfully be applied to complete or incomplete hydraulic jumps such as those shown in Figure 2.3. According to this figure, and using an axis parallel to the channel, a one-dimensional form of the momentum equation may be written:

$$P_1 - P_2 + W \sin\phi - F_f = M_2 - M_1$$

where P_1 and P_2 are the pressure forces (lbs, N) at sections (1) and (2), respectively; W is the weight (lbs, N) of the fluid within the control volume; ϕ is the bed slope angle (degrees) from the horizontal; Ff is the force of friction (lbs, N) caused by the channel or conduit; and M_1 and M_2 are the momentum fluxes (lbs, N) at sections (1) and (2), respectively.

$$P_1 = \rho_1 g \bar{z}_1 A_1 \cos\phi$$

$$\rho_1 = \rho_w$$

where ρ_1 is the density of water (slugs/ft3, kg/m3) at section (1); g is the acceleration (ft/s2, m/s2) due to gravity; $\bar{z}_1$ is the distance (ft, m) from the water surface to the centroid of the cross-sectional area at section (1), perpendicular to the channel; and A_1 is

the cross-sectional area (ft^2, m^2) at section (1). Again assuming hydrostatic pressure distribution, the pressure force at section (2) is given by:

$$P_2 = \rho_2 g \bar{z}_2 A_2 \cos\phi$$

where ρ_2 is the average density of the water (slugs/ft^3, kg/m^3) at section (2); $\bar{z}_2$ is the distance (ft., m) from the water surface to the centroid of the cross-sectional area at section (2), perpendicular to the channel; and A_2 is the cross-sectional area (ft^2, m^2) at section (2). Due to air entrainment within the jump, the density of the water leaving the control volume is on average less than that entering it, such that ρ_2 is given approximately by:

$$\rho_2 \approx \frac{\rho_w}{1 + \beta_a}$$

where β_a is the ratio of air to water after the jump. Kalinske and Robertson (1943) and Haindl and Sotornik (1957) found this to be a function of the upstream Froude number only, regardless of channel shape or slope:

$$\beta_a = 0.0066(F_{r1} - 1)^{1.4}$$

The weight of the fluid within the control volume may be expressed in a variety of different ways. Conceptually, if the distance (ft., m) parallel to the channel or conduit axis is measured from section (1) downstream, denoted by x, then the weight may be approximated mathematically as the integral of the incremental weight of the water summed over the entire control volume, given by:

$$W = \int dW = \int \rho g dV = \int_0^{L_j} \rho g A dx$$

The frictional force may also be expressed in a variety of ways, but conceptually it is the cumulative shear stress (psf, Pa), τ_0, over the wetted surface between sections (1) and (2). If the distance (ft, m) around the wetted perimeter (P_w) from one side to a point along the wetted perimeter at any point (x) along the jump is measured, denoted by λ, then the frictional force may be approximated mathematically as the integral of the shear stress over the cumulative wetted area, given by:

$$F_f = \int \tau_0 dA = \int_0^{L_j} \left(\int_0^{P_w} \tau_0 d\lambda \right) dx$$

On the right side of the momentum equation, the momentums at sections (1) and (2) are given by:

$$M_1 = \beta_1 \rho_1 Q V_1$$

$$M_2 = \beta_2 \rho_2 Q V_2$$

where β_1 and β_2 are the Boussinesq velocity distribution coefficients at sections (1) and (2), respectively, V_1 and V_2 are the velocities (ft/s, m/s) at sections (1) and (2), respectively, and Q is the flow rate (cfs, cms) through the channel or conduit. By continuity, $V_1 = Q/A_1$ and $V_2 = Q/A_2$. Combining these equations, the momentum equation in its full form may be written as:

$$\rho_W g \bar{z}_1 A_1 \cos\phi - \left(\frac{\rho_w}{1+\beta_a} \right) g \bar{z}_2 A_2 \cos\phi + \left(\int_0^{L_j} \rho g A dx \right) \sin\phi - \int_0^{L_j} \left(\int_0^{P_w} \tau_0 d\lambda \right) dx$$

$$= \frac{\beta_2 \rho_w Q^2}{A_2(1+\beta_a)} - \frac{\beta_1 \rho_w Q^2}{A_1}$$

Dividing through by ρ_w and assuming a horizontal bed slope (i.e. $\phi = 0^0$), no air entrainment (i.e. $\beta_a = 0$), no friction (i.e. $\tau_0 = 0$), and uniform velocity distributions at section (1) and (2) (i.e. $\beta_1 = \beta_2 = 1$), the momentum equation may be reduced to its simplest form:

$$g(\bar{z}A)_1 - g(\bar{z}A)_2 = \frac{Q^2}{A_2} - \frac{Q^2}{A_1}$$

If T_1 is defined as the top width of flow at section (1), then by rearranging and multiplying both sides of by ${T_1}/{{A_1}^3}$, the following relationship may be found (Montes 1998):

$$\frac{Q^2 T_1}{g{A_1}^3} = \frac{T_1 A_2[(\bar{z}A)_2 - (\bar{z}A)_1]}{{A_1}^2(A_2 - A_1)}$$

B.4 Incomplete Jump Theory (excepts from Lowe 2008)

Incomplete hydraulic jumps are defined here as closed conduit jumps in which the downstream subcritical flow becomes pressurized, i.e. y2 ≥ D (see Figure). In this the sequent depth $y_2$does not exist except in theory, because the water surface meets the top of the conduit within the control volume before such a depth can be reached. The depth y_2 may instead be considered as the pressure head (ft, m) at section (2), measured from the conduit bottom, or the sum of the rise of the conduit, D, and the pressure head (ft, m), H, above the conduit (Montes 1998). In its dimensionless form, y'_2 is therefore expressed as:

$$y'_2 = 1 + H'$$

where $H' \equiv H/D$ is the dimensionless pressure head above the conduit.

The flow area A2 cannot exceed the cross sectional area of the conduit itself, so for pressure flow the subscript '2' is replaced by 'f' to denote full conditions (i.e. y'f = 1). The centroid may also be considered as the sum of the centroid at full conditions, $\bar{z}_f$ and the pressure head above the top of the conduit, H. With this notation, Equation on page 135 $\frac{Q^2 T_1}{g {A_1}^3} = \frac{T_1 A_2 [(\bar{z}A)_2 - (\bar{z}A)_1]}{{A_1}^2 (A_2 - A_1)}$ may be rewritten in a dimensionless form for incomplete jumps:

$$Fr_1^{\,2} = \frac{T'_1 A'_f \left[(\bar{z}A)'_f + H' A'_f - (\bar{z}A)'_1\right]}{{A'_1}^2 \left(A'_f - A'_1\right)}$$

In this case only H' is a function of y'2, such that it may be solved for explicitly:

$$H' = \frac{1}{T_1 {A'_f}^2}\left\{{Fr_1}^2 {A'_1}^2\left(A'_f - A'_1\right) - T_1 A'_f\left[(\bar{z}A)'_f - (\bar{z}A)'_1\right]\right\}$$

Combining Equations (${Fr_1}^2$) and (H') results in the following explicit solution for y'2:

$$y'_2 = 1 + \frac{1}{T_1 {A'_f}^2}\left\{{Fr_1}^2 {A'_1}^2\left(A'_f - A'_1\right) - T'_1 A'_f\left[(\bar{z}A)'_f - (\bar{z}A)'_1\right]\right\}$$

The top width (Γ), area (Ω), and centroid-area (Ψ) functions for rectangular conduits are given by the following equations (Sturm 2001):

$$\Gamma(rect.y') = T' = \frac{T}{B} = \frac{B}{B} = 1$$

$$\Omega(rect.y') = \frac{A}{BD} = \frac{By}{BD} = \frac{y}{D} = y'$$

$$\Psi(rect.y') = \frac{\bar{z}A}{BD^2} = \frac{By^2}{2BD^2} = \frac{1}{2}\left(\frac{y}{D}\right)^2 = \frac{1}{2}(y')^2$$

$$y'_i \equiv \frac{y_i}{D}$$

$$T'_i \equiv \frac{T_i}{B} = \Gamma\left(shape.y'_i\right)$$

$$A'_i \equiv \frac{A_i}{BD} = \Omega\left(shape.y'_i\right)$$

$$(\bar{z}A)'_i \equiv \frac{(\bar{z}A)_i}{BD^2} = \Psi\left(shape.y'_i\right)$$

Inserting equations (Γ), (Ω), (Ψ), (y'_i), (T'_i), (A'_i) and (($\bar{z}A)'_i$) into equation (y'_2) yields the following equation:

$$y'_2 = 1 + \frac{1}{(1)\left(y'_f\right)^2}\left\{{Fr_1}^2 (y'_1)^2\left(y'_f - y'_1\right) - (1)y'_f\left[\frac{1}{2}\left(y'_f\right)^2 - \frac{1}{2}(y'_1)^2\right]\right\}$$

By combining like terms and rearranging, and noting that y'_f by definition equals 1, the following equation is obtained for incomplete jumps:

$$y'_2 = \frac{1}{2} + \left(Fr_1{}^2 + \frac{1}{2}\right)(y'_1)^2 - Fr_1{}^2(y'_1)^3$$

B.5 Example Calculations

B.5.1 Example 1: Box Culvert (experiment 12C)

Determine the subcritical sequent depth of an incomplete hydraulic jump in a box culvert with a 150 ft span and a 10 ft rise, passing a flow of 1.6883 cfs at an upstream depth of 6.47 ft. with approach velocity of 6.059 ft./s.

GIVEN: B = 150 ft, D = 10 ft, Q = 1.6883 cfs, y_1 = 6.47 ft., $V_1 = 6.059$ ft/s

Find: y_2

SOLUTION:

Step 1: Calculate dimensionless upstream depth

$$y'_1 = \frac{y_1}{D} = \frac{6.47\ ft}{10 ft} = 0.65$$

Step 2: Calculate upstream Froude number

$$F_{r1} = \frac{V_1}{\sqrt{g y_1}} = \frac{6.059\ ft/s}{\sqrt{(32.2 ft/s^2)6.47\ ft}} = 1.87$$

Step 3: Calculate downstream depth (y_2)

$$y'_2 = \frac{1}{2} + \left(Fr_1{}^2 + \frac{1}{2}\right) y'_1{}^2 - Fr_1{}^2 y'_1{}^3$$

$$y'_2 = \frac{1}{2} + \left((1.87)^2 + \frac{1}{2}\right)(0.65)^2 - (1.87)^2(0.65)^3 = 1.23$$

$$y_2 = y'_2 * D = 1.23 * 10\ ft = \underline{12.3\ ft.}$$

B.6 Orifice Plate

An orifice plate is a device used for measuring the volumetric flow rate. It uses the same principle as a Venturi nozzle, namely Bernoulli's principle that states that there is a relationship between the pressure of the fluid and the velocity of the fluid. When the velocity increases, the pressure decreases and vice versa.

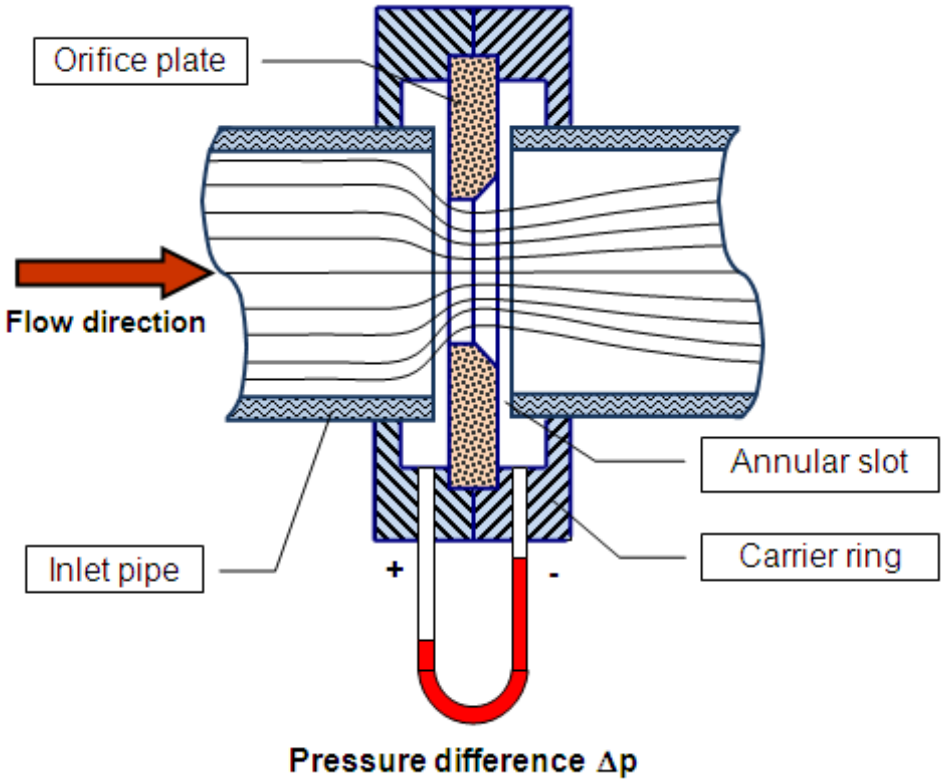

$$P_1 - P_2 = \frac{1}{2} \cdot \rho \cdot V_2^2 - \frac{1}{2} \cdot \rho \cdot V_1^2$$

$$Q = C_d \, A_2 \sqrt{\frac{1}{1-\beta^4}} \sqrt{2 \, (P_1 - P_2)/\rho}$$

$$\dot{m} = \rho \, Q = C \, A_2 \sqrt{2 \, \rho \, (P_1 - P_2)}$$

B.7 Flowrate Table

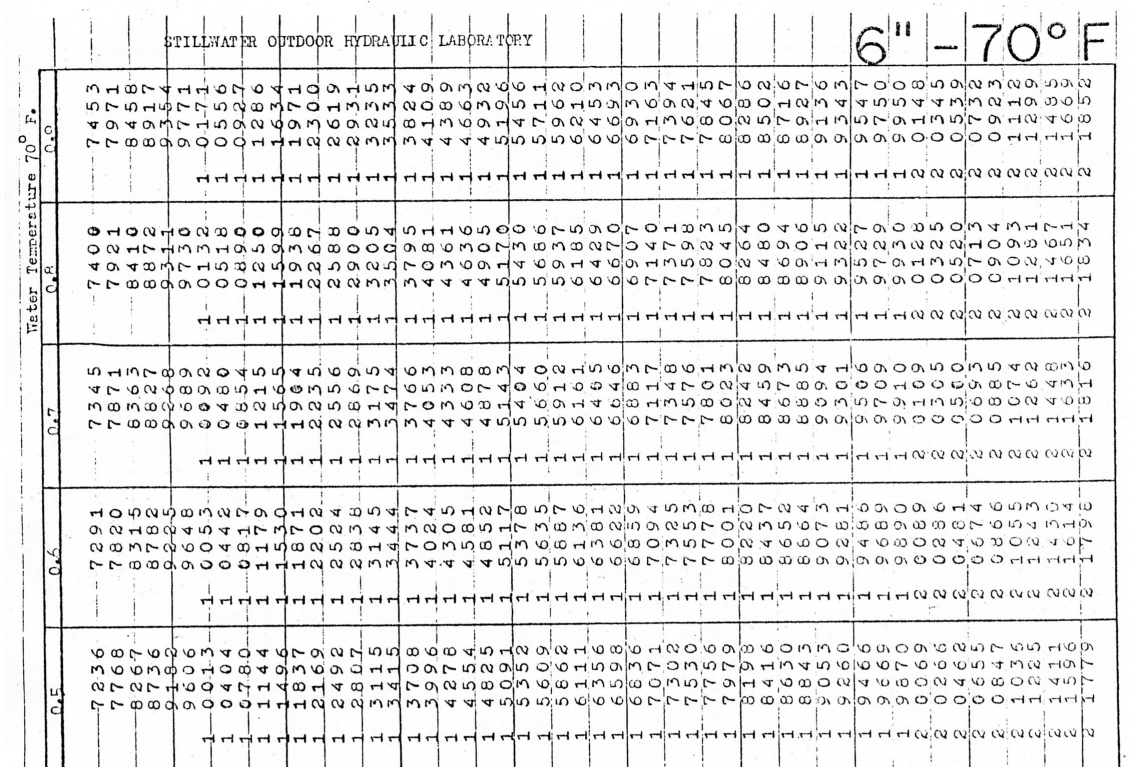

STILLWATER OUTDOOR HYDRAULIC LABORATORY

ORIFICE SIZE 6 in. #4642100010056 Water Temperature 70° F.

6" – 70° F

H	0.0	0.1	0.2	0.3	0.4	0.5	0.6	0.7	0.8	0.9
5	0 6954	0 7011	0 7068	0 7124	0 7180	7236	7291	7345	7400	7453
7	0 7507	0 7560	0 7613	0 7665	0 7717	7768	7820	7871	7921	7971
9	0 8021	0 8071	0 8120	0 8169	0 8218	8267	8315	8363	8410	8458
10	0 8505	0 8551	0 8598	0 8644	0 8690	8736	8782	8827	8872	8917
11	0 8962	0 9006	0 9050	0 9094	0 9138	9182	9225	9268	9311	9354
12	0 9396	0 9439	0 9481	0 9523	0 9565	9606	9648	9689	9730	9771
13	0 9812	0 9852	0 9893	0 9933	0 9973	1 0013	1 0053	1 0092	1 0132	1 0171
14	1 0210	1 0249	1 0288	1 0327	1 0365	1 0404	1 0442	1 0480	1 0518	1 0556
15	1 0594	1 0631	1 0669	1 0706	1 0743	1 0780	1 0817	1 0854	1 0890	1 0927
16	1 0963	1 1000	1 1036	1 1072	1 1108	1 1144	1 1179	1 1215	1 1250	1 1286
17	1 1321	1 1356	1 1391	1 1426	1 1461	1 1496	1 1530	1 1565	1 1599	1 1634
18	1 1668	1 1702	1 1736	1 1770	1 1804	1 1837	1 1871	1 1904	1 1938	1 1971
19	1 2004	1 2038	1 2071	1 2104	1 2137	1 2169	1 2202	1 2235	1 2267	1 2300
20	1 2332	1 2364	1 2396	1 2428	1 2460	1 2492	1 2524	1 2556	1 2588	1 2619
21	1 2651	1 2682	1 2714	1 2745	1 2776	1 2807	1 2838	1 2869	1 2900	1 2931
22	1 2962	1 2993	1 3023	1 3054	1 3084	1 3115	1 3145	1 3175	1 3205	1 3235
23	1 3266	1 3296	1 3325	1 3355	1 3385	1 3415	1 3444	1 3474	1 3504	1 3533
24	1 3562	1 3592	1 3621	1 3650	1 3679	1 3708	1 3737	1 3766	1 3795	1 3824
25	1 3853	1 3882	1 3910	1 3939	1 3967	1 3996	1 4024	1 4053	1 4081	1 4109
26	1 4137	1 4166	1 4194	1 4222	1 4250	1 4278	1 4305	1 4333	1 4361	1 4389
27	1 4416	1 4444	1 4471	1 4499	1 4526	1 4554	1 4581	1 4608	1 4636	1 4663
28	1 4690	1 4717	1 4744	1 4771	1 4798	1 4825	1 4852	1 4878	1 4905	1 4932
29	1 4958	1 4985	1 5011	1 5038	1 5064	1 5091	1 5117	1 5143	1 5170	1 5196
30	1 5222	1 5248	1 5274	1 5300	1 5326	1 5352	1 5378	1 5404	1 5430	1 5456
31	1 5481	1 5507	1 5533	1 5558	1 5584	1 5609	1 5635	1 5660	1 5686	1 5711
32	1 5737	1 5762	1 5787	1 5812	1 5837	1 5862	1 5887	1 5912	1 5937	1 5962
33	1 5987	1 6012	1 6037	1 6062	1 6086	1 6111	1 6136	1 6161	1 6185	1 6210
34	1 6234	1 6259	1 6283	1 6308	1 6332	1 6356	1 6381	1 6405	1 6429	1 6453
35	1 6477	1 6502	1 6526	1 6550	1 6574	1 6598	1 6622	1 6646	1 6670	1 6693
36	1 6717	1 6741	1 6765	1 6788	1 6812	1 6836	1 6859	1 6883	1 6907	1 6930
37	1 6954	1 6977	1 7000	1 7024	1 7047	1 7071	1 7094	1 7117	1 7140	1 7163
38	1 7187	1 7210	1 7233	1 7256	1 7279	1 7302	1 7325	1 7348	1 7371	1 7394
39	1 7417	1 7439	1 7462	1 7485	1 7508	1 7530	1 7553	1 7576	1 7598	1 7621
40	1 7644	1 7666	1 7689	1 7711	1 7733	1 7756	1 7778	1 7801	1 7823	1 7845
41	1 7867	1 7890	1 7912	1 7934	1 7956	1 7979	1 8001	1 8023	1 8045	1 8067
42	1 8089	1 8111	1 8133	1 8155	1 8177	1 8198	1 8220	1 8242	1 8264	1 8286
43	1 8307	1 8329	1 8351	1 8372	1 8394	1 8416	1 8437	1 8459	1 8480	1 8502
44	1 8523	1 8545	1 8566	1 8588	1 8609	1 8630	1 8652	1 8673	1 8694	1 8716
45	1 8737	1 8759	1 8780	1 8801	1 8822	1 8843	1 8864	1 8885	1 8906	1 8927
46	1 8948	1 8969	1 8990	1 9011	1 9032	1 9053	1 9073	1 9094	1 9115	1 9136
47	1 9157	1 9177	1 9198	1 9219	1 9240	1 9260	1 9281	1 9301	1 9322	1 9343
48	1 9363	1 9384	1 9404	1 9425	1 9445	1 9465	1 9486	1 9506	1 9527	1 9547
49	1 9567	1 9588	1 9608	1 9628	1 9649	1 9669	1 9689	1 9709	1 9729	1 9750
50	1 9770	1 9790	1 9810	1 9830	1 9850	1 9870	1 9890	1 9910	1 9930	1 9948
51	2 0016	2 0036	2 0056	2 0076	2 0096	2 0116	2 0136	2 0155	2 0175	2 0195
52	2 0214	2 0234	2 0253	2 0273	2 0292	2 0312	2 0331	2 0350	2 0370	2 0389
53	2 0408	2 0427	2 0446	2 0465	2 0484	2 0503	2 0522	2 0541	2 0560	2 0579
54	2 0598	2 0617	2 0636	2 0655	2 0674	2 0693	2 0712	2 0731	2 0750	2 0769
55	2 0787	2 0806	2 0825	2 0844	2 0862	2 0881	2 0900	2 0918	2 0937	2 0955
56	2 0974	2 0993	2 1011	2 1030	2 1048	2 1067	2 1085	2 1104	2 1122	2 1141
57	2 1159	2 1178	2 1196	2 1214	2 1233	2 1251	2 1269	2 1288	2 1306	2 1324
58	2 1342	2 1361	2 1379	2 1397	2 1415	2 1433	2 1451	2 1469	2 1487	2 1505
59	2 1523	2 1541	2 1559	2 1577	2 1595	2 1613	2 1631	2 1649	2 1667	2 1685

VITA

JAMES ALFRED BROWN

Candidate for the Degree of

Master of Science

Title of Study: LABORATORY MODELING OF ENERGY DISSIPATION IN SIX-FOOT DROP BROKEN-BACK CULVERTS

Major Field: CIVIL ENGINEERING WATER RESOURCES

Biographical:

Education:

Completed the requirements for the Master of Science in Civil Engineering at Oklahoma State University, Stillwater, Oklahoma in December 2012.

Completed the requirements for the Bachelor of Science in Civil Engineering at Oklahoma State University, Stillwater, Oklahoma in 2006.

Experience:

Environmental Engineer / 72 ABW/CEAN
Tinker AFB May 2011 – Present

Graduate Research and Teaching Assistant / Oklahoma State University
Stillwater, OK April 2009 – May 2011

Civil Engineer In Training / JGVEngineering
Oklahoma City, OK January 2006 – January 2007

Civil Engineering Intern / Poe And Associates
Tulsa, OK May 2004 – August 2004

Professional Memberships: ASCE